The Generation and Maintenance of T Helper 17 Cells in Response to Bacterial Infection

A DISSERTATION
SUBMITTED TO THE FACULTY OF
UNIVERSITY OF MINNESOTA
BY

Jonathan L. Linehan

IN PARTIAL FULFILLMENT OF THE REQUIREMENTS
FOR THE DEGREE OF
DOCTOR OF PHILOSOPHY

Marc K. Jenkins, Ph.D., Advisor

SEPTEMBER 2012

Acknowledgements

I would like to thank my mentor Dr. Marc Jenkins and my Thesis Committee: Dr. Stephen Jameson, Dr. Daniel Kaplan, and Dr. David Masopust for their advice and direction throughout my doctoral training. I would also like to thank members of the Jenkins lab for invaluable insights and assistance throughout my graduate career, particularly Dr. Marion Pepper for collaboration on the helper T cell memory aspect of this dissertation. Special thanks go Dr. P. Patrick Cleary and Dr. Thamotharampillai Dileepan, for initiating our collaboration to study T_H17 cell differentiation in response to bacterial infection. Without their expertise and assistance, this dissertation would not have come to fruition. Lastly, I would like to thank the faculty, staff, and my classmates in the Microbiology, Immunology, and Cancer Biology graduate program and my colleagues in the Center for Immunology for providing an intellectually enriching environment to carry out my graduate studies.

Dedication

I dedicate this dissertation to my mother, Elaine.

Abstract

Multiple studies have identified Interleukin-6 (IL-6) and Transforming Growth Factor-β1 (TGF-β1) as sufficient to induce T helper type 17 (T_H17) differentiation *in vitro*, but it is unclear whether these factors are necessary, and if so, what the cellular source of these factors is in the context of a T_H17 inducing infection *in vivo*. Moreover, studies of the T_H17 response have focused mainly on the effector phase and it is currently unclear whether these cells persist into the memory phase. To address these questions, we used mouse models of immunity to the extracellular bacterium Group A *Streptococcus pyogenes* (GAS) and the intracellular bacterium *Listeria monocytogenes* (LM), along with a sensitive peptide:Major Histocompatibility Complex II (pMHCII) tetramer and magnetic bead-based enrichment method to study the differentiation of naïve, polyclonal, GAS or LM pMHCII-specific $CD4^+$ cells into T_H17 cells. We found that an intranasal route of infection resulted in T_H17 differentiation, while an intravenous route of infection resulted in T helper type 1 (T_H1) differentiation after either GAS or LM infection. We also found that IL-6 and TGF-β1 were necessary for T_H17 differentiation in response to intranasal GAS infection *in vivo*. We identified a hematopoietic source of IL-6 and a dendritic cell source of TGF-β1 necessary for this differentiation. Lastly, we found that intravenous LM infection induced a long-lived T_H1 memory population, while intranasal LM infection induced a short-lived T_H17 population. Combined, this work supports a model whereby dendritic cells residing in upper respiratory tissues induce T_H17 cell differentiation through the production of IL-6 and TGF-β1, resulting in a short-lived population of T_H17 cells.

Table of Contents

List of Figures

Chapter 2

Chapter 3

Chapter 1:

Background and Introduction

1.1 Helper T cell Development

Helper T cell development begins when progenitors from the bone marrow seed the thymus (Love and Bhandoola, 2011). In the thymus, these progenitors differentiate into thymocytes and begin to rearrange their αβ T cell antigen receptors (TCRs) through the process of random VDJ gene segment somatic recombination (Taghon and Rothenberg, 2008). This process ends at the $CD4^+$ $CD8^+$ stage of thymocyte development. At this time, thymocytes survey self-peptide:MHC (pMHC)-expressing cortical thymic epithelial cells via their unique TCRs. Thymocytes with a TCR that binds self-pMHC with low affinity will receive a signal through their TCR that allows for survival on to the next stage through the process of Positive Selection (Starr et al., 2003). Thymocytes that express a TCR that does not bind self-pMHC will not receive a survival signal and will undergo apoptosis. Clones with TCRs that recognize self-pMHCI will become $CD8^+$ cytotoxic T cells, while clones that recognize self-pMHCII will become $CD4^+$ helper T cells (Jameson et al., 1995; Singer et al., 2008). Positively selected thymocytes then migrate to the thymic medulla. Here they interact with medullary thymic epithelial cells and dendritic cells (DCs) displaying self-pMHC molecules. At this developmental stage, if a thymocyte expresses a TCR that binds self-pMHC with too high avidity, it will undergo apoptosis in a process termed negative selection. However, some $CD4^+$ thymocytes survive this process and go on to become natural regulatory T cells ($nT_{REG}s$) (Hogquist et al., 2005). The surviving thymocytes together form a

repertoire of T cells containing weakly self-pMHC binding TCRs that go on to seed the secondary lymphoid organs of the body. These organs include the spleen, lymph nodes, Peyer's patches, and nasal associated lymphoid tissue (NALT).

The totality of T cell development results in a diverse repertoire of mature T cells that discriminate self from non-self pMHC molecules and are thereby able to mount effective responses against pathogens. Additionally, autoimmunity is averted through the deletion of autoreactive T cells.

1.2 Primary Helper T Cell Response

In the context of an infection, immature DCs become activated through interaction of pathogen recognition receptors, such as Toll-like receptors, with pathogen-associated molecular patterns residing on the microbe. Upon activation, DCs begin to upregulate genes involved in antigen processing, pMHCII presentation, costimulatory molecules, and cytokines (Banchereau et al., 2000; Janeway and Medzhitov, 2002). This can happen in lymphoid or non-lymphoid tissue. In the former, resident DCs capture the antigen from afferent draining lymph or blood. In the latter, the DC must capture the antigen and then migrate to the draining lymphoid tissue (Catron et al., 2004; Gonzalez et al., 2011). These DCs process pathogen-derived protein antigens, load peptides onto MHCII, and present them on the cell membrane (Jenkins et al., 2001). Within secondary lymphoid tissues, naïve helper T cells ($CD4^+$ T cells) become activated and proliferate upon engagement of their epitope-specific TCR and CD28 by pathogen-derived pMHCII and costimulatory ligands residing on activated DCs, respectively (Glimcher and

Murphy, 2000). These pathogen-derived pMHCII-specific naïve $CD4^+$ T cells are extremely rare (a frequency of about $1/10^5$-$1/10^6$ of all $CD4^+$ T cells in a mouse) (Jenkins et al., 2010). Naïve $CD4^+$ T cells can differentiate into three known distinct effector subsets, each dependent on the presence of specific cytokines provided in the lymphoid environment at the time of activation: T helper 1 (T_H1), T_H2, and T_H17 (Murphy and Reiner, 2002). Each subset carries out distinct functions and secretes a specific cytokine profile. Although each subset has unique functionality, activated $CD4^+$ T cells are generally known to promote B cell, phagocyte, and $CD8^+$ T cell function (Jenkins et al., 2001). T_H17 cells are thought to primarily orchestrate protective immunity to extracellular bacterial and fungal pathogens, predominantly at epithelial surfaces (Korn et al., 2009). They secrete the signature effector cytokine Interleukin-17A (IL-17A), which has proinflammatory properties and is involved in the activation, recruitment, and migration of neutrophils (Korn et al., 2009). IL-17A also acts on many other cell types to induce the expression of cytokines, chemokines, antimicrobial peptides, and metalloproteinases (Korn et al., 2009). Upon differentiation, many of these cells exit lymphoid organs and circulate through the blood to locations throughout the body, including sites of infection (Reinhardt et al., 2001). Upon resolution of infection, most $CD4^+$ effector cells will undergo apoptosis. However, a small percentage of $CD4^+$ T cells will remain in the body as memory cells.

1.3 Helper T Cell Memory

About 10% of the total pMHCII-specific $CD4^+$ cells that existed at the peak of proliferation remain as memory cells. These cells are mostly quiescent, but some can self-renew (Seder and Ahmed, 2003). $CD4^+$ memory cells can be classified into two groups: central memory (T_{CM}) and effector memory (T_{EM}) (Sallusto et al., 1999). T_{CM} cells express lymphoid tissue homing receptors, therefore they tend to reside in these tissues. They are thought to be primarily involved in secondary responses in these organs exclusively (Sallusto et al., 2004). Upon TCR stimulation, these cells produce the cytokine IL-2, proliferate extensively, and differentiate into effector cells (Sallusto et al., 2004). T_{EM} cells express homing receptors that bring them to non-lymphoid tissues of the body. These cells are known to produce effector cytokines quickly upon stimulation through their TCR (Sallusto et al., 1999). In this respect, T_{EM} cells more closely resemble effector cell subsets and have been shown to derive from effector cells in several *in vitro* and *in vivo* studies (Harrington et al., 2008; Lohning et al., 2008; Pepper and Jenkins, 2011). T_{EM} cells are thought to be a line of immediate defense at sites of pathogen entry into the body (Sallusto et al., 2004).

A general characteristic of memory T cells is that they are capable of long-term survival within the host, independent of further TCR stimulation from the inducing pMHC ligand (Pepper and Jenkins, 2011; Seder and Ahmed, 2003). Oldstone and colleagues studied this after acute infection with lymphocytic choriomeningitis virus (LCMV). They tracked the stability of LCMV-specific T_H1 and $CD8^+$ effector memory cells over time and identified that T_H1 effector memory cells were less stable over time

than their $CD8^+$ counterparts (Homann et al., 2001). They attributed this to reduced expression of the anti-apoptotic molecule Bcl-2 in T_H1 compared to $CD8^+$ effector memory cells. The finding that T_H1 effector memory cells behaved differently had major implications to the protective capacity of these cells. Two other *in vivo* studies have identified putative T_H2 effector memory cells, however, to date there have been no other studies to investigate the stability of other $CD4^+$ memory cell subsets (Mohrs et al., 2001; Zaph et al., 2006). Many questions remain such as: does this attrition occur for $CD4^+$ memory populations induced from other infections, do T_H17 cells survive to the memory phase, and if so, do they decline over time similarly to memory cells in the Oldstone study?

1.4 Cytokine Requirements for T_H17 Differentiation

In 2005, two important studies identified a new class of $CD4^+$ T cells distinct from the classically described T_H1 and T_H2 subsets. This new subset developed independently of, and was inhibited by, T_H1 and T_H2 specific transcriptional regulators (Harrington et al., 2005; Park et al., 2005). These cells were termed T_H17 cells because they produced a signature cytokine, IL-17A, in large amounts. Subsequently, the transcription factor RORγt was identified as both necessary and sufficient to drive T_H17 differentiation (Ivanov et al., 2006; Wilson et al., 2007). In rapid succession following this discovery, the minimal cytokines sufficient to differentiate naïve $CD4^+$ T cells into T_H17 cells *in vitro* were identified. These factors were transforming growth factor (TGF)-β1 and interleukin (IL)-6 (Bettelli et al., 2006; Mangan et al., 2006; Veldhoen et

al., 2006). The fact that TGF-β1 was involved came as a surprise since this cytokine was historically associated with anti-inflammatory effects and was now implicated in the differentiation of a pro-inflammatory $CD4^+$ T cell subset. Later three other cytokines IL-21, IL-23, and IL-1β were identified, which enhanced or stabilized the T_H17 phenotype, but none were required for initial induction of these cells *in vitro* (Chung et al., 2009; Korn et al., 2007; McGeachy et al., 2009). The establishment that TGF-β1 and IL-6 were required for T_H17 differentiation *in vitro* still left open the question of whether these factors are necessary for differentiation *in vivo* and, if so, the potential cellular sources. Recent work by Flavell and colleagues showed that T cell-produced TGF-β1 may play a role in the induction of T_H17 cells (Li et al., 2007). In this study, after genetically ablating the *Tgfb1* gene in T cells, the authors found a significant reduction in IL-17A-producing cells after experimental autoimmune encephalomyelitis (EAE) induction. Although this is an important finding, the authors induced a T cell response to a self-pMHCII (MOG peptide), which could have confounded their conclusions. This result may not apply to T cell responses to a foreign pMHCII, such as those generated in infection. Additionally, the necessity for IL-6 *in vivo* has come under scrutiny as a recent study found that IL-21 may be involved in an alternative pathway to IL-6 dependent T_H17 generation in IL-$6^{-/-}$ mice (Korn et al., 2007). This study was also undertaken utilizing the EAE model, therefore, the conclusions may not be universal for the same reason stated above. It will be important to determine the necessity and cellular sources of these factors under the more physiological conditions of a T_H17 cell-inducing infection.

1.5 IL-6 Signaling in Helper T cells

IL-6 is a cytokine with pleiotropic properties within the immune system and is produced by a multitude of cell types in the body including: DCs, macrophages, neutrophils, and epithelial cells (Ericson et al., 1998; Iwasaki, 2007; Jung et al., 1995). IL-6 mediates its effects on $CD4^+$ T cells via engaging its receptor, IL6Rα, on the cell surface. In order for a signal to be transduced though, a homodimer of the membrane-spanning receptor molecule gp130 must be recruited to the IL-6/IL-6Rα complex. Upon engagement with this complex, gp130 recruits the Janus kinase JAK1 to its intracellular domain. JAK1 then activates the transcription factor signal transducer and activator of transcription (STAT)-3 via phosphorylation (Vanden Berghe et al., 2000). Phosphorylated STAT3 then dimerizes and mobilizes to the nucleus, helping to initiate the T_H17 differentiation program (Heinrich et al., 2003; Korn et al., 2009). STAT3 is necessary but not sufficient to induce RORγt, suggesting that other factors are involved. This is also evidenced by the fact that full induction of RORγt is achieved only in the presence of TGF-β1 and IL-6 *in vitro* (Korn et al., 2009). IL-6 signaling in naïve $CD4^+$ T cells also leads to the upregulation of IL-23R and IL-21, which as mentioned earlier, are important for further T_H17 development (Ivanov et al., 2006; Zhou et al., 2007).

1.6 TGF-β1 Signaling in Helper T cells

Like IL-6, TGF-β1 has pleiotropic effects on the immune system including functioning in T cell development, homeostasis, and tolerance (Li and Flavell, 2008). This cytokine is also produced by many cell types in the body. Relevant potential

sources of this factor to T cells include lymphocytes, dendritic cells, and epithelial cells (Iwasaki, A., 2007; (Wang et al., 2006). Owing to its many roles in the body, TGF-β1 is complexly regulated. It is synthesized in an inactive form consisting of a TGF-β1 dimer in association with latency-associated protein (LAP). Latent TGF-β1 is either secreted directly or can form a complex with latent-TGF-β1-binding protein (LTBP), which allows for binding to the extracellular matrix (ECM) (Li and Flavell, 2008). Latent TGF-β1 becomes activated upon engagement of a TGF-β1 activator, such as $\alpha_v\beta_6$ integrins on epithelial cells or $\alpha_v\beta_8$ on DCs (Korn et al., 2009). This binding alters the conformation of LAP, allowing active TGF-β1 to bind to its receptor on the surface of $CD4^+$ T cells (Li and Flavell, 2008). This receptor is composed of a tetrameric complex of TGF-β1 receptor I (TGF-β1RI) and TGF-β1 receptor II (TGF-β1RII) dimers. Upon binding, TGF-β1RI becomes activated and phosphorylates the transcription factors Smad2 and Smad3, triggering their translocation into the nucleus in a complex with Smad4. Once in the nucleus, these Smad complexes associate with additional transcription factors and cofactors to regulate gene expression programs (Li and Flavell, 2008). Currently, the downstream factors that Smad proteins interact with in $CD4^+$ T cells remain unknown, but it is has been suggested that TGF-β1 downstream signaling leads to suppressed expression of the transcription factors T-bet and GATA3, limiting differentiation to T_H1 and T_H2 fates (Das et al., 2009). Study of TGF-β1 and its role in T_H17 differentiation has been complicated by the observation that mice lacking this cytokine or its receptor subunits develop a fatal, systemic T cell-mediated autoimmune disease (Letterio and Roberts, 1998; Shull et al., 1992; Yang et al., 1999).

1.7 Detection of Polyclonal Epitope-specific $CD4^+$ T Cells with p:MHCII Tetramers

The Jenkins laboratory has recently developed a technique to detect numerically rare, polyclonal, epitope-specific $CD4^+$ T cells utilizing pMHCII tetramers along with magnetic enrichment and flow cytometry (Moon et al., 2007). To do this, a tissue is processed into a single-cell suspension and incubated with fluorochrome-labeled pMHCII tetramers. The sample is then incubated with anti-fluorochrome-conjugated magnetic beads. Next, the sample is put through a magnetic column, thereby enriching the sample for tetramer-bound cells. Using this method, detection of low frequency, endogenous, epitope-specific $CD4^+$ T cell populations can be achieved, which was not previously possible. Using this method, the technique of transferring TCR transgenic T cells to study T cell responses, with its presently identified potential pitfalls, is avoided (Badovinac et al., 2007; Garcia et al., 2007; Hataye et al., 2006; Marzo et al., 2005).

1.8 Statement of Thesis

Multiple studies have identified IL-6 and TGF-β1 as sufficient to induce T_H17 differentiation *in vitro*, but it is unclear whether these factors are necessary, and if so, what the cellular source of these factors is in the context of a T_H17 inducing infection *in vivo*. Moreover, studies of the T_H17 response have focused mainly on the effector phase and it is currently unclear whether these cells persist into the memory phase. This dissertation tests the hypothesis that T_H17 differentiation *in vivo* is controlled by the production of IL-6 and TGF-β1 by dendritic cells residing in anatomically distinct

lymphoid tissues of the body. We predict that these interactions lead to the generation of a phenotypically and functionally short-lived population of T_H17 cells. We used mouse models of immunity to the extracellular bacterium Group A *Streptococcus pyogenes* (GAS) and the intracellular bacterium *Listeria monocytogenes* (LM), along with a sensitive pMHCII tetramer and magnetic bead-based enrichment method to study the differentiation of naïve, polyclonal, GAS or LM pMHCII-specific $CD4^+$ cells into T_H17 cells. We found that IL-6 and TGF-β1 were necessary for T_H17 differentiation in response to GAS infection *in vivo*. We identified a hematopoietic source of IL-6 and a dendritic cell source of TGF-β1 necessary for this differentiation. We also found that an intranasal route of infection resulted in T_H17 differentiation, while an intravenous route of infection resulted in T_H1 differentiation after either GAS or LM infection. Lastly, we found that intravenous LM infection induced a long-lived T_H1 memory population, while intranasal LM infection induced a short-lived T_H17 population. Combined, this work supports a model whereby dendritic cells residing in upper respiratory tissues induce T_H17 cell differentiation through the production of IL-6 and TGF-β1, resulting in a short-lived population of T_H17 cells.

Chapter 2:

Robust Antigen Specific T_H17 T Cell Response to Group A Streptococcus is Dependent on IL-6 and Intranasal Route of Infection

2.1 Introduction

Group A streptococcus (GAS, *Streptococcus pyogenes*) is an important bacterial pathogen that causes many different clinical conditions ranging from pharyngitis, impetigo, toxic shock syndrome, necrotizing fasciitis to post infectious autoimmune sequelae like acute rheumatic fever and glomerulonephritis (Cunningham, 2008; Guilherme et al., 2005). GAS is an important cause of morbidity and mortality worldwide. Estimates are that 500,000 deaths occur each year due to severe GAS infections (Carapetis et al., 2005). GAS produces a wide variety of virulence factors that play important roles in adhesion, immune evasion, dissemination, tissue destruction and toxicity (Cunningham, 2008; Tart et al., 2007). Remarkably, one third of those treated with antibiotics continue to shed streptococci and a significant number of these carriers have recurrent disease by the same strain (Martin et al., 2004; Quinn and Federspiel, 1973). Carrier state is an important public health problem because it maintains the cycle of disease in a community. Tonsils are known to harbor and shed streptococci, even after intense antibiotic therapy. Osterlund *et al* found that 93% of tonsils excised from children retained intracellular GAS, and others reported isolation of GAS from excised tonsils, confirming that this secondary lymphoid tissue is an important reservoir (Osterlund et al., 1997).

The capacity of GAS to survive in lymphoid tissue is not understood. Although GAS induces a humoral immune response in most individuals, streptococci can still persist. GAS also induces a $CD4^+$ T cell response (Park et al., 2004). $CD4^+$ T cells express T cell antigen receptors (TCR) that recognize short peptides bound to MHCII molecules (pMHCII) expressed by host antigen-presenting cells. During primary infection, the rare naïve $CD4^+$ T cells, which by chance express TCRs complementary to bacterial pMHCII complexes, proliferate and differentiate into Th1, Th2, or Th17 effector cells that produce cytokines such as IFN-γ, IL-4 or IL-17, respectively, which help to eliminate the pathogen. Which of these effector cell types will develop during infection is determined by cytokines produced by cells of the innate immune system. For example in mice, the differentiation of Th17 cells *in vitro* depends on IL-6 and Transforming Growth Factor-beta (TGF-β) (Bettelli et al., 2006). We recently demonstrated that GAS infection of the NALT, the murine equivalent of the tonsils, generates Th17 cells, which contribute to immune protection (Wang et al., 2010). Lu *et al* have shown that Th17 cells protect against other streptococcal infections as well (Lu et al., 2008).

Previous studies used adoptive transfer of monoclonal TCR transgenic T cells to study T cell responses to infection with antigen tagged GAS (Costalonga et al., 2009; Park et al., 2004). A drawback of this approach is that it results in an abnormally large number of naïve precursors, which experience inefficient activation due to competition for limiting pMHCII (Blair and Lefrancois, 2007; Catron et al., 2006; Hataye et al., 2006). Therefore, the nature of the $CD4^+$ T cell response to GAS infection under physiological conditions is still unknown.

To avoid these limitations, we used a new cell enrichment method based on fluorochrome-labeled pMHCII tetramers and magnetic beads (Moon et al., 2009) to characterize the endogenous polyclonal $CD4^+$ T cell response to GAS. This approach depended on the availability of a tetramer of the I-A^b MHCII molecule of the preferred C57BL/6 mouse strain bound to a peptide from the GAS proteome. Unfortunately, no such peptide has been identified to date. We therefore produced a recombinant GAS strain that expresses an immunogenic peptide (EAWGALANWAVDSA) called 2W (Rees et al., 1999) fused to the M1 protein on its surface. 2W:I-A^b tetramer staining and magnetic bead enrichment was used to characterize 2W:I-A^{b+} $CD4^+$ T cells from NALT and other lymphoid tissues after intranasal GAS-2W infection. Our results demonstrate that an intranasal infection is critical for mounting an effective IL-6-dependent pMHCII-specific Th17 response. A lack of this response led to a preponderance of Th1 cells and failure to control GAS infection. This work defines the Th17 response to GAS infection, and may shed light on the basis for the carrier state and autoimmune complications in humans.

2.2 Materials and Methods

Bacterial Strains and Growth

Streptococci were grown in Todd-Hewitt broth supplemented with 2% neopeptone (THB-Neo) or on solid media containing Difco blood agar base and sheep blood at 37°C in 5% CO_2. All growth media were purchased from Difco Laboratories, Detroit, MI. Strain 90-

226 (serotype M1) was originally isolated from the blood of a septic patient (Dombek et al., 1999).

Mice

Five to six weeks old female C57BL/6 mice were purchased from Taconic farms (Germantown, NY) and used at 7–8 weeks of age. *IL-6*$^{-/-}$ mice in C57BL/6 background were purchased from the Jackson Laboratory (Bar Harbor, ME) (Kopf et al., 1994). Mice were housed under specific pathogen-free conditions at RAR facilities of University of Minnesota. Mice inoculated with GAS were housed in biosafety level 2 facilities.

Generation of a Recombinant GAS Strain that Expresses the 2W Epitope in M Protein

An M1 GAS strain 90–226 was genetically engineered to express the 14 amino acid 2W peptide (EAWGALANWAVDSA) on the bacterial surface as a fusion protein with streptococcal M protein (Fig. 2.1). The corresponding chimeric protein is composed of the 2W epitope inserted in-frame after the first five amino acids of the mature M1 surface protein. The hybrid emm1.0::2W gene was constructed using standard molecular biology techniques and then introduced into the chromosomal emm1.0 gene locus by allelic replacement. Briefly, the emm1.0 gene of strain 90–226 is contiguous with mga at the 5' end and with the sic gene at the 3' end, and has its own promoter. Plasmid pFW5 has two multiple cloning sites on either side of a spectinomycin resistance gene (Dombek et al., 1999; Park et al., 2004). The entire sic gene with its promoter was PCR amplified and

inserted into the multiple cloning site downstream of the spectinomycin resistance gene in pFW5. A fragment containing the C-terminal half of mga through the entire emm1.0 gene was PCR amplified by a two-step method to insert the sequence of the 2W epitope into the emm1.0 gene. In the first step, DNA fragments, each coding for part of the 2W epitope sequence (overlapping) were amplified by PCR. In the second step these overlapping fragments were annealed, extended and further amplified to generate a 2.5-kb fragment, which was inserted into the multiple cloning site upstream of the spectinomycin resistance gene in pFW5. This plasmid was transformed into strain 90–226 emm1.0::km for gene replacement, and transformants were selected on spectinomycin (100µg/ml). The spectinomycin-resistant transformants were then screened for kanamycin sensitivity. Positive clones ($Spec^{R}Kan^{S}$) were screened for gene replacement and the entire region including the 2W insertion was amplified and sequence verified. The resulting strain was designated *Streptococcus pyogenes* 90-226 emm1.0::2W (GAS-2W). A whole blood phagocytosis assay was used to test whether GAS-2W streptococci are M^{+} (Hyland et al., 2007).

Intranasal Inoculation

C57BL/6 mice were anesthetized with isoflurane/oxygen mixture for 1 min and inoculated intranasally with GAS-2W by placing appropriate doses in a total volume of 15 µl PBS (7.5 µl /nostril). Fractionated droplets were placed with a pipette tip near the entrance of the nostril and the inoculum was involuntarily aspirated into the nasal cavity.

In Vitro Stimulation with PMA-Ionomycin

NALT, Cervical lymph nodes (CLN) and Spleen from C57BL/6 mice were harvested by dissection, disrupted on a nylon screen in 1-2 ml of complete EHAA medium (cEHAA). Resulting single cell suspensions were filtered over a nylon screen and washed with cEHAA before invitro stimulation and staining. Freshly made single cell suspensions in cEHAA were stimulated in vitro with PMA and ionomycin for 4 hours. PMA and ionomycin were added at 50 ng/ml and 500 ng/ml final concentrations, respectively. Cells were incubated at 37C for 1 hour and Brefeldin A (BrA) was added to disrupt golgi and prevent cytokines from being secreted into the medium (1:1000 of 10 mg/ml DMSO stock) and incubated for three additional hours before proceeding to tetramer enrichment.

Tetramer Production

2W:I-A^b tetramers were generated as described in detail by Moon *et al* (Moon et al., 2009; Moon et al., 2007). Briefly, 2W:I-A^b was expressed in S2 cells. S2 cells were co-transfected with plasmids encoding the I-A^b alpha chain, the I-A^b beta chain and BirA gene. Transfected cells were selected, passaged in serum-free media, and cultures scaled up to one liter cultures. Expression was induced with copper sulfate and biotinylated 2W:I-A^b heterodimers were purified from supernatants with a Ni^{++} affinity column. Bound 2W:I-A^b molecules were eluted and purified. Tetramers were created by mixing biotinylated 2W:I-A^b molecules with Phycoerythrin (PE) or Allophycocyanin (APC)-conjugated streptavidin.

Peptide-MHC-II Tetramer Based Magnetic Bead Enrichment

2W:I-A^b-specific $CD4^+$ T cells were enriched as described previously (Moon et al., 2009; Moon et al., 2007; Pepper et al., 2010). Briefly mice were euthanized and NALT, cervical lymph nodes and Spleen were harvested separately. Single cell suspensions were prepared in 200 µl of Fc block (supernatant from 2.4G2 hybridoma cells grown in serum-free media + 2% mouse serum, 2% rat serum, 0.1% sodium azide) from each tissue. Phycoerythrin (PE) or Allophycocyanin (APC) conjugated tetramer was added at a final concentration of 10 nM and the cells were incubated at room temperature for 1 hr, followed by a wash in 15 ml of ice-cold FACS buffer (PBS + 2% fetal bovine serum, 0.1% sodium azide). The tetramer-stained cells were then resuspended in a volume of 200 µl of FACS buffer and mixed with 50 µl of anti-PE or anti-APC antibody conjugated magnetic microbeads (Miltenyi Biotech, Auburn, CA) and incubated on ice in dark for 30 min, followed by one wash with 10 ml of FACS buffer. The cells were resuspended in 3 ml of FACS buffer and passed over a magnetized LS column (Miltenyi Biotech). The column was washed with 3 ml of FACS buffer three times and then removed from the magnetic field. The bound cells were eluted by pushing 5 ml of FACS buffer through the column with a plunger. The resulting enriched fractions were resuspended in 0.1 ml of FACS buffer, and a small volume was removed for cell counting while the rest of the sample was stained with a cocktail of fluorochrome-labeled antibodies.

In Vivo Stimulation with Heat-killed GAS-2W

GAS-2W was grown in THB-Neo media to O.D.$_{600}$ of 0.5, washed once with PBS, pelleted and resuspended in appropriate volume of PBS and incubated at 60C for 30 minutes. Viability of bacteria was confirmed by plating out on blood agar plates. Heat-killed GAS-2W was stored in aliquots at -20C until use. To induce cytokine production by 2W:I-A^{b}-specific CD4^{+} T cells in vivo, 2 X 10^{8} CFU heat-killed GAS-2W in 200 µl of PBS was inoculated intravenously through tail vein. Mice were sacrificed after 3-4 hrs and single cell suspensions of spleen were made in cEHAA medium supplemented with BrA.

Intracellular Cytokine Staining

Intracellular cytokine staining for IL-17A and IFN-γ was done using BD Cytofix/Cytoperm fixation-permeabilization solution and anti-IL-17A-PE and anti-IFN-γ-PE-Cy7 antibodies according to manufacturer's protocols. Briefly cells stimulated in vivo with heat-killed GAS-2W or in vitro with PMA-ionomycin were subjected to 2W-MHCII tetramer enrichment. Enriched cells were stained for surface markers, washed and fixed with 250 µl of Fixation / Permeabilization solution (BD Biosciences) per sample for 20 min on ice. All samples were washed with 1 ml of 1X Perm/Wash buffer (BD Biosciences) and anti IL-17A PE and anti IFN-γ-PE-Cy7 antibodies were added in 100 µl of 1X Perm/Wash buffer and incubated overnight at 4C in dark. The following day cells were washed with 1 ml of 1X Perm/Wash buffer and resuspended in 400 µl of FACS

buffer and transferred to a micro tube within a FACS tube for analysis in LSR-II flow cytometer.

Flow Cytometry and Antibodies

A Becton Dickinson LSR-II flow cytometer was used to collect and analyze events that have the light scatter properties of lymphocytes and are $CD4^+$ and 2W:I-A^{b+}. Pacific Blue-conjugated anti-B220, CD11b, F4/80 (Caltag), CD11c (eBioscience, San Diego, CA); Pacific Orange-conjugated CD8 (eBioscience); PerCP-conjugated CD4 (BD PharMingen); PE-Cy7-conjugated IFN-γ (eBioscience); PE conjugated IL-17A; APC-AF780 conjugated CD4 and AlexaFluor 700-conjugated CD44 (eBioscience); PE-conjugated CD4; FITC-conjugated CD4; PB-conjugated CD4; APC-conjugated CD4; AF700-conjugated CD4; PerCP-Cy5.5-conjugated CD4; APC-AF750-conjugated CD4. Antibodies were purchased from the indicated sources. FACS acquisition was performed using FACSDiva software and analysis was done using FlowJo (Tree Star, Ashland, OR).

Statistics

All values are expressed as mean ± SEM. Differences between groups were analyzed using Student's t-test by GraphPad Prism (Version 4.03 for Windows, GraphPad Software, San Diego, CA). Differences are considered significant at $P < 0.05$.

2.3 Results

Generation of Recombinant GAS Strain that Expresses the M1-2W Fusion Protein

An M1 GAS strain 90–226 was genetically engineered to express the 14 amino acid 2W peptide (EAWGALANWAVDSA) as a cell wall surface hybrid M1 fusion protein. The hybrid emm1.0::2W gene was constructed in plasmid pFW5 in *E. coli* and then introduced into the chromosomal emm1.0 gene by allelic replacement (Dombek et al., 1999). The corresponding chimeric protein is composed of the 14 amino acid 2W peptide inserted in frame after the first five amino acids of the mature M1 surface protein (Fig. 2.1A). The strain, designated 90–226 emm1.0::2W (GAS-2W), is genetically stable without spectinomycin selection due to replacement of the wild-type gene in the chromosome. The anti-phagocytic property of the M1-2W fusion protein was assessed to test whether insertion of the 2W peptide altered the function of the M protein. GAS-2W was as resistant to phagocytosis as the wild-type 90-226 in whole blood bactericidal assays (Fig. 2.1B). An M^- variant 90-226 emm1.0::km (GAS-ΔM) (Dombek et al., 1999) was included as a negative control and was susceptible to phagocytic killing as expected. Furthermore, the GAS-2W strain colonized mouse NALT as efficiently as the wild type (Fig. 2.1C).

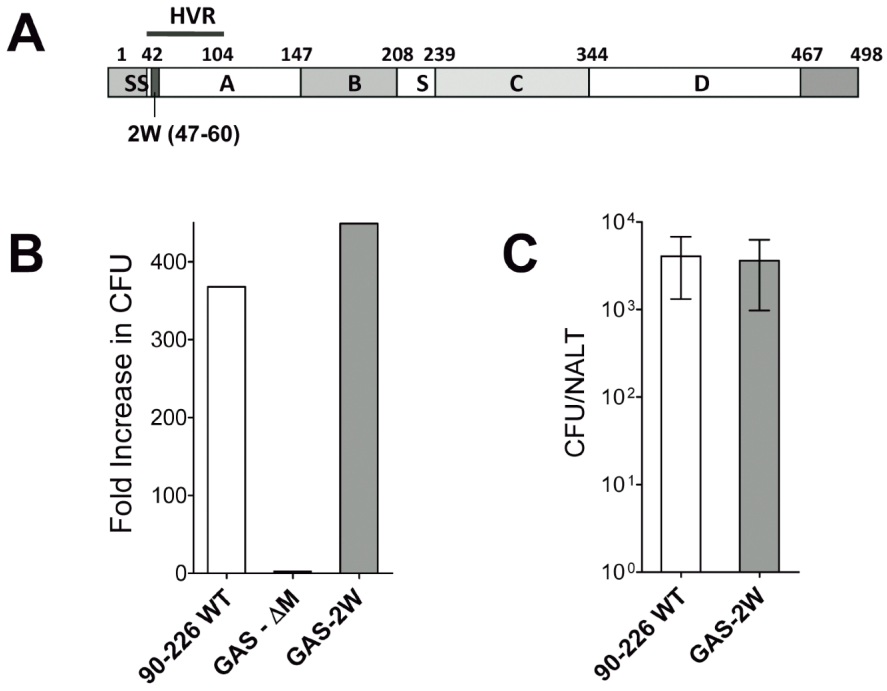

Figure 2.1. Construction of a Group A Streptococcus 90-226 strain that expresses the 2W (GAS-2W). (A) Schematic diagram of emm1.0::2W fusion protein that is expressed on the surface of GAS-2W. SS-Signal sequence; A - A region; B - B repeats; S - spacer region; C – C repeats; D – D region; HVR – Hyper-variable region; Cell wall anchor (466-496) (B) Survival and growth of strain GAS-2W in phagocytic human blood. 90-226 WT is the parent of GAS-2W and the M protein negative mutant GAS-ΔM. Fold increase was calculated as the number of CFU after 3 h in rotated blood divided by the initial number of CFU. Representative result from one of two independent experiments is shown. (C) Colonization of mouse NALT by intranasally administered Streptococci. Viable counts of 90-226-WT or GAS-2W streptococci recovered from homogenized NALT 24h following inoculation with $2x10^8$ CFU. The bars represent the mean $\pm$ SEM of four mice per group.

Intranasal Infection with GAS-2W Induced a Strong Antigen-specific T_H17 response in C57BL/6 Mice

Spleen and lymph node cells from mice were pooled for quantification of 2W:I-A^b-specific $CD4^+$ T cells by pMHCII-based cell enrichment at various times after infection with GAS-2W. Each C57BL/6 mouse had between 200 and 250 2W:I-A^b-specific $CD4^+$ T cells before infection, and these cells expressed small amounts of CD44 ($CD44^{Lo}$) on the surface as expected for naïve cells (Fig. 2.2A) (Moon et al., 2009; Moon et al., 2007). In mice that were inoculated intranasally with GAS-2W, this naïve 2W:I-A^b-specific $CD4^+$ T cell population expanded to ~10^5 cells in seven days (Fig. 2.2A). Most of these cells expressed large amounts of CD44 ($CD44^{Hi}$), indicative of pMHCII-dependent activation. Expansion of 2W:I-A^b-specific $CD4^+$ T cells was first detected three days after primary infection with GAS-2W and increased rapidly to a peak seven days after inoculation (Fig. 2.2B). 2W:I-A^b-specific $CD4^+$ T cells then began to decline and reached 10% of the maximum level by day 20-post infection. Expansion of these $CD4^+$ T cells was proportional to the dose of GAS-2W used for infection (Fig. 2.2C).

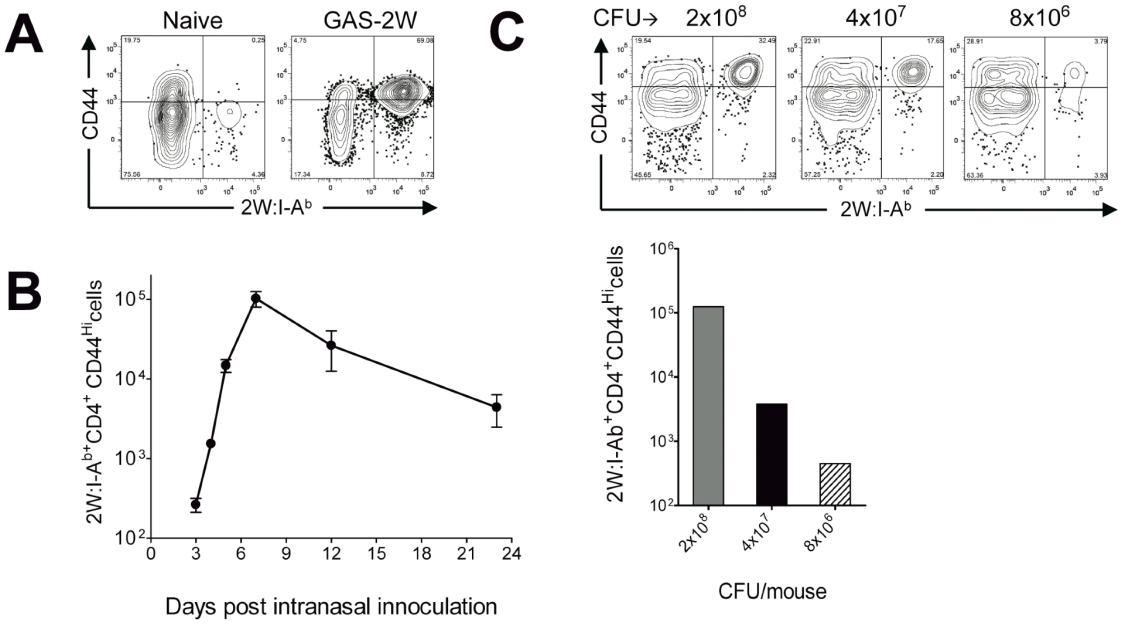

Figure 2.2. 2W:I-A^b-specific naïve CD4$^+$ T cells expanded in response to intranasal infection with GAS-2W. (A) B6 mice were infected with GAS-2W (intranasal, 2x10^8 CFU). Seven days later CD4$^+$2W:I-A^{b+} cells were enriched from cervical lymph nodes and spleens and analyzed by flow cytometry. One representative of at least ten independent experiments is shown. CD44 indicates the number of antigen experienced CD4$^+$ T cells (B) Change in the total number of 2W:I-A^b-specific CD4$^+$ T cells after a primary infection over time (n=28). (C) Mean number of antigen specific CD4$^+$2W:I-A^{b+} T cells is dose dependent. B6 mice were inoculated intranasally with 2x10^8, 4x10^7 and 8x10^6 CFU / mouse, respectively. Seven days after infection CD4$^+$2W:I-A^{b+} cells were isolated from cervical lymph nodes and spleen, and analyzed.

In vivo lymphokine production was measured by rechallenging mice with heat-killed GAS-2W (HK-GAS-2W) and then measuring intracellular lymphokines produced by 2W:I-A^b-specific T cells 3 hours later (Pepper et al., 2010). 2W:I-A^{b+} cells in mice infected intranasally with live GAS-2W one week earlier produced IL-17A, but not IFN-γ

after challenge with HK-GAS-2W (Fig. 2.3A). 2W:I-A^{b+} cells in mice inoculated intranasally with HK-GAS-2W one week earlier also produced IL-17A after challenge with HK-GAS-2W (Fig. 2.3). Therefore, exposure of NALT to either live or dead GAS induced bacterial pMHCII-specific Th17 cells. In order to compare the approximate percentage of 2W:I-A^{b}-specific Th17 cells to total GAS induced Th17 cells, B6 mice were inoculated once intranasally with $2x10^{8}$ CFU of GAS-2W. Ten days after the infection mice were restimulated in vivo by IV injection of heat killed GAS-2W. 2W:I-A^{b+} $CD4^{+}$ T cells from spleen were stained and enriched as described in the methods. Both bound (2W:I-A^{b+} $CD4^{+}$ T cells) and unbound (2W:I-A^{b-} $CD4^{+}$ T cells or flow through) fractions were collected and analyzed for intracellular cytokines IL-17A and IFN-γ. Total numbers of $CD4^{+}$2W:I-A^{b+}IL-$17A^{+}$ and $CD4^{+}$2W:I-A^{b-}IL-$17A^{+}$ cells were calculated for the entire spleen. The approximate ratio of 2W:I-A^{b+}IL-$17A^{+}$ cells to total 2W:I-A^{b-} IL-$17A^{+}$ cells ranged from 1:7 to 1:12 (Fig. 2.4).

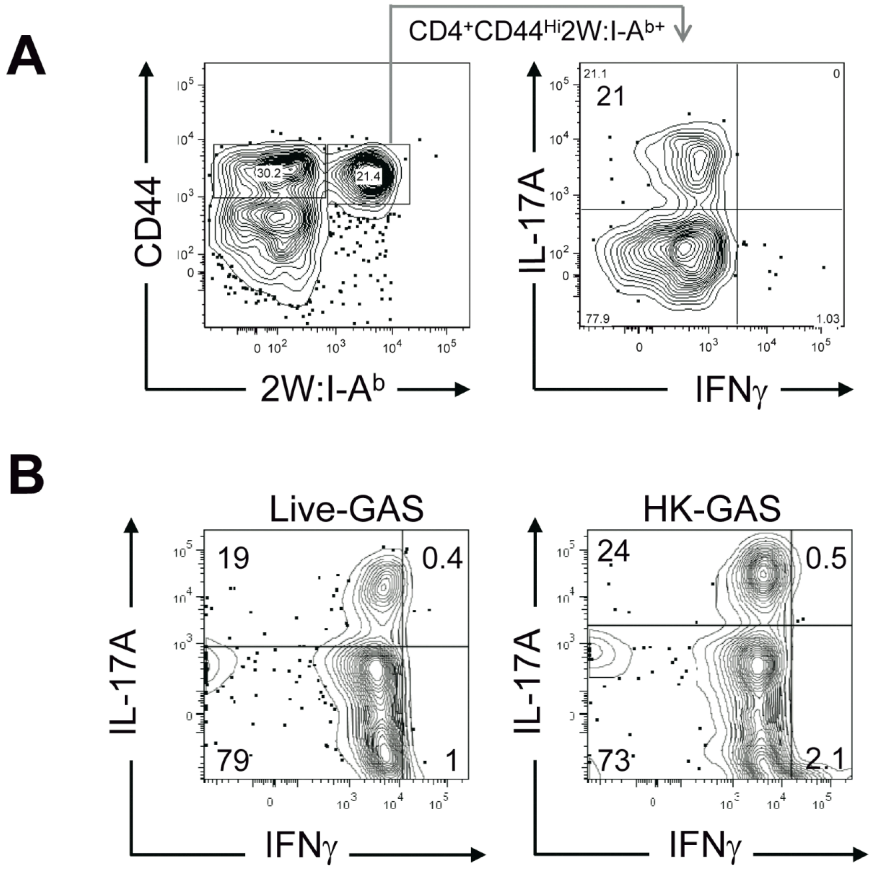

Figure 2.3. Primary intranasal GAS infection induces a Th17 response. Mice were inoculated once intranasally with $2x10^8$ CFU or equivalent numbers of heat-killed streptococci HK-GAS. (A) $CD4^+CD44^{Hi}2W:I\text{-}A^{b+}$ cells enriched from spleens of mice that were inoculated with live GAS-2W and restimulated after a week in vivo by IV injection of heat killed GAS-2W (HK-GAS-2W). (B) $CD4^+CD44^{Hi}2W:I\text{-}A^{b+}$ cells from mice that were inoculated intranasally with heat-killed GAS-2W and restimulated in vivo with HK-GAS-2W. One representative of three independent experiments is shown.

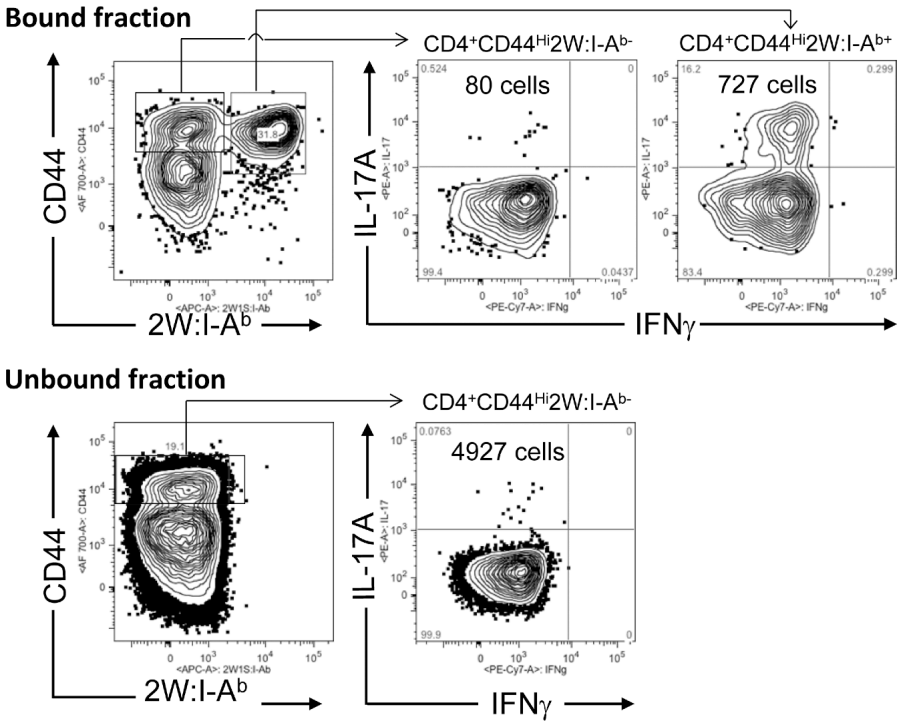

Figure 2.4. Primary intranasal GAS infection induces a Th17 response in both 2W:I-A^{b+} and 2W:I-A^{b-} CD4^{+} T cell populations. B6 Mice were inoculated once intranasally with 2x10^{8} CFU of GAS-2W. 10 days after the infection mice were restimulated in vivo with IV injection of heat killed GAS-2W. 2W:I-A^{b+} CD4^{+} T cells from spleen were enriched on magnetized columns. Both bound and unbound fractions were collected and analyzed for intracellular cytokines IL-17A and IFN-γ. Upper panel shows the bound fraction and cells shown in the middle and right columns are gated on CD4^{+}CD44^{Hi} cells. Lower panels shows the unbound (flow through) fraction. One representative of two independent experiments is shown. Numbers of CD4^{+}IL-17A^{+} T cells shown in the quadrants above were calculated for the whole spleen. The approximate ratio of 2W:I-A^{b+}IL-17A^{+} cells to streptococcus activated total 2W:I-A^{b-} IL-17A^{+} cells ranged from 1:7 to 1:12.

Li *et al* reported that the Streptococcal superantigen, which contaminates commercial peptidoglycan preparations induced human lymphocytes to produce IL-17A (Li et al., 2008); therefore, experiments were performed to determine whether 2W:I-A^b-specific $CD4^+$ T cell clonal expansion was pMHCII-specific. B6 mice were inoculated three times at weekly intervals with either $2x10^8$ CFU of GAS-2W or wild type $2W^-$ GAS (GAS-WT). Three days after the last infection, mice were euthanized and enriched $CD4^+$2W:I-A^{b+} T cells from spleen, cervical lymph nodes (CLN), and NALT were analyzed (Fig 2.5). Expansion of 2W:I-A^b-specific $CD4^+$ T cells only occurred in mice inoculated with GAS-2W (Fig. 2.5A), and not in mice inoculated with GAS-WT that lacked the 2W epitope. The number of $CD4^+$2W:I-A^{b+} T cells in tissue from mice infected with GAS-WT was less than 200, similar to that of naïve mice. This indicates that the clonal expansion of 2W:I-A^b-specific $CD4^+$ T cells is a pMHCII-specific response and not due to superantigens produced by this strain of GAS (Fig.2.5A). The same samples were restimulated *in vitro* with pharmacologic TCR mimics, PMA and ionomycin, and stained for intracellular cytokines in order to evaluate their cytokine phenotype. Most of the 2W:I-A^b-specific $CD4^+$ T cells from NALT, CLN and spleen produced IL-17A (Fig. 2.5B); greater than 75% of the 2W:I-A^b-specific $CD4^+$ T cells from all three tissues had a Th17 phenotype (Fig. 2.5B). The response was more robust in NALT, which is a preferred target of intranasal GAS infection. In NALT pMHCII-specific IL-17A producers reached more than 90% of the total 2W:I-A^b-specific $CD4^+$ T cells.

Even though initial priming and expansion of $CD4^{+}$2W:I-A^{b+} T cells is independent of superantigen as shown above, it was possible that cytokine activation in T cells from infected mice was mediated by superantigens associated with heat-killed bacteria. To address specificity of the recall response, B6 mice that were inoculated twice with GAS-2W streptococci and then were restimulated *in vivo* by intravenous injection of either HK-GAS-2W or heat killed wild-type $2W^{-}$GAS (HK-GAS-WT) bacteria. $CD4^{+}CD44^{Hi}$2W:I-A^{b+} cells from mice that were primed with GAS-2W had expanded significantly, produced IL-17A 21 days later following restimulation with HK-GAS-2W, but not with $2W^{-}$ HK-GAS-WT bacteria (Fig. 2.5C). Thus both priming of $CD4^{+}$ T cells and recall of cytokine expression by GAS is antigen-specific and independent of superantigens in this animal model.

Children often experience multiple episodes of GAS pharyngitis before reaching the age of 15. Therefore, we investigated whether repeated infection amplified, shifted or dampened the Th17 response. Following multiple infections, most of the $CD4^{+}CD44^{Hi}$2W:I-A^{b+} T cells had elevated levels of intracellular IL-17A (Fig. 2.5B). The response was more robust in NALT, the major infection site following intranasal GAS infection.

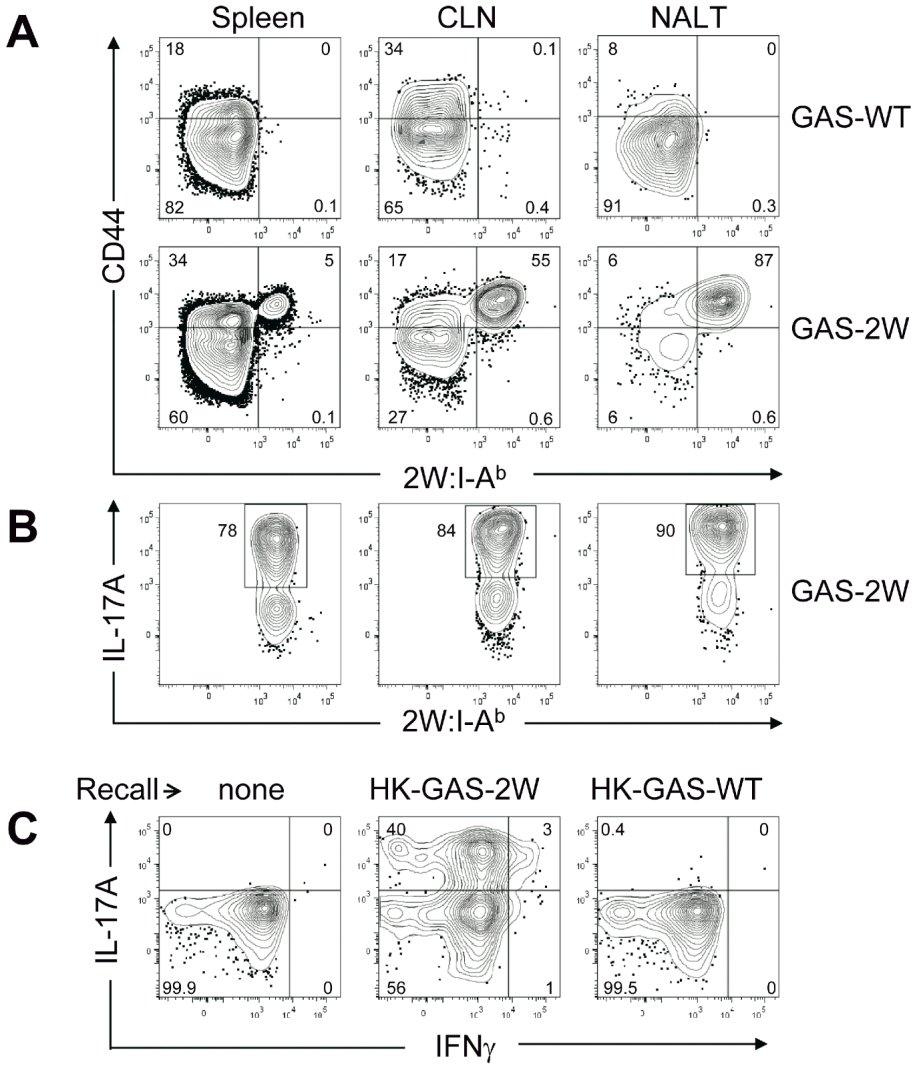

Figure 2.5. Clonal expansion of 2W:I-A^b-specific CD4$^+$ T cells and recall of IL-17A is antigen-specific and not due to Superantigens produced by GAS. (A) Tetramer enriched CD4$^+$ T cells from Spleen, CLN and NALT of mice after three inoculations at weekly intervals. Top panel is from wild type GAS (GAS-WT) infected B6 mice and the lower panel is from B6 mice inoculated with (GAS-2W). (B) Analysis of IL-17A expression by CD4$^+$ CD44^{Hi} 2W:I-A^b-specific T cells in NALT, CLN and Spleen from the lower panel of part A. (C) Analysis of the specificity of IL-17A activation in CD4$^+$ 2W:I-A^{b+} T cells originally primed by GAS-2W infection (twice). Primed mice were restimulated in vivo by IV injection of heat killed GAS-2W (HK-GAS-2W) or heat killed 2W negative GAS (HK-GAS-WT) 21 days

after the last infection. $CD4^{+}CD44^{Hi}$2W:I-A^{b+} cells were isolated as described in methods and analyzed for IL-17A and IFN-γ expression.

Route of Inoculation Influences the T_H17 Phenotype to GAS Infection

Recently, Pepper *et al* showed that the intranasal route was important for the generation of IL-17-producing 2W:I-A^{b}-specific T cells in response to a recombinant strain of *Listeria monocytogenes* that expressed the 2W peptide (LM-2W) (Pepper et al., 2010). Most GAS infections naturally involve oro-pharyngeal tissue and preferably colonize tonsils in humans and NALT in mice. Experiments were therefore performed to assess the impact of the intranasal route of inoculation of GAS on the $CD4^{+}$ T cell response. B6 mice were inoculated with HK-GAS-2W intranasally, intravenously or subcutaneously. HK-GAS-2W bacteria were used to avoid spread of infection from the site of inoculation. 2W:I-A^{b}-specific T cells expanded in the spleens of these mice in response to all routes of inoculation. Intranasal infection with GAS-2W induced IL-17A-producing 2W:I-A^{b}-specific T cells; whereas intravenous and subcutaneous inoculations induced IFN-γ-producing cells (Fig. 2.6). The Th17/Th1 ratio was more than 40 times higher in cells from intranasally inoculated mice compared to that from mice inoculated intravenously or subcutaneously. Thus, the intranasal route of infection was critical for the generation of Th17 cells during GAS infection.

To compare the relative magnitude of Th17 induction by GAS and LM intranasal infections, mice were inoculated either intranasally or intravenously with either GAS-2W or LM-2W. Intranasally both GAS-2W and LM-2W induced primarily a Th17 response.

Notably, however, a larger fraction of the 2W:I-A^b-specific T cell population produced IL-17A following intranasal GAS-2W infection than following intranasal LM-2W infection (Fig. 2.6B) (Pepper et al., 2010). Furthermore, both GAS and LM primarily induced a Th1 response to intravenous inoculation but LM induced a significantly greater Th1 response than GAS (Fig. 2.6B). Therefore, the PAMPs expressed by or nature of GAS infections creates an environment more conducive to priming the Th17 phenotype than those of LM. Moreover, these data suggest that the 2W epitope does not influence the Th phenotype per se, since the same naïve 2W:I-A^b-specific $CD4^+$ T cell population has expanded and differentiated into different phenotypes in response to alternative routes of infection.

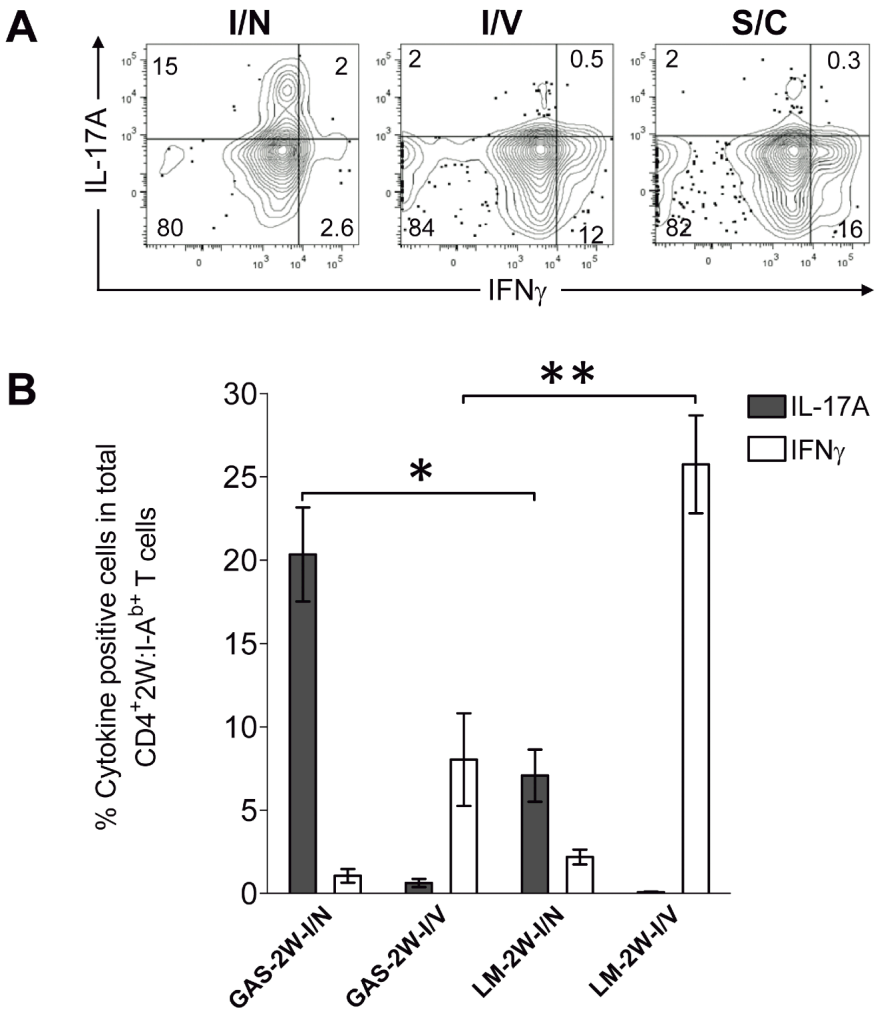

Figure 2.6. Route of inoculation determines the Th17 phenotype to GAS infection. (A) B6 mice were inoculated intranasally (I/N), intravenously (I/V) or subcutaneously (S/C) with HK-GAS-2W. After one week mice were restimulated in vivo with HK-GAS-2W for 4 hours and then $CD4^{+}CD44^{Hi}$2W:I-A^{b+} cells from spleen were stained for cytokines IL-17A and IFN-γ and analyzed by flow cytometry. (B) Comparison of the $CD4^{+}CD44^{Hi}$2W:I-A^{b+} T cell response to GAS-2W or *Listeria monocytogenes* (LM-2W) intranasal and intravenous infections. Three weeks after a single intranasal or intravenous inoculation with bacteria, single cell suspensions from spleens were incubated with PMA and ionomycin for 4 hrs. $CD4^{+}CD44^{Hi}$2W:I-A^{b+} cells were then enriched, stained and analyzed for IL-17A and IFN-γ expression by

flow cytometry. (n=7-12 mice per group). The bars represent the mean ± SEM. *= P < 0.002, ** = P < 0.001, Mann Whitney test.

IL-6-deficient Mice Fail to Develop a T_H17 Response and to Clear Group A Streptococci from NALT.

Although IL-6 is known to be critical for some Th17 responses in mice, it is not known whether this is the case for streptococcal infection. We therefore compared the primary T cell response to GAS infection of B6 IL-6 knockout mice *(IL-6 $^{-/-}$)* mice to age matched wild type B6 mice, inoculated intranasally with $2x10^8$ cfu of GAS-2W. There was no significant difference in the colonization of both groups of mice 24 hrs after inoculation with this sublethal dose of bacteria. However, over the next 7 days nearly a third of the *IL-6 $^{-/-}$* mice succumbed to infection (*P = 0.0473, Logrank Test) (Fig. 2.7). In contrast, wild-type B6 mice had no casualties and most had reduced their bacterial load in NALT. *IL-6$^{-/-}$* mice that survived infection continued to harbor high bacterial counts for up to 60 days; whereas, all wild-type mice completely cleared the bacteria from NALT by day 7.

IL-6$^{-/-}$ mice that survived the first week of infection returned to health even though they retained significant numbers of GAS-2W organisms in NALT. T cells from both wild-type and *IL-6$^{-/-}$* mice were restimulated *in vivo* after one week by intravenous injection of HK-GAS-2W. The 2W:I-A^{b+} cells from *IL-6$^{-/-}$* mice (Fig. 2.7A) had proliferated in response to infection with GAS-2W streptococci but failed to produce IL-17A. Instead, many of these cells produced IFN-γ (Fig. 2.7A). These results confirm that

IL-6 is required to promote a Th17 response after GAS infection. Long-term persistence of GAS-2W in NALT from *IL-6*$^{-/-}$ mice is consistent with the possibility that clearance from NALT and perhaps human tonsils requires a vigorous Th17 adaptive response and that IFN-γ^{+} T cells lack potential to eliminate streptococci from lymphoid tissue.

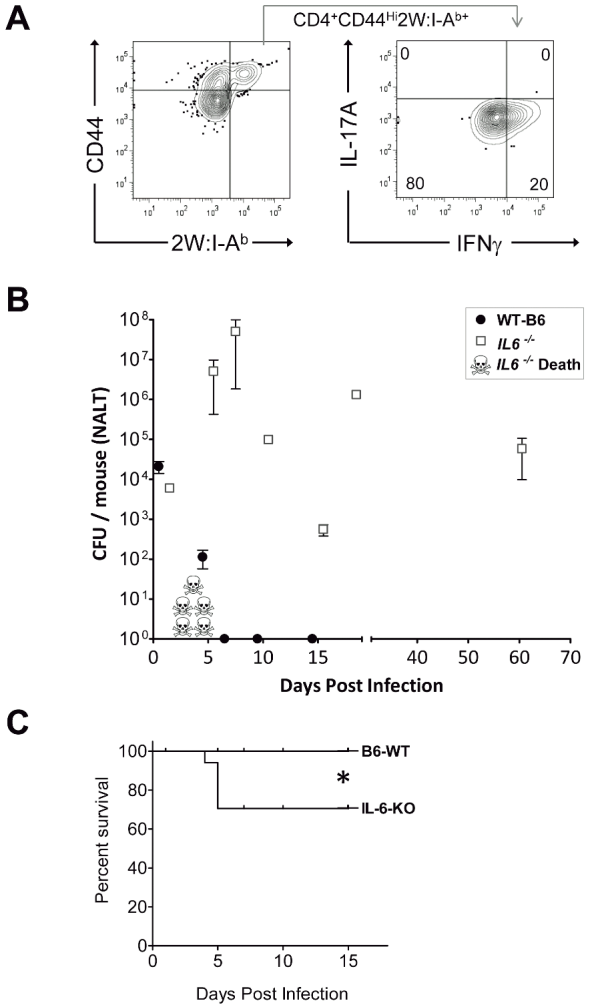

Figure 2.7. Mice deficient in Th17 cells fail to clear primary GAS infections from NALT and become chronic carriers. (A) Analysis of IL-17A and IFN-γ expression of CD4^{+}CD44^{Hi}2W:I-A^{b+} T cells from IL-6 knockout mice (*IL-6*$^{-/-}$) infected with GAS-2W. CD4^{+}CD44^{Hi}2W:I-A^{b+} cells were enriched from spleens of *IL-6*$^{-/-}$ mice that were intranasally inoculated with HK-GAS-2W and restimulated in vivo after a

week by IV injection of HK-GAS-2W. (B) Comparison of *IL-6*$^{-/-}$ mice (n=17) to age matched wild type B6 mice (n=14) for susceptibility to intranasal GAS infection. Mice were inoculated with 2 x10^8 CFU/mouse intranasally. Mice were euthanized at different time points after inoculation and CFU associated with NALT were assessed. Data are presented as mean CFU $\pm$ SEM. (C) Kaplan-Meier survival curve of *IL-6*$^{-/-}$ and WT-B6 mice (*P < 0.04, Logrank Test.)

Recurrent GAS Infection Shifts the Antigen-specific Population Toward an IL-17A$^+$ IFN-γ$^+$ Double Positive Phenotype in NALT.

The Th17 phenotype is less stable than the Th1 phenotype (Annunziato and Romagnani, 2010; Peck and Mellins, 2010; Pepper et al., 2010). For example, IL-17A$^+$ T cells were observed to acquire the capacity to produce IFN-γ *in vitro* by varying the cytokine environment (Lee et al., 2009). The regulatory program and precursor to these double positive T cells is unclear, as is the impact of infection on this phenotype. These considerations prompted experiments to test the influence of multiple intranasal infections on the Th17 population in NALT. Wild-type B6 mice usually clear GAS from NALT 5-7 days after an intranasal inoculation (Park et al., 2003). For recurrent infection, B6 mice were inoculated intranasally with 2x10^8 GAS-2W CFU at weekly intervals for 12 weeks. One week after the last inoculation cells were harvested from NALT, CLN and spleen, activated *in vitro* with PMA and ionomycin, and analyzed for intracellular cytokines IL-17A and IFN-γ. After repeated exposure to GAS-2W, IL-17A$^+$ IFN-γ$^+$ 2W:I-A^b-specific CD4$^+$ cells preferentially accumulated in the NALT, whereas the primary phenotype of CD4$^+$CD44^{Hi}2W:I-A^{b+} cells in spleen and CLN from the same mice retained a Th17 phenotype (Fig. 2.8A and 2.8B). More than 60% of CD4$^+$CD44^{Hi}2W:I-

A^{b+} cells were positive for both cytokines; whereas, fewer than 12% from spleens and cervical lymph nodes were double positive. The implications of this change will be discussed below.

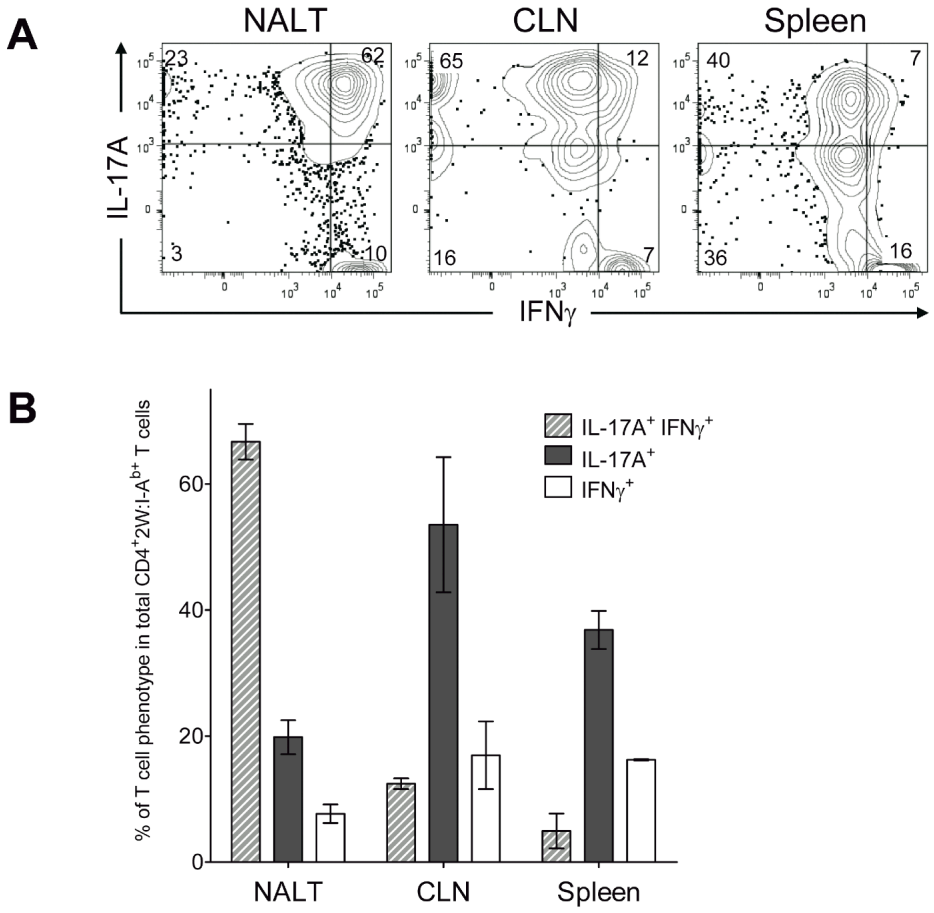

Figure 2.8. Recurrent GAS infection shifts the cytokine profile of $CD4^+$ 2W:I-A^{b+} T cells to IL-$17A^+$, IFN-γ^+ population in NALT. (A) B6 mice were inoculated intranasally with $2X10^8$ CFU at weekly intervals for 12 weeks. $CD4^+CD44^{Hi}$2W:I-A^{b+} T cells from Spleens, CLNs and NALT of infected mice were restimulated in vitro with PMA and ionomycin, stained and analyzed for IL-17A and IFN-γ and analyzed by flow cytometry. Representative result from one of two independent experiments is shown. (B) Pooled results of two independent experiments shown. (n=4)

2.4 Discussion

We recently discovered that GAS induces a polyclonal, TGF-β1 dependent Th17 response in intranasally infected mice. Moreover, adoptive transfer of $CD4^+$ IL-$17A^+$ T cells imparted partial protection to naïve mice against intranasal infection. That investigation raised several questions, which could be more definitively answered using pMHCII tetramers to quantify antigen specific T cells that recognize a streptococcal expressed antigen. In lieu of identifying immunodominant bacterial specific T cell epitopes, the surrogate 14 amino acid peptide 2W was fused to M1 protein and expressed on the streptococcal surface. The recombinant serotype M1 strain, GAS-2W, was constructed and M protein function confirmed by phagocytosis assays using human blood. Moreover, the GAS-2W strain colonized mouse NALT as efficiently as wild type 90-226 streptococci.

For unknown reasons, humans often fail to develop protective immunity after a single episode of pharyngitis or tonsillitis, and persistence of GAS in tonsils even after antibiotic intervention is common (Osterlund et al., 1997). This problem could be explained by failure to develop a sufficient Th17 immune response. However, we found that a single intranasal infection with GAS-2W rapidly induced a robust 2W:I-A^b-specific Th17 population, which paralleled the clearance of bacteria in mice. The 2W:I-A^b-specific Th17 population represented ~10 % of the total GAS specific Th17 induced (Fig. 2.4).

Superantigens are powerful mitogens that induce massive TCR V beta chain-specific clonal expansion of T cells. Group A streptococci, including the GAS-2W strain

are known to produce many superantigens, which have been implicated in highly lethal streptococcal toxic shock and autoimmune sequelae (Cunningham, 2008; Sriskandan et al., 2007). Such superantigens do not account for the expansion of 2W:I-A^b-specific $CD4^+$ T cells following GAS-2W infection, despite the fact that some of these T cells express the relevant TCR V beta chains (Moon et al., 2007). This conclusion may not reflect the situation during human infections because murine T cells are known to be relatively refractory to bacterial superantigens. Dominance of the Th17 response to GAS is impressive relative to that observed for other bacterial pathogens like Listeria. After a single infection 20-39% of the 2W-specific T cells produced IL-17A. By comparison, only about 5-12% of 2W:I-A^b-specific $CD4^+$ cells produced IL-17A in response to primary LM-2W intranasal infection (Fig.5, (Pepper et al., 2010)). Furthermore, both GAS and LM primarily induced a Th1 response to intravenous inoculation and as expected LM induced a more robust Th1 response than GAS (Fig. 2.6B). Therefore, GAS might have other features that make for more efficient Th17 induction than LM. Furthermore, these results suggest that the 2W epitope per se does not influence the out come of the $CD4^+$ T cell response. The more robust Th17 response could reflect the GAS tropism for NALT (Park et al., 2004) and human tonsils (Tart et al., 2007), the potential for these bacteria to induce TGF-β1 production in these sites (Wang et al., 2010), expression of a unique pathogen-associated molecular patterns (PAMPs), or a combination of these factors. GAS was shown to induce TGF-β1 and IL-6 in NALT (Wang et al., 2010), but the specific PAMPs that lead to expression of these cytokines are unknown. The substantial hyaluronic acid capsule or its degradation products are known

to induce TLR2- and TLR4-mediated inflammation (Jiang et al., 2005; Scheibner et al., 2006), and TLR2 agonists are known to promote Th17 differentiation (Reynolds et al., 2010). M1 protein is also a TLR2 agonist (Sigurdardottir et al., 2010) and known to induce inflammatory cytokines, including IL-6 (Pahlman et al., 2006) and TGF-β1 (Nishikawa et al., 2000), and is, therefore, another potential PAMP that could direct a Th17 response. The finding that intranasal inoculation, even with heat-killed GAS-2W cells induces an antigen-specific Th17 response, while other routes induce a Th1 response also has important implications for development and delivery of vaccines to protect against GAS and other mucosal pathogens. The pathogenic potential of IL-17A$^+$ T cells and their short half-life questions the potential safety and utility of intranasal vaccines.

We previously observed that single cell suspensions of NALT, spleen, and cervical lymph nodes from intranasally infected mice secrete TGF-β1, IL-6 and IL-17 upon *ex vivo* restimulation (Wang et al., 2010). Although IL-17 secretion was dependent on TGF-β1 receptor signals, dependence on IL-6 was not tested. As predicted (Korn et al., 2009), *IL-6*$^{-/-}$ mice failed to mount a Th17 response and instead developed IFN-γ$^+$ T cells following intranasal infection. As reported by Diao *et al*, we found high mortality in *IL-6*$^{-/-}$ mice infected with GAS (Diao and Kohanawa, 2005), perhaps as a consequence of exuberant TNF-α expression. Nearly a third of *IL-6*$^{-/-}$ mice, inoculated intranasally, developed lethal systemic infections; however, survivors fully recovered without subsequently developing systemic infections even though they retained large numbers of GAS in NALT (Fig. 2.7). This suggests that protection is compartmentalized, ie. opsonic

antibody is required to clear bacteria from blood, but does not efficiently remove them from NALT or tonsils. On the other hand a robust Th17 cellular response would be required to eliminate streptococci from those lymphoid organs. Secretory antibody that bathes mucosal surfaces may also protect against pharyngitis, but may not be able to reach bacteria sequestered within NALT. These findings are also consistent with studies of Th17 protection induced by intranasal infections of mice with encapsulated *S. pneumoniae* (Lu et al., 2008). It is theoretically possible that local activation of antigen specific T cells could recruit phagocytes with potential to ingest other unrelated bacteria at that site, but recruitment of phagocytes to those infectious foci would still be antigen specific. In addition, *IL-6*$^{-/-}$ mice developed a robust antigen specific Th1 response (Fig. 2.7) but failed to clear the bacteria from NALT. This finding is consistent with the observation that *IFN-γ*$^{-/-}$ mice (Hyland et al., 2009) cleared streptococci from NALT more rapidly than normal mice. We postulate that efficient elimination of GAS depends on IL-17A production by Streptococcal specific $CD4^+$ T cells to attract neutrophils to infected NALT, a capacity that IFN-γ-producing T cells lack. Persistence of large numbers of GAS in NALT of *IL-6*$^{-/-}$ mice is reminiscent of the situation in human immune carriers who may also fail to develop an adequate Th17 response.

The Th17 response is known to contribute to immune protection against infections by several pathogens (Conti et al., 2009; Ishigame et al., 2009; Lin et al., 2009; Lu et al., 2008; Wang et al., 2010); however, these T cells can also be pathogenic, as demonstrated in murine autoimmune models, such as experimental encephalomyelitis (EAE) (Aranami and Yamamura, 2008; Oukka, 2008). A potentially important discovery from our

experiments is that repeated intranasal exposure to GAS-2W results in the accumulation of an IL-17A^{+} IFN-γ^{+} (double positive) 2W:I-A^{b}-specific CD4^{+} T cells in NALT. In contrast, 2W:I-A^{b}-specific CD4^{+} T cells in CLN and spleens from the same mice predominantly retained the Th17 phenotype. Preferential accumulation of double positive T cells in NALT could be explained by a unique homing potential, by more rapid expansion or a longer half-life of double positive cells relative to those only able to produce IL-17A. Whether the large population of antigen-specific IL-17^{+} IFN-γ^{+} double positive cells observed in NALT following recurrent GAS infection is associated with an autoimmune response is unknown: however, repeated intranasal infection of mice was reported to occasionally produce endocarditis and valvular lesions(Stephen et al., 1998), suggesting a link to human autoimmune disease.

Chapter 3:

The Generation of Peptide:MHCII-specific T_H17 Cells in Response to Intranasal Bacterial Infection Requires IL-6 and Dendritic Cell-Produced TGF-β1

3.1 Introduction

T_H17 cells are a subset of $CD4^+$ helper T cells that orchestrate protective immunity to extracellular bacterial and fungal pathogens, predominantly at epithelial surfaces (Korn et al., 2009). TCR recognition of a pMHCII ligand on antigen presenting cells (APC) causes T_H17 cells to secrete the signature cytokine IL-17A, which has pro-inflammatory properties and acts primarily by increasing chemokine production in epithelial tissues to enable the recruitment, activation, and migration of neutrophils and monocytes (Korn et al., 2009). IL-17A also acts on many other cell types to induce the expression of cytokines, chemokines, antimicrobial peptides, and metalloproteinases (Korn et al., 2009).

Several studies have shown that T_H17 cells are preferentially generated by mucosal infections (Conti et al., 2009; Pepper et al., 2010; Woolard et al., 2008), while intravenous infections generate T_H1 cells. *In vitro* studies have shown that naive $CD4^+$ T cells differentiate into T_H17 cells when stimulated by pMHCII ligands in the presence of TGF-β1 and IL-6 (Betelli et al., 2006; Mangen et al., 2006; Veldhoen et al., 2006). Similarly, TGF-β1 is required for T_H17 differentiation during the induction of experimental autoimmune encephalomyelitis (EAE) (Li et al., 2007) and we found that IL-6 was required for the generation of T_H17 cells in response to intranasal infection with *Streptococcus pyogenes* (Dileepan et al., 2011). However, evidence exists that T_H17 cell

formation in the lamina propria of the small intestine does not depend on TGF-β1 (Ghoreschi et al., 2010), and requires IL-1β but not IL-6 (Shaw et al., 2012). In addition, Kuchroo and colleagues also reported that T_H17 differentiation was normally dependent on IL-6, but could occur in its absence through an IL-21-dependent pathway that operated when T_{REG} cells were depleted (Korn et al., 2007).

These findings suggest that the IL-6/TGF-β1-dependent pathway of T_H17 generation operates preferentially during intranasal infections. The extracellular, gram-positive bacterium Group A *Streptococcus pyogenes* (GAS) normally causes infections of the upper respiratory tract, which are controlled by T_H17 cells (Wang et al., 2010). We tracked GAS pMHCII-specific T cells during intranasal GAS infection to test the hypothesis that T_H17 cell formation is promoted by specialized dendritic cells that occupy the lymph nodes that drain the nasal mucosa. We found that GAS-induced T_H17 formation depended on IL-6 produced from hematopoietic cells. We also found that dendritic cell-produced TGF-β1 was important for GAS-induced T_H17 differentiation. Thus, the tendency of intranasal infection to induce T_H17 cells is related to cytokine production by specialized dendritic cells that drain this site.

3.2 Materials and Methods

Mice

Seven to eight-week-old C57BL/6 (B6), B6.SJL-Ptprca *Pep3b/BoyJ* (CD45.1), IL-$6^{-/-}$ (Kopf et al., 1994), 129;CF-1-*Rag2*^{tm1Fwa}*Tgfb1*^{tm1Doe} (*Tgfb1*-deficient) (Engle et al.,

1999), C57BL/6J-Tg(Itgax-cre,-EGFP)4097Ach/J (CD11c-Cre) (Stranges et al., 2007), B6.Cg-Tg(Cd4-cre)1Cwi/BfluJ (CD4-Cre) (Lee et al., 2001), and B6.129P2(Cg)-*Rorc*^{tm2Litt}/J (Eberl et al., 2004) mice were from the Jackson Laboratory or the National Cancer Institute. *Tgfb1*$^{f/f}$ (Li et. al. 2007) were obtained from D. Kaplan (University of Minnesota). *TgfbrII*$^{f/f}$ (Chytil et al., 2002) were obtained from S. Jameson (University of Minnesota). All mice were housed in specific-pathogen-free conditions in accordance with guidelines of the University of Minnesota and National Institutes of Health. The Institutional Animal Care and Use Committee of the University of Minnesota approved all animal experiments.

Bone Marrow Irradiation Chimeras

Bone marrow cells were harvested from femurs, tibias, and humeri. T cells were depleted from bone marrow cell suspensions with anti-Thy1.2 (30-H12, Bio X Cell) and low-toxicity rabbit complement (Cedarlane Laboratories). In some cases, CD45.1$^+$CD45.2$^+$ wild-type bone marrow cells were mixed in a 2:1 ratio with CD45.2$^+$ CD4-Cre, *TgfbrII*$^{f/f}$ bone marrow cells. 5–10x10^6 total bone marrow cells were injected into lethally irradiated (1,000 rads) CD45.1$^+$ mice.

Infections

Mice were injected intranasally or intravenously with $2x10^8$ GAS-WT or GAS-2W expressing *Streptococcus pyogenes* bacteria as previously described (Dileepan et. al. 2011).

***In Vivo* Stimulation with Heat-killed GAS-2W**

GAS-2W was grown in THB-Neo media to $O.D._{600}$ of 0.5, washed once with PBS, pelleted and resuspended in appropriate volume of PBS and incubated at 60C for 30 minutes. Viability of bacteria was confirmed by plating out on blood agar plates. Heat-killed GAS-2W was stored in aliquots at -20C until use. To induce cytokine production by 2W:I-A^b-specific $CD4^+$ T cells *in vivo*, 5 X 10^8 CFU heat-killed GAS-2W in 100 µl of PBS was inoculated intravenously through tail vein. Mice were sacrificed after 3hrs and single cell suspensions of spleen were made in cEHAA medium supplemented with BrA.

Cell Enrichment and Flow Cytometry

All antibodies were from eBioscience unless noted. Spleen and lymph node cells were prepared and stained for 1 hr at room temperature with 2W:I-Ab-streptavidin-allophycocyanin tetramers. Samples were then enriched for bead-bound cells on magnetized columns and a portion was removed for counting as described (Moon et al.,

2007). For identification of surface phenotype, the rest of the sample underwent surface staining on ice with a mixture of antibodies specific for B220 (RA3-6B2), CD11b (MI-70), CD11c (N418), CD8a (5H10; Caltag), CD4 (RM4-5), CD3ε (145-2C11), CD44 (IM7), CCR6 (140706), CD69 (H1.2F3), CD45.1 (A20), and/or CD45.2 (104), each conjugated with a different fluorochrome. In experiments designed to detect cytokines, the cells were surface stained, then treated with BD Cytofix/Cytoperm (Becton Dickinson) for 20 minutes and stained for 1 hour on ice with antibodies against IL-17A (TC11), IFN-γ (XMG1.2), IL-17F (18F10), IL-22 (1H8PWSR), IL-10 (JES5-16E3), and IL-2 (JES6-5H4) in Perm Wash solution (Becton Dickinson). In all cases, cells were then analyzed on an LSR II or Fortessa (Becton Dickinson) flow cytometer. Data were analyzed with FlowJo software (TreeStar).

Cell Transfer

For wild-type B6 $CD4^+$ T cell transfer experiments, spleen and lymph node cells were isolated from naïve $CD45.1^+$ B6 mice and negatively selected over magnetic columns ($CD4^+$ T cell isolation kit, Miltenyi). One mouse equivalent of >95% pure $CD4^+$ cells were then injected intravenously per $CD45.2^+$ recipient, which were then infected one day later intranasally with $2x10^8$ GAS-2W bacteria. Seven days later, the phenotype of 2W:I-A^b-specific T cells was determined after tetramer-based cell enrichment as described above.

Cell Enrichment and qRT-PCR

Tissues were isolated from naïve or GAS-2W infected mice and digested with Collagenase D (Roche). $CD11c^+$ cells were enriched over magnetic columns ($CD11c^+$ microbeads, Miltenyi). RNA was isolated (RNeasy column, Qiagen), DNase digested (Turbo DNA-free kit, Ambion), and cDNA was made (High-capacity cDNA reverse transcription kit, Applied Biosystems). Quantitative reverse transcription polymerase chain reaction was run using taqman primers (Taqman gene expression assays: *Il6*-Mm00446190_m1, *Tgfb1*-Mm01178820_m1, *Hprt*-Mm00446968_m1; Taqman universal master mix II, Applied Biosystems)

Statistical Analysis

Differences between two data sets were analyzed by a paired or unpaired two-tailed Student's t test with Prism (Graphpad) software.

3.3 Results

Detection of pMHCII-specific $CD4^+$ T cells

We used a p:MHCII tetramer-based approach to track $CD4^+$ T cells specific for a peptide called 2W bound the I-A^b MHCII molecule of C57BL/6 (B6) mice during

intranasal GAS infection. The 2W peptide is a variant of a similar peptide from the I-Eα chain but contains 2 tryptophan substitutions at TCR contact positions that increase its immunogenicity (Rees et al., 1999). GAS bacteria were engineered to express the 2W peptide fused to the cell wall surface-anchored M1 protein (Dileepan et al., 2011). The GAS-2W bacteria cause the same transient intranasal infection that was eliminated 7 days after inoculation as wild-type GAS organisms (Dileepan et al., 2011). $CD4^+$ T cells expressing TCRs specific for 2W:I-A^b complexes were detected by staining spleen and lymph node cells from individual mice with fluorochrome-labeled 2W:I-A^b tetramers and anti-fluorochrome magnetic beads followed by enrichment of the tetramer-bound cells on magnetized columns (Moon et al., 2007). The cells that bound to the column were stained with antibodies specific for the TCR (CD3e) and a mixture of non-T cell lineage-specific markers to aid in identification of genuine T cells.

We first analyzed the clonal expansion of 2W:I-A^b-specific $CD4^+$ T cells in response to intranasal (i.n.) GAS-2W infection. Uninfected B6 mice contained a small population of about 250-300 primarily $CD44^{low}$ 2W:I-A^b tetramer-binding cells (Fig. 3.1A). The sample contained little to no $CD8^+$ 2W:I-A^b tetramer-binding cells indicating that $CD4^+$ T cells bound this MHCII tetramer via the TCR (Fig. 3.1A). Mice infected i.n. 7 days earlier with the non-engineered, parental strain of GAS (GAS-WT) also contained about 300 naive $CD44^{low}$ 2W:I-A^{b+} $CD4^+$ cells (Fig. 3.1B). However, mice infected i.n. 7 days earlier with GAS-2W, the peak of clonal expansion for 2W:I-A^b-specific $CD4^+$ T cells induced after this infection (Dileepan 2011), contained a large population of $CD44^{high}$ 2W:I-A^{b+} $CD4^+$ T cells in the spleen and lymph nodes that could still be

detected more than 200 days past infection (Fig. 3.1B).

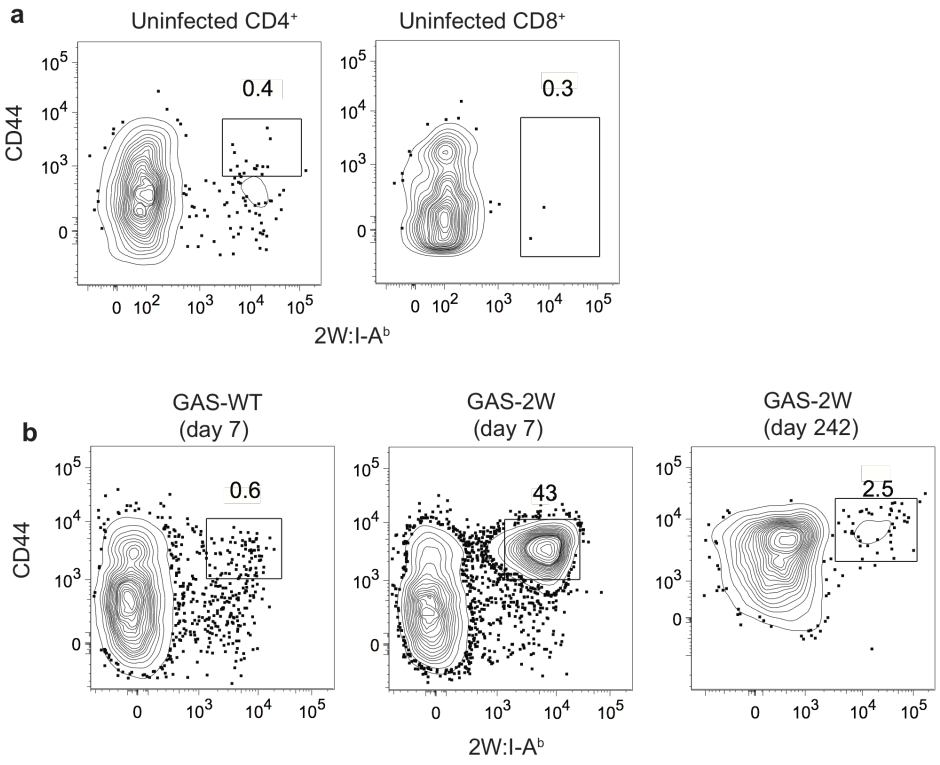

Fig 3.1. Infection with GAS-2W induces the clonal expansion of 2W–I-A^{b}–specific cells. Flow cytometry to identify CD4^{+} or CD8^{+} T cells in enriched fractions, for events gated on CD11c^{-}CD11b^{-} B220^{-}CD3^{+} cells. (a) CD4^{+} T cells (left) or CD8^{+} T cells (right) from an uninfected B6 mouse with gates on CD44^{hi} 2W–I-A^{b+} (left) or all 2W–I-A^{b+} cells (right). (b) CD4^{+} T cells in enriched samples from a B6 mouse 7 d after intranasal infection of GAS-WT (left) or 7 d (middle) or 242 d (right) after intranasal infection of GAS-2W. Numbers above outlined areas indicate percent cells in gate. Data are representative of five independent experiments.

Intranasal Infection with GAS-2W Induces a 2W:I-A^b-specific T_H17 Response

To test for induction of T_H17 cells, we measured lymphokine production by 2W:I-A^b-specific $CD4^+$ cells by direct *ex vivo* intracellular staining (Khoruts et al., 1998) in mice that were i.n. infected 7 days before with GAS-2W and then challenged intravenously for 3 hours with heat-killed GAS-2W or GAS-WT (hk-GAS-2W or hk-GAS-WT) (Dileepan et al., 2011). We found that none of the 2W:I-A^b-specific cells expressed CD69 or produced IL-17A or IFN-γ after challenge with GAS-WT (Fig. 3.2A,B). However, 10-30% of the cells produced IL-17A after challenge with hk-GAS-2W (Fig. 3.2A), whereas none of these cells produced IFN-γ (Fig. 3.2B) or IL-4 (data not shown). A similar result was obtained following stimulation of spleen and lymph node cells from day 7 infected mice *in vitro* with the soluble TCR signal mimics phorbol 12-myristate 13-acetate and ionomycin (data not shown), indicating that the *in vivo* challenge technique was optimal. The failure of the majority of 2W:I-A^b-specific $CD4^+$ cells to make IL-17A after challenge was not solely due to a lack of 2W:I-A^b recognition after challenge, as many of the cells expressed the TCR signal-dependent CD69 molecule but did not make IL-17A (Fig. 3.2A). Therefore, about one fifth of the 2W:I-A^b-specific $CD4^+$ cells induced by intranasal infection resembled T_H17 cells, whereas the remainder did not produce any T_H1, T_H2, or T_H17 related cytokines.

To place the T_H17 cells in the context of other T_H17 "subtypes" that have been recently described (Rutz et al., 2011; Zielinski et al., 2012), we investigated what other T_H17-associated cytokines these cells expressed. GAS-2W-induced 2W:I-A^b-specific $CD4^+$ cells that produced IL-17A also produced IL-2, IL-22, and IL-17F (Fig. 3.2C) but

not IL-10 (data not shown). This places T_H17 cells induced by intranasal GAS infection under a more "classical" T_H17 cytokine profile (Bettelli et al., 2008).

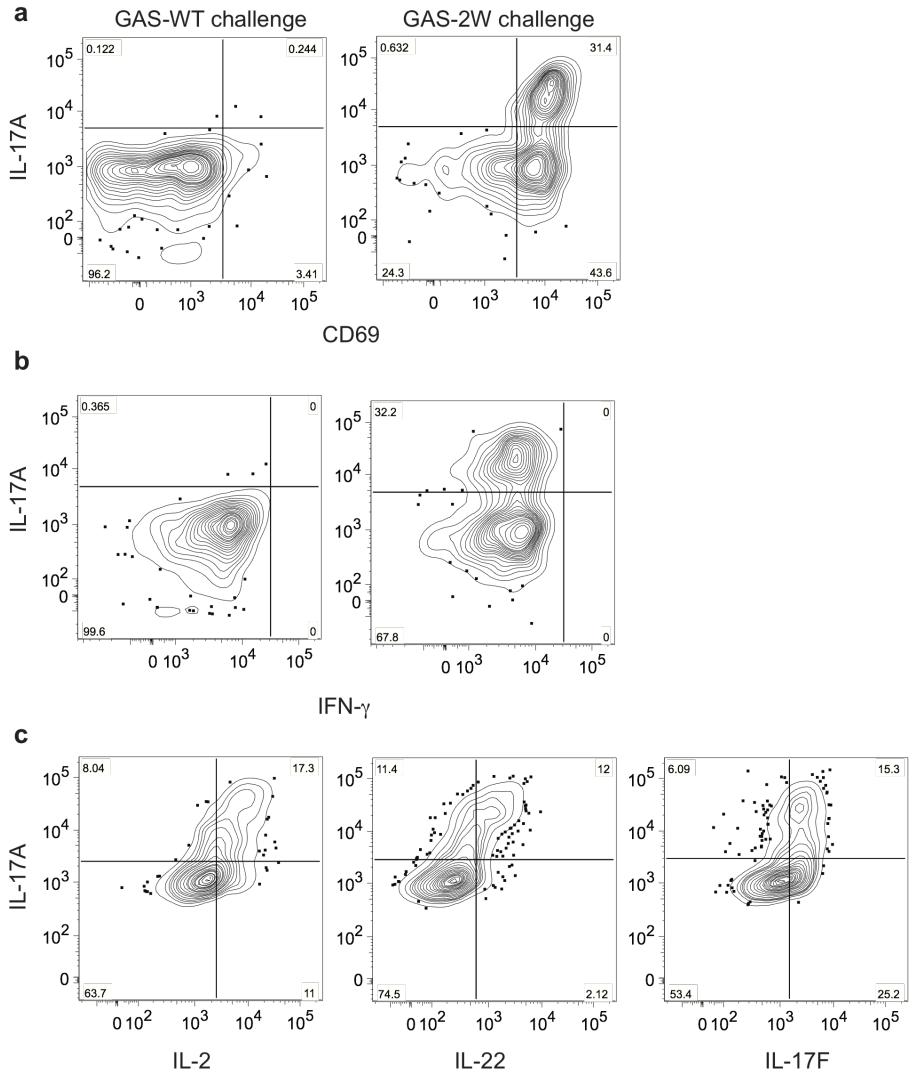

Figure 3.2. Lymphokine production by 2W–I-A^b–specific CD4$^+$ T cells. (a,b) Expression of CD69 (a) or IL-17A (a,b) and IFN-γ production (b) by 2W–I-A^b–specific T cells 3 h after intravenous heat-killed challenge of mice (a,b) with GAS-WT (left) or GAS-2W (right). Numbers in quadrants indicate percent of cells in each. (c) Expression of IL-17A and IL-2, IL-22, or IL-17F by 2W–I-A^b–specific T cells

3 h after intravenous challenge of mice with GAS-2W. Data are representative of three (a,b) or two (c) independent experiments.

Route of Infection Determines T_H17 and T_H1 Subset Differentiation

We next sought to determine whether the T_H17 differentiation induced by GAS infection was a result of bacterial determinants (i.e.-pathogen associated molecular patterns) or the route of infection. Mice were infected i.n. or intravenously (i.v.) with GAS-2W and challenged 7 days later with hk-GAS-2W or 2W:I-A^b-specific T cell to elicit cytokine production by the effector cells. About 20% of the 2W:I-A^b-specific T cells from mice that had been infected i.n. produced IL-17A and none produced IFN-γ. However, cells from mice that were infected i.v. produced no IL-17A, whereas ~10% produced IFN-γ (Fig. 3.3). This result indicates that the lymphoid environment plays a primary role in determining whether a $CD4^+$ T cell will differentiate down the T_H17 lineage. The same response was observed after immunization with hk-GAS-2W by both routes, indicating that the $CD4^+$ T cell response is not a result of route-dependent antigen expression by GAS-2W (data not shown).

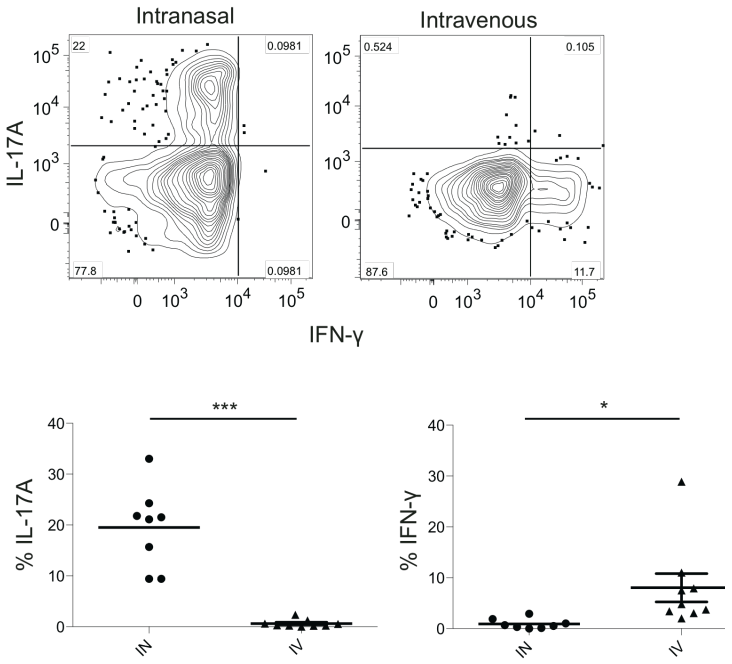

Figure 3.3 Intranasal infection induces IL-17A-producing, while intravenous infection induces IFN-γ-producing 2W:I-A^b-specific CD4$^+$ cells. Cytokine expression by 2W–I-A^b–specific T cells 3 h after intravenous heat-killed GAS-2W challenge of mice previously infected intranasally with GAS-2W. ***$P < 0.0005$, *$P < 0.05$ (unpaired two-tailed Student's *t*-test). Data are representative of three independent experiments.

Anatomy of 2W:I-A^b-specific T_H17 Response to i.n. GAS-2W Infection

The preferential induction of T_H17 cells after intranasal infection indicated that there was something special in this regard about one of the secondary lymphoid organs associated with this site. We focused first on the NALT, a secondary lymphoid organ that is functionally equivalent to human tonsils, which is the primary site of infection after i.n. GAS inoculation (Park et al., 2003). Notably, however, 2W:I-A^b-specific T cells were not detected in the NALT before infection or for up to 5 days after infection. In contrast,

naive 2W:I-A^b-specific T cells were detected in the CLN and spleen. Beginning at day 3 after infection, some of the 2W:I-A^b-specific cells in CLN, but not the spleen had increased CD44 and become blasts, indicating activation began in the CLN. About 15% of the 2W:I-A^b-specific T cells in CLN on day 3 expressed the T_H17 master regulator transcription factor RORγt and the T_H17-associated chemokine receptor CCR6 indicating that T_H17 differentiation had also begun at this time (Fig. 3.4). By day 4 after i.n. GAS-2W infection, the 2W:I-A^b-specific T cells in the CLN had increased dramatically in number and some were still blasts (Fig. 3.4). At this time, $CD44^{high}$ 2W:I-A^b-specific T cells appeared in the spleen. However, these cells were not blasts suggesting that they were activated in the CLN then migrated to the spleen. Beginning on day 5 after infection, non-blasting $CD44^{hi}$ 2W:I-A^b-specific T cells, about 60% expressing RORγt, finally appeared in the NALT and accumulated in this location to a peak number on day 7 (Fig. 3.4). Together, these results indicated that naive 2W:I-A^b-specific T cells were first activated in the CLN after intranasal GAS-2W infection, then proliferated, differentiated into T_H17 cells, and migrated to the spleen and NALT.

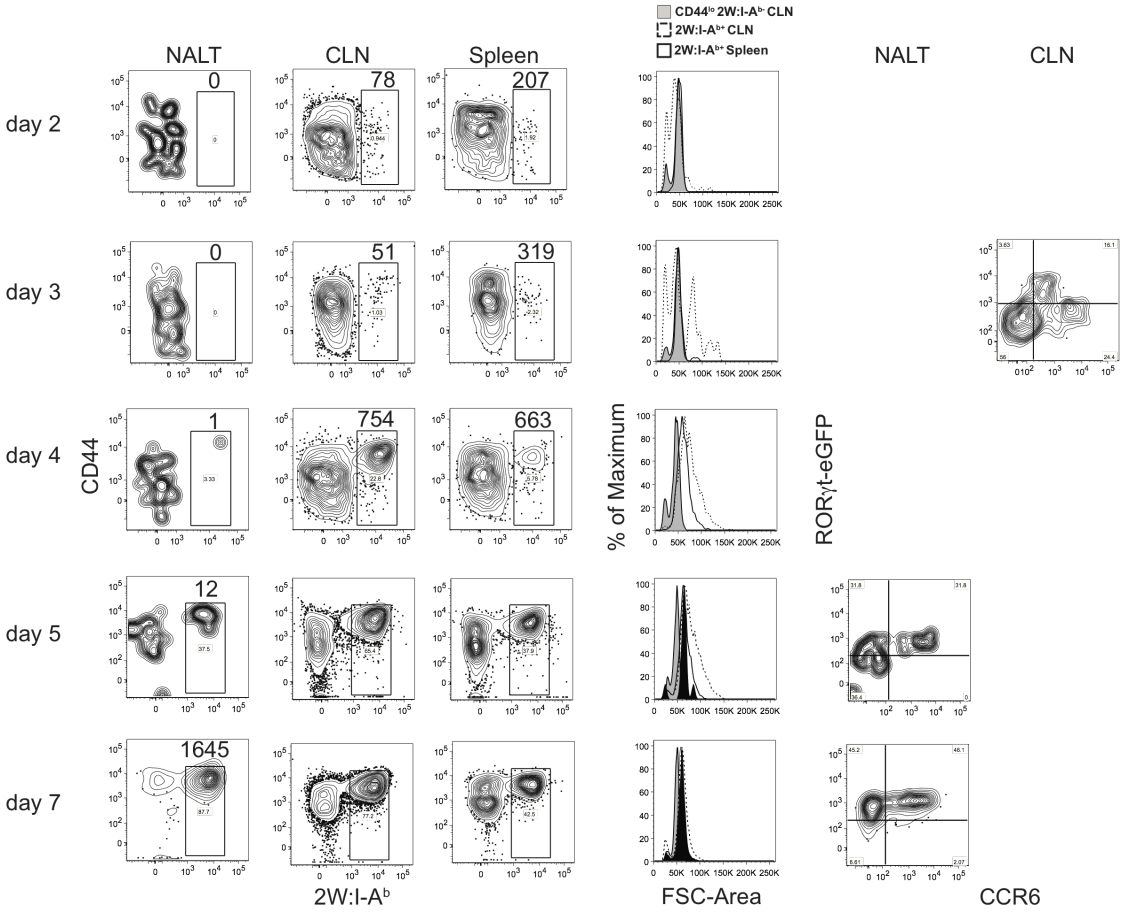

Figure 3.4. 2W:I-A^b-specific cells are activated and differentiate into T_H17 cells in the CLNs after intranasal GAS-2W infection. Mice were infected and tissues were enumerated for 2W:I-A^b-specific T cells at various times thereafter. For NALT and CLNs, three mice were pooled per sample, for spleen, one mouse per sample. Data are representative of three independent experiments.

IL-6 is Necessary for T_H17 Differentiation in Response to i.n. GAS-2W Infection

Having identified the i.n. route as a mucosal environment important for the differentiation of T_H17 cells *in vivo*, we sought to identify the factors necessary to induce this differentiation.

We first focused on IL-6, as this was one of the first cytokines to be described,

along with TGF-β1, as being sufficient to drive T_H17 differentiation *in vitro* (Betelli et al., 2006; Mangen et al., 2006; Veldhoen et al., 2006). Recently, we identified the necessity for IL-6 for T_H17 differentiation after i.n. GAS-2W infection and reported that the majority of *Il-6*$^{-/-}$ mice inoculated i.n. with GAS-2W die or develop a persistent infection (Dileepan et al., 2011). We investigated this issue by giving *Il-6*$^{-/-}$ mice hk-GAS-2W intranasally to ensure that the mice survived until completion of the experiment. Seven days later, about 20% of 2W:I-A^b-specific T cells from inoculated wild-type B6 mice produced IL-17A and none produced IFN-γ, while comparable cells from *Il-6*$^{-/-}$ mice produced no IL-17A and about 10% produced IFN-γ (Fig. 3.5A). The loss of IL-17A production by 2W:I-A^b-specific cells in IL-6-deficient mice was not accompanied by a gain in Foxp3$^+$ cells as reported in the EAE model (data not shown) (Korn et al., 2007). Therefore, IL-6 was necessary for T_H17 differentiation and suppression of Th1 but not T_{REG} cell production after i.n. GAS-2W infection.

We next sought to identify which cell type produced the IL-6 needed during this infection for T_H17 differentiation. The literature suggested that hematopoietic or non-hematopoietic cells could be involved. (Harker et al., 2011). These possibilities were assessed using radiation bone marrow chimeras in which IL-6 was produced by hematopoietic or non-hematopoietic cells. Chimeras were inoculated i.n. with GAS-2W and evaluated for cytokine production 7 days later. About 13% of the CD44^{high} 2W:I-A^b-specific T cells in control chimeras produced by transplanting wild-type bone marrow cells into irradiated wild-type recipients produced IL-17A and none produced IFN-γ (Fig. 3.5B). The same was true for mice in which wild-type bone marrow cells were

transplanted into IL-6-deficient recipients. However, wild-type mice transplanted with IL-6-deficient bone marrow contained 2W:I-A^b-specific T cells that produced little to no IL-17A and instead had a few cells that produced IFN-γ (Fig. 3.5B). Therefore, hematopoietic cells were the source of IL-6 necessary for T_H17 differentiation after i.n. infection with GAS-2W bacteria.

The early generation of T_H17 cells in the CLN implicated dendritic cells in this location as candidate sources of IL-6. Dendritic cell expression of the *Il6* gene was measured by quantitative reverse transcriptase-polymerase chain reaction (qRT-PCR) to address this possibility. The analysis was performed on RNA from $CD11c^+$ cells from B6 mice before and 3 days after i.n. or i.v. GAS-2W infection (Fig. 3.5C). Dendritic cells in the NALT, but not the CLN and spleens of uninfected mice contained high basal expression of *Il6* transcripts. However, *Il6* transcripts increased 2-3-fold in $CD11c^+$ cells in the CLN and NALT, but not the spleen 3 days after i.n. GAS-2W infection (Fig. 3.5C). *Il6* gene expression was also not induced in $CD11c^+$ cells in the spleen after i.v. GAS-2W infection. These results suggest that infection induced expression of IL-6 by $CD11c^+$ cells in the NALT and/or CLN, but not the spleen, is a primary factor driving T_H17 differentiation after intranasal infection.

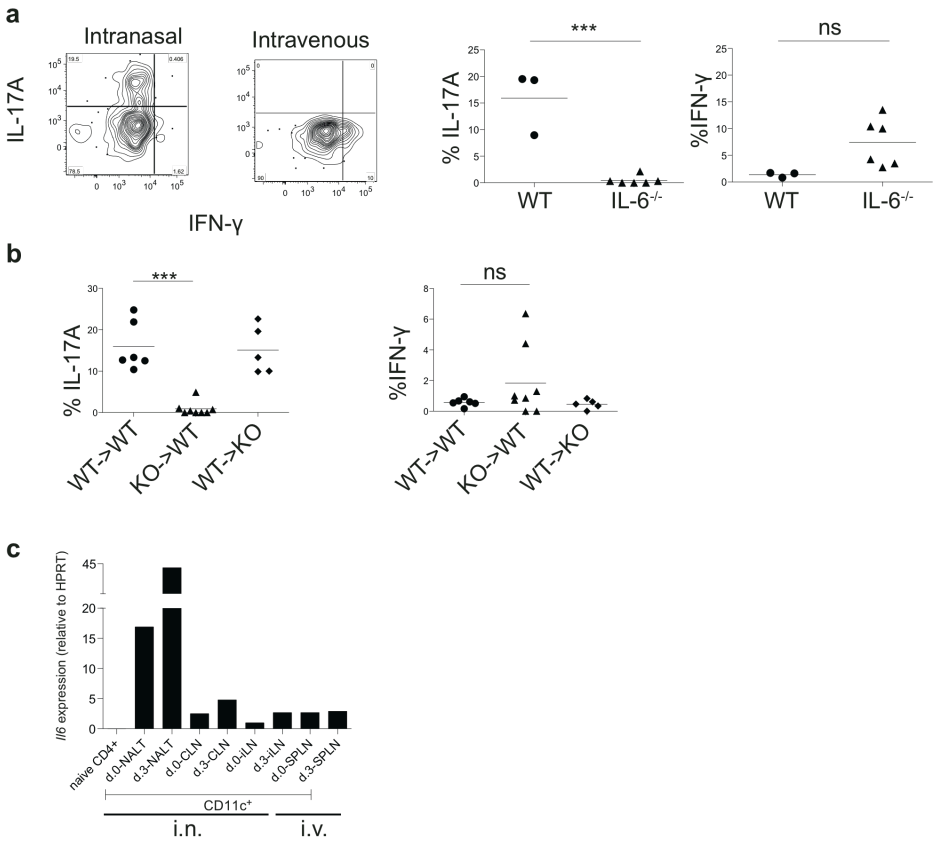

Figure 3.5. Hematopoietic cell derived IL-6 is necessary for 2W:I-A^{b}-specific T$_{H}$17 differentiation after intranasal GAS-2W infection. (a,b) Cytokine expression by 2W–I-A^{b}–specific T cells 3 h after intravenous heat-killed GAS-2W challenge of (a) wild-type or IL6$^{-/-}$ mice and (b) bone marrow chimeras composed of wild-type or IL6$^{-/-}$ donor marrow previously infected intranasally with GAS-2W. ***$P < 0.0005$ (unpaired two-tailed Student's *t*-test). (c) qRT-PCR for *Il6* relative to *Hprt* from magnetically enriched CD11c^{+} cells from various tissues of uninfected or GAS-2W day 3 intranasally infected wild-type mice. Each sample composed of three pooled mice. Data are representative of three independent experiments.

TGF-β1 is Necessary for T_H17 Differentiation in Response to i.n. GAS-2W Infection

We next sought to determine the role of TGF-β1 in T_H17 differentiation after i.n. GAS-2W infection. Although, the requirement of this cytokine for T_H17 differentiation *in vitro* is well established (Betelli et al., 2006; Mangen et al., 2006; Veldhoen et al., 2006), its role *in vivo* is controversial. Flavell and colleagues reported that T cell produced TGF-β1 was necessary for T_H17 differentiation *in vivo* in the EAE model, while O'Shea and colleagues showed that TGF-β1 is dispensable for the development of gut Th17 cells (Li et al., 2007; Goreschi et al., 2011).

The role of TGF-β1 in Th17 differentiation induced by intranasal GAS infection was first studied using a radiation bone marrow chimeras containing a mixture of wild-type T cells, and T cells lacking the TGF-β1 receptor II. On day 7 after i.n. GAS-2W infection, about 12% of the wild-type 2W:I-A^b-specific cells produced IL-17A following challenge with hk-GAS-2W, whereas the TGF-β1receptor II-deficient T cell population lacked IL-17A producing cells and instead contained a population of ~10% IFN-γ producing cells (Fig 3.6A). Therefore, TGF-β1 signaling to $CD4^+$ T cells is necessary for T_H17 differentiation after i.n. GAS-2W infection.

We next determined the cellular source of TGF-β1 necessary for T_H17 differentiation under these conditions using radiation bone marrow chimeras in which TGF-β1 was produced by hematopoietic or non-hematopoietic cells. After immune reconstitution, chimeric mice were infected i.n. with GAS-2W bacteria and then cytokine production was measured on day 7 after challenge with hk-GAS-2W. About 20% of the $CD44^{high}$ 2W:I-A^b-specific T cells in chimeras produced by transplanting wild-type bone

marrow cells into irradiated wild-type or TGF-β1-deficient recipients produced IL-17A but not IFN-γ (Fig. 3.6B). In contrast, the 2W:I-A^b-specific T cells in chimeras produced by transplanting TGF-β1-deficient bone marrow into irradiated wild-type mice did not produce IL-17A and about 10 % produced IFN-γ (Fig. 3.6B). Therefore, hematopoietic cells are the source of TGF-β1 required for T_H17 differentiation after i.n. GAS-2W infection.

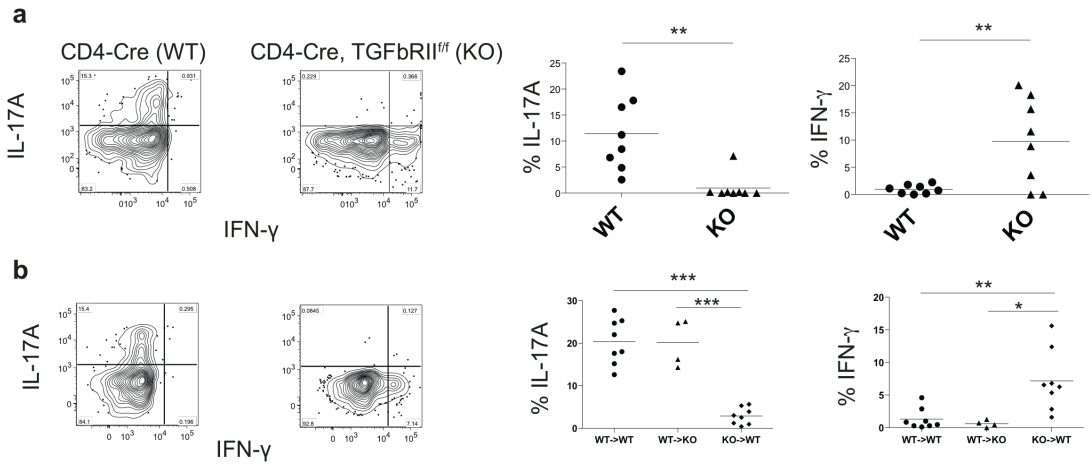

Figure 3.6. Hematopoietic cell derived TGF-β1 is necessary for 2W:I-A^b-specific T_H17 differentiation after intranasal GAS-2W infection. (a,b) Cytokine expression by 2W–I-A^b–specific T cells 3 h after intravenous heat-killed GAS-2W challenge of (a) CD4-Cre^+ or CD4-Cre^+, *Tgfbrll*$^{f/f}$ mice and (b) bone marrow chimeras composed of wild-type or *Tgfb1*$^{-/-}$ donor marrow previously infected intranasally with GAS-2W. ***$P < 0.0005$, **P<0.005, *P<0.05 (unpaired two-tailed Student's *t*-test). Data are representative of three independent experiments.

CD11c$^+$ Produced TGF-β1 is Necessary for T_H17 Differentiation in Response to i.n. GAS-2W Infection

Other studies suggested that the likely hematopoietic sources of TGF-β1 were autocrine from CD4$^+$ T cells (Gutcher et al., 2011) or paracrine from dendritic cells (Iwasaki and Kelsall, 2001). The latter possibility was tested in CD11c-Cre x *Tgfb1*$^{f/f}$ mice in which the *Tgfb1* gene was disrupted in CD11c$^+$ cells. These mice or CD11c-Cre control mice were infected i.n. with GAS-2W bacteria and then challenged with hk-GAS-2W on day 7 to elicit cytokine production by 2W:I-A^b-specific T cells. As expected, about 30% of the 2W:I-A^b-specific effector cells produced IL-17A and few if any produced IFN-γ producing cells in control mice (Fig. 3.7A). The population of 2W:I-A^b-specific T cells in mice lacking the *Tgfb1* gene in CD11c$^+$ cells contained significantly fewer IL-17A-producing cells than the control mice (10%) and also contained some IFN-γ producing (8%) cells, indicating that CD11c$^+$ cells were important contributors of TGF-β1 for T_H17 differentiation (Fig. 3.7A). Since some T_H17 differentiation still occurred in mice lacking TGF-β1 in dendritic cells, other sources of this cytokine must also contribute.

A potential confounding factor to this experiment was identified when we crossed CD11c-Cre$^+$ x *Tgfb1*$^{f/f}$ mice to *Rosa26*-stopflox-eYFP reporter mice. Although eYFP was expressed by all CD11c$^+$ cells as expected, 10-40% of the T and B cell cells in these mice also expressed eYFP (Fig. 3.7B). Similar reporter expression in T and B cells was described in an independently created CD11c-Cre x *Rosa26*-stopflox-eYFP transgenic mouse (Caton et al., 2007). This result is likely explained by transient expression of

CD11c at some point during T and B cell development. However, it raised the possibility that TGF-β1 deficiency in T cells caused the defects in Th17 differentiation observed in CD11c-Cre x *Tgfb1*$^{f/f}$ mice.

Adoptive transfer of congenically-marked wild-type CD4$^+$ T cells into mice lacking TGF-β1 in CD11c$^+$ cells was performed to address this issue. The transferred 2W-I-A^b-specific effector T cell population generated by GAS-2W infection in CD11c-Cre recipient mice contained a subset of about 20% that produced IL-17A, while no cells produced IFN-γ following challenge with hk-GAS-2W (Fig. 3.7C). In contrast, only 5% of the transferred 2W-I-A^b-specific T cell population in CD11c-Cre x *Tgfb1*$^{f/f}$ mice produced IL-17A and a few cells even made IFN-γ. The fact that wild-type CD4$^+$ T cells had reduced T_H17 differentiation after i.n. GAS-2W infection in mice lacking TGF-β1 in CD11c$^+$ cells indicated that TGF-β1 was likely derived as a paracrine source from dendritic cells and not an autocrine source from T cells in this system. However, this result does not exclude the possibility that T cells could be producing TGF-β1 in a paracrine manner.

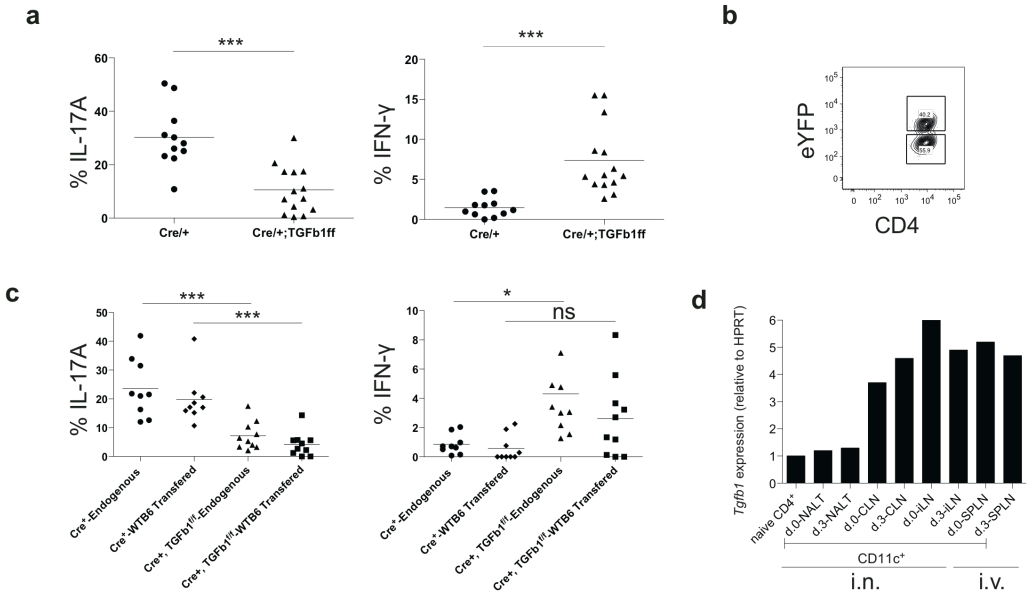

Figure 3.7. Dendritic cell derived TGF-β1 is necessary for 2W:I-A^{b}-specific T$_{H}$17 differentiation after intranasal GAS-2W infection. (a,c) Cytokine expression by 2W–I-A^{b}–specific T cells 3 h after intravenous heat-killed GAS-2W challenge of (a) CD11c-Cre^{+} or CD11c-Cre^{+}, *Tgfb1*$^{f/f}$ mice and (c) purified total wild-type CD4^{+} T cells adoptively transferred into CD11c-Cre^{+} or CD11c-Cre^{+}, *Tgfb1*$^{f/f}$ hosts previously infected intranasally with GAS-2W. ***P < 0.0005, *P<0.05 (unpaired two-tailed Student's *t*-test). (b) eYFP expression by total CD4^{+} T cells in CD11c-Cre^{+}, *Tgfb1*$^{f/f}$, *Rosa26*^{stopflox}-eYFP mice. (d) qRT-PCR for *Tgfb1* relative to *Hprt* from magnetically enriched CD11c^{+} cells from various tissues of uninfected or GAS-2W day 3 intranasally infected wild-type mice. Each sample composed of three pooled mice. Data are representative of three independent experiments.

To determine whether $CD11c^+$ cells produced TGF-β1 in response to infection, qRT-PCR was performed on cDNA isolated from purified $CD11c^+$ cells from various tissues before and after i.n. GAS-2W infection (Fig. 3.7D). Low amounts of *Tgfb1* transcripts were observed in $CD11c^+$ cells in the NALT before and after i.n. infection. $CD11c^+$ cells in the CLN expressed four times higher amounts of *Tgfb1* transcripts than $CD11c^+$ cells in the NALT, but again these amounts did not change after i.n. infection. *Tgfb1* transcripts were also detected in the spleen at the same level before and after i.v. infection (Fig. 3.7D). These results suggest that TGF-β1 is expressed constitutively at different levels in different secondary lymphoid organs and does not change after i.n. GAS-2W infection. Therefore, preferential TGF-β1 expression in $CD11c^+$ cells in the NALT or CLN is not a likely explanation for the tendency of the i.n route of infection to induce Th17 cells.

3.4 Discussion

Our results indicate that infections of nasal mucosa drive Th17 differentiation due to early effects of specialized dendritic cells in the secondary lymphoid organs that collect material from these sites. A previous study showed that i.n. GAS infection resulted in the early activation of adoptively transferred TCR transgenic $CD4^+$ T cells in the NALT, which directly samples the contents of the nasal mucosa (Park et al., 2004). It was therefore surprising to find that the earliest activation of endogenous 2W:I-A^b-specific $CD4^+$ T cells after i.n. GAS-2W infection occurred in the CLN not the NALT. The lack of early activation in the NALT was likely due to a limitation in the T cell

repertoire in this small secondary lymphoid organ. 2W:I-A^b-specific T cells exist in the pre-immune repertoire at a frequency of about 10 cells per million $CD4^+$ T cells (Jenkins and Moon, 2012). Since the murine NALT contains fewer than 1 million $CD4^+$ T cells, it is possible the NALT of many mice did not contain any 2W:I-A^b-specific T cells at the time of infection. In contrast, adoptive transfer of a large number of naive TCR transgenic T cells ensures that these cells are always present in the NALT. The fact that the TCR transgenic T cells became activated very early after i.n. infection showed that dendritic cells in this location produce GAS p:MHCII ligands. However, in the normal situation, dendritic cells that take up bacteria in the NALT or nasal submucosa and migrate to the CLN, or take up bacteria in the CLN directly, may initiate the T cell response in the CLN because enough relevant naive T cells are located in or circulate through this site.

GAS p:MHCII-specific Th17 cells were detected in the CLN as early as 3 days after i.n. GAS infection, indicating that this is the initial site of Th17 differentiation. Our results suggest that the dendritic cells in the CLN drive Th17 differentiation because of IL-6 and TGF-β1 production. These dendritic cells may have migrated from the NALT, which contained the dendritic cells that produced *Tgfb1* mRNA and the largest amounts of *Il6* mRNA after GAS infection, as was found in another study of a Toll-like receptor agonist (Zygmunt et al., 2009). It also possible that dendritic cells that took up GAS bacteria in the CLN were the key drivers of Th17 differentiation since these cells also expressed *Il6* and *Tgfb1* mRNA after infection. The failure of Th17 development in the spleen after i.v. GAS infection correlated with low *Il6* mRNA and protein production by

dendritic cells in this location. Thus, the i.n. route of infection may be better than the i.v. route for induction of Th17 cells because of the presence of a potent IL-6-producing dendritic cell in the CLN that is not present in the spleen.

It is worth noting that ablation of TGF-β1 production by dendritic cells did not completely inhibit GAS-induced Th17 formation, indicating that other cells of hematopoietic origin provide TGF-β1 for this purpose. Autocrine TGF-β1 production by $CD4^+$ T cells was a good candidate based on the work of Li and colleagues in the EAE model (Gutcher et al., 2011). However, we found no role for autocrine TGF-β1 production by $CD4^+$ T cells in GAS-driven Th17 differentiation.

Our finding that Th17 differentiation in response to i.n. GAS infection depends on IL-6 and TGF-β1 production supports early *in vitro* studies that reached a similar conclusion. However, these results are in contrast to other *in vivo* studies, which showed that IL-1β and IL-23, not IL-6 and TGF-β1 (Shaw et al., 2012; Ghoreschi et al., 2010), are required for Th17 differentiation in the intestinal mucosa. Thus, it appears that two separate pathways of Th17 differentiation exist for the upper respiratory and intestinal mucosal surfaces.

Weak Th1 cell differentiation was observed in cases where Th17 differentiation in response to i.n. GAS infection was impaired due to a lack of IL-6 or TGF-β1, as has been reported previously (Li et al., 2007; Dileepan et al., 2010). This finding indicates that IL-6 and/or TGF-β1 suppress Th1 differentiation, perhaps through an effect on IL-12 production (Lyakh et al., 2005). Notably, 2W:I-A^b-specific T cells did not become $Foxp3^+$ cells in IL-6-deficient GAS-2W-infected mice as observed in the EAE model

(Korn et al., 2007). Therefore, exposure of p:MHCII-activated T cells to TGF-β1 without IL-6 does not necessarily lead to Treg cell differentiation in all cases.

Chapter 4:

Different Routes of Bacterial Infection Induce Long-lived T_H1 Memory Cells and Short-lived T_H17 Cells

4.1 Introduction

Vaccination or prior encounter with a microbe generally results in immunity to subsequent infection with that microbe. This immunity is mediated by memory T cells and B cells, which are generated from naive precursor cells after exposure to microbial antigens. Binding of the T cell antigen receptor (TCR) to microbe-derived peptide bound to major histocompatibility complex (pMHC) molecules causes naive T cells to proliferate and differentiate into effector cells able to produce microbicidal cytokines (Jenkins et al., 2001). Although ~90% of the effector cells die, some survive to become long-lived memory cells capable of a rapid and protective response to reinfection with the relevant microbe (Ahmed and Gray, 1996).

Two main subsets of memory T cells have been described: central memory T cells (T_{CM} cells) and effector memory T cells (T_{EM} cells) (Masopust et al., 2001; Reinhardt et al., 2001; Sallusto et al., 1999). T_{CM} cells express the chemokine receptor CCR7 and L-selectin, which allows recirculation through lymph nodes. T_{EM} cells lack CCR7 and L-selectin yet express other homing receptors needed for migration into nonlymphoid organs (Seder and Ahmed, 2003). When stimulated with antigen, T_{EM} cells are immediately capable of effector cytokine production and cytolysis, whereas T_{CM} cells proliferate to produce new effector cells, which then acquire these functions. Heterogeneity in lymphokine production potential also exists in the case of $CD4^+$ T cells.

Naive $CD4^+$ T cells differentiate into T helper type 1 (T_H1), T_H2 or interleukin 17 (IL-17)-producing T helper (T_H17) effector cells when stimulated *in vitro* with antigen and specific combinations of cytokines (Zhou et al., 2009). In addition, certain infections induce $CD4^+$ effector cells with the properties of T_H1 or T_H2 cells (Reiner and Locksley, 1995).

However, it is still not clear that $CD4^+$ memory T cells specific for peptide–MHC class II (pMHCII) exist as discrete T_H1, T_H2 or T_H17 subsets *in vivo* because such cells are difficult to detect in normal hosts. To circumvent this problem, researchers have studied immune memory by $CD4^+$ T cells *in vitro* (Swain et al., 1999) or *in vivo* (Jenkins et al., 2001; Li et al., 2003; Lohning et al., 2008) by adoptive transfer of TCR-transgenic T cells. These approaches are artificial in that memory T cells are generated from disrupted lymphoid tissue (Li et al., 2003; Lohning et al., 2008; Swain et al., 1999) or are so abundant that normal homeostasis is perturbed (Badovinac et al., 2007; Hataye et al., 2006; Marzo et al., 2005). Thus, it is not clear how well polyclonal $CD4^+$ memory T cells fit into the T_H1, T_H2, T_H17 or T_{CM} and T_{EM} categories.

Here we addressed this problem with a sensitive pMHCII tetramer–based approach that allowed detection of polyclonal pMHCII-specific $CD4^+$ T cells in normal mice after infection with *Listeria monocytogenes*. We found that intravenous and intranasal infection induced T_H1 and T_H17 $CD4^+$ effector T cells, respectively, although the most abundant cells in both cases did not resemble any of the canonical helper T cell subsets. In addition, we found that T_H1 cells were much more likely than T_H17 cells to persist in the memory cell pool.

4.2 Materials and Methods

Mice

Six- to eight-week-old B6, B6.129S6-*Tbx21*^{tm1Glm}/J, B6.129P2(Cg)-*Rorc*^{tm2Litt}/J and B6.PL-Thy1^{a}/CyJ mice were from the Jackson Laboratory or the National Cancer Institute (B6). All mice were housed in specific pathogen–free conditions in accordance with guidelines of the University of Minnesota and National Institutes of Health. All animal experiments were approved by the Institutional Animal Care and Use Committee of the University of Minnesota.

L. monocytogenes Infection

Mice were injected intravenously (1×10^7 bacteria) or intranasally (1×10^7 bacteria) with *ActA*-deficient *L. monocytogenes* expressing a recombinant protein consisting of chicken ovalbumin fused to the 2W peptide (EAWGALANWAVDSA) or ESAT6 peptide. In some experiments, mice were challenged intravenously after primary infection with 5×10^8 live LM-2W or LM-ESAT6. Challenged mice were killed 2 h later for analysis.

BrdU Labeling

For analysis of homeostatic proliferation, mice were infected with LM-2W and at least 40 d later were given BrdU (0.8 mg/ml) in the drinking water for 12–14 d. In some cases, mice were injected intraperitoneally with complexes of recombinant mouse IL-15Rα–Fc chimera (7 μg per mouse) and recombinant mouse IL-15 (1.5 μg per mouse; both from

R&D Systems) formed as described (Rubinstein et al., 2006; Stoklasek et al., 2006). Mice were injected once a day for 2 d with IL-15–IL-15Rα complexes and BrdU (2 mg per mouse by intraperitoneal injection) and then BrdU was added to the drinking water (0.8 mg/ml) for an additional 3 d before spleens and lymph nodes were collected and stained as described below.

Tetramer Production

Biotin-labeled soluble 2W:I-A^b molecules were produced and were expressed in *Drosophila melanogaster* S2 cells, then were purified and were made into tetramers with streptavidin-phycoerythrin or streptavidin-allophycocyanin (Prozyme) as described (Moon et al., 2007).

Tetramer Enrichment and Flow Cytometry

Spleen and lymph node cells or leg bone marrow cells were prepared and then were stained for 1 h at 25 °C with 2W:I-A^b–streptavidin-phycoerythrin or 2W:I-A^b–streptavidin-allophycocyanin tetramer and peridinin chlorophyll protein–cyanine 5.5–conjugated antibody to CCR7 (anti-CCR7; 4B12; eBioscience) and then with anti-phycoerythrin and/or anti-allophycocyanin magnetic beads. Samples were then enriched for bead-bound cells on magnetized columns and a portion was removed for counting as described .(Moon et al., 2007) It was assumed that the leg bones contained one fifth of the bone marrow in the body (Boggs, 1984). The rest of the sample underwent surface

staining on ice with Pacific Blue– or eFluor 450–conjugated anti-B220 (RA3-6B2; all antibodies from eBioscience unless otherwise noted), anti-CD11b (MI-70), anti-CD11c (N418) and anti-F4/80 (BM8; Caltag); Pacific Orange–conjugated anti-CD8α (5H10; Caltag); fluorescein isothiocyanate–conjugated anti-CD27 (LG.7F9); allophycocyanin–Alexa Fluor 750– or allophycocyanin–eFluor780–conjugated anti-CD4 (RM4-5); phycoerythrin-indotricarbocyanine–conjugated anti-CD3ϵ (145-2C11); phycoerythrin-conjugated anti-CD122 (5H4); and Alexa Fluor 700–conjugated anti-CD44 (IM7). For intracellular cytokine experiments, spleen and lymph node cells from challenged mice or *in vitro*–stimulated cultures containing phorbol 12-myristate 13-acetate (50 ng/ml), ionomycin (200 ng/ml) and brefeldin A (10 μg/ml; Sigma) underwent the tetramer enrichment and anti-CCR7 staining described above in buffer containing brefeldin A (10 μg/ml; Sigma) to prevent cytokine secretion. Surfaces of enriched cells were stained with combinations of antibodies listed above, then cells were treated with BD Cytofix/Cytoperm and stained with phycoerythrin-indotricarbocyanine–conjugated anti-IFN-γ (XMG1.2) or phycoerythrin-conjugated anti-IL-17A (TC11-18H10; BD Pharmingen). In some experiments, surfaces of enriched cells were stained, then cells were treated with Foxp3 Fixation/Permeabilization Concentrate and Diluent (eBioscience) and stained with phycoerythrin-conjugated anti-T-bet (eBio 4B10) or phycoerythrin-conjugated anti-RORγt (AFKJS-9), or they were treated with BD Cytofix/Cytoperm and stained with phycoerythrin-conjugated anti-Bcl-2 (3F11; BD Pharmingen). For BrdU labeling, surfaces of enriched cells were stained and incorporated BrdU was detected with a BrdU Flow kit according to the manufacturer's specifications

(BD Pharmingen). In all cases, cells were then analyzed on an LSR II (Becton Dickinson). Data were analyzed with FlowJo software (TreeStar).

Memory Cell Transfer

Spleens and lymph nodes were collected from B6 mice infected at least 20 d earlier with LM-2W. For transfer of $CD27^-$ cells, samples were depleted of $CD27^+$ cells (95–97% purity) with biotin-conjugated anti-CD27, anti-biotin beads (Miltenyi) and LD columns (Miltenyi). For transfer of $CD27^+$ cells, samples were enriched for $CD4^+$ memory cells by the addition of biotin-conjugated anti-CD45RB (0.1 μg/ml) to the biotin-labeled antibody 'cocktail' provided in the Miltenyi CD4 Isolation kit, followed by the removal of biotin-labeled cells on an LS column. The remaining cells were stained with fluorochrome-labeled anti-CD44 and anti-CD27 before sorting of $CD44^+CD27^+$ events with a FACSAria (Becton Dickinson). Purified cells were injected intravenously into B6.PL-Thy-1^a recipients. Then, 1 d or 14 d later, spleen and lymph node cells from the recipients were collected, were stained for 1 h at 25 °C for 2W:I-A^b–streptavidin–allophycocyanin tetramer and peridinin chlorophyll protein–cyanine 5.5–conjugated anti-CCR7 (4B12), then with phycoerythrin-conjugated anti-CD90.2 (53-2.1) and anti-phycoerythrin magnetic beads. Bead-bound cells were then stained with the non–T lineage–specific antibodies listed above (anti-CD8α, anti-CD4, anti-CD27 and anti-CD44) and cells were then analyzed on an LSR II (Becton Dickinson). Data were analyzed with FlowJo software (TreeStar).

Statistical Analysis

Differences between data sets were analyzed by a paired or unpaired two-tailed Student's *t*-test. In Figure 3, a two-way analysis of variance with a Bonferroni's post-test was used to determine significance.

4.3 Results

Detection of pMHCII-specific $CD4^+$ Memory T cells

We used a pMHCII tetramer–based approach to identify $CD4^+$ T cells specific for a pMHCII complex produced during bacterial infection. The pMHCII tetramer consisted of the I-A^b MHC class II molecule bound to a variant of amino acids 52–68 from the I-E α-chain called 2W (2W–I-A^b) (Rees et al., 1999). The 2W peptide is highly immunogenic in C57BL/6 (B6) mice because of a relatively large naive population able to recognize 2W–I-A^b (Moon et al., 2007). We infected B6 mice with an attenuated strain of *L. monocytogenes* (ΔActA) engineered to secrete a fusion protein containing a portion of chicken ovalbumin and the 2W peptide (LM-2W) (Ertelt et al., 2009) or a mycobacterial peptide ESAT6 (LM-ESAT6) (Muller et al., 2008). These bacteria replicate for several days in mice and are then completely eliminated by innate and adaptive immune mechanisms (Portnoy et al., 2002). We stained cells from each mouse with a fluorochrome-labeled 2W–I-A^b tetramer and anti-fluorochrome magnetic beads at various times after infection and enriched them on a magnetized column (Moon et al., 2009). We then stained the bound fraction with antibodies specific for CD3, CD4, CD8,

CD44 and a 'cocktail' of non–T cell lineage–specific antibodies to aid in the identification of $CD4^+$ memory T cells.

Because effector and memory T cells express many of the same surface markers, we identified the latter cells as the population that stabilized after the expansion and contraction phases of the primary response (Kaech et al., 2002). Initial analyses involved standard intravenous infection. Mice that were not infected contained a small population of about 300 2W–I-A^b–binding $CD3^+CD4^+$ cells in the spleen and lymph nodes, the vast majority of which were $CD44^{lo}$, as expected for naive cells (Fig. 4.1A). The tetramer bound to these T cells via the TCR, as shown by the finding that we detected no 2W–I-A^b–binding cells among the $CD8^+$ MHC class I–restricted T cells. Mice infected 7 d earlier with LM-ESAT6 also contained about 300 $CD44^{lo}$ 2W–I-A^{b+} $CD4^+$ naive T cells (Fig 4.1B). In contrast, mice infected with LM-2W 7 d earlier contained a large population of $CD44^{hi}$ 2W–I-A^{b+} $CD4^+$ T cells in the spleen and lymph nodes that could still be detected on day 190 and beyond. The number of 2W–I-A^b–specific $CD4^+$ T cells peaked at ~140,000 cells by day 5 after LM-2W infection and then decreased rapidly to 20,000 cells by day 20 (Fig 4.2). This contraction phase ended abruptly on day 20, after which the population slowly decreased until day 250 with a half-life of about 40 d (Fig 4.2). By day 250, only about 200 $CD44^{hi}$ 2W–I-A^{b+} $CD4^+$ T cells remained in the spleen and lymph nodes, and this number remained stable for the next 150 d. Although we did not detect 2W–I-A^{b+} $CD4^+$ T cells in the bone marrow in uninfected mice (data not shown), about 1,500 $CD44^{hi}$ 2W–I-A^{b+} $CD4^+$ T cells appeared in the bone marrow by day 20 and then decreased to 150 cells by day 300. Thus, 2W–I-A^b–specific $CD4^+$ T cell

populations expanded to a peak number on day 5, contracted until day 20, and then entered a memory phase characterized by slow numerical decrease for the next 230 d. In addition, some of the 2W–I-A^b–specific memory CD4$^+$ T cells were present in the bone marrow, although more were present in the spleen and lymph nodes.

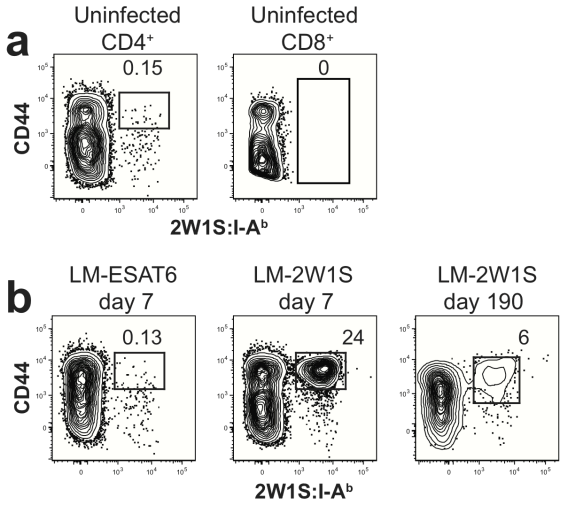

Figure 4.1. Infection with LM-2W induces the clonal expansion of 2W–I-A^b–specific memory cells. Flow cytometry to identify CD4$^+$ or CD8$^+$ T cells in enriched fractions, for events gated on CD11c$^-$ CD11b$^-$F4/80$^-$B220$^-$CD3$^+$ cells. (**a**) CD4$^+$ T cells (left) or CD8$^+$ T cells (right) from an uninfected B6 mouse with gates on CD44^{hi} 2W–I-A^{b+} (left) or all 2W–I-A^{b+} cells (right). (**b**) CD4$^+$ T cells in enriched samples from a B6 mouse 7 d after intravenous infection of LM-ESAT6 (left) or 7 d (middle) or 190 d (right) after intravenous infection of LM-2W. Numbers above outlined areas indicate percent cells in gate. Data are representative of over twenty (**a**) or two to five (**b**) independent experiments.

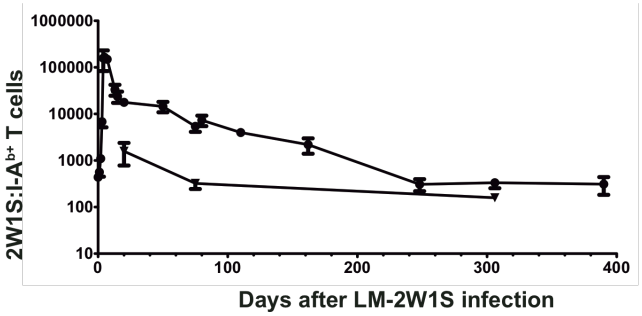

Figure 4.2. The 2W–I-A^{b}–specific CD4^{+} memory T cells decay after infection with LM-2W. CD4^{+} 2W–I-A^{b+} T cells in the spleen and lymph nodes (circles) or bone marrow (triangles) after intravenous infection of LM-2W (n ³ 3 mice per data point). A nonlinear regression fit of the spleen and lymph node data yielded a half-life of 43 d for points between days 20 and 248 (R^2 = 0.94; 95% confidence interval, 30–73 d). Data are representative of five experiments (mean ± s.e.m.).

Infection Route Influences CD4^{+} T Cell Differentiation

We next determined whether CD4^{+} memory cells induced by intravenous infection resembled any of the canonical helper T cell subsets. We measured lymphokine production by 2W–I-A^{b}–specific CD4^{+} memory cells by direct *ex vivo* intracellular staining (Khoruts et al., 1998) in mice that were infected 24 d before with LM-2W and then challenged for 2 h with LM-2W or LM-ESAT6. We chose 2 h because this is the time of maximal *in vivo* lymphokine production by antigen-experienced CD4^{+} T cells stimulated by intravenous injection of peptide (Pape et al., 1998) or infection with LM-2W (data not shown). We found that 2W–I-A^{b}–specific CD4^{+} memory cells did not express CD69 (Fig. 4.3A) or produce interferon-γ (IFN-γ) or IL-17A after challenge with

LM-ESAT6 (Fig. 4.3A,B). In contrast, about 30–40% of the memory cells produced IFN-γ after challenge (Fig. 4.3A,B) with LM-2W, whereas none of these cells produced IL-17A (Fig. 4.3B)or IL-5 (data not shown). The failure of the majority of 2W–I-A^b–specific $CD4^+$ memory cells to make IFN-γ after challenge was not related solely to a lack of 2W–I-A^b recognition after challenge, as many of the cells expressed the TCR signal–dependent CD69 molecule but did not make IFN-γ (Fig. 4.3B). Therefore, about one third of the 2W–I-A^b–specific $CD4^+$ memory cells induced by intravenous infection resembled T_H1 cells, whereas the remainder did not produce any of the canonical T_H1, T_H2 or T_H17 cytokines.

It was possible that many of the 2W–I-A^b–specific $CD4^+$ memory cells that were $CD69^+$ but were not making cytokines 2 h after challenge would have gone on to produce cytokines. To address this issue, we stimulated spleen and lymph node cells from mice infected 22 d earlier with LM-2W *in vitro* with the soluble TCR signal mimics phorbol 12-myristate 13-acetate (PMA) and ionomycin in the presence of an exocytosis inhibitor. IFN-γ-producing cells peaked at about 50% of the total 2W–I-A^b-specific $CD4^+$ memory population between 3.5 and 6 h of stimulation (Fig. 4.3C). As IFN-γ should accumulate in these conditions, these results indicated that only a subset of the 2W–I-A^b–specific $CD4^+$ memory cell population had the potential to produce IFN-γ. This conclusion was supported by the finding that about 50% of the 2W–I-A^b–specific $CD4^+$ memory cells induced by intravenous infection expressed the T_H1-associated transcription factor T-bet (Szabo et al., 2000) before challenge, whereas none expressed the T_H17-associated

transcription factor RAR-related orphan receptor gamma (RORgt) (Ivanov et al., 2006) (Fig. 4.3D) and none became Foxp3$^+$ regulatory T cells (Ertelt et al., 2009). As T-bet expression controls the T_H1 differentiation program in most cases (Szabo et al., 2000), this finding indicates that only a subset of the memory cells induced by intravenous infection had differentiated into T_H1 cells.

One potential factor driving the induction of T_H1 but not T_H17 or T_H2 cells was the intravenous route of infection. We therefore studied the effect of intranasal administration of LM-2W based on reports that IL-17A-producing T cells are induced during mucosal bacterial infection (Woolard et al., 2008; Zhang et al., 2009). Indeed, we found that about 7% of the 2W–I-A^b–specific CD4$^+$ T cells in the spleen and lymph nodes of mice 24 d after intranasal infection with LM-2W produced IL-17A, whereas very few produced IFN-γ, 2 h after challenge with LM-2W but not after challenge with LM-ESAT6 (Fig. 4.3B). In addition, about 15% of the 2W–I-A^b-specific T cells induced by intranasal infection expressed RORgt, as shown by expression of green fluorescent protein in mice heterozygous for expression of green fluorescent protein–tagged RORgt (Rorc(gt)$^{+/GFP}$) or by intracellular staining for RORgt (Fig. 4.3D). These results demonstrate that intranasal infection with LM-2W induced some of the 2W–I-A^b–specific T cells to differentiate into T_H17 cells. However, as with intravenous infection, the main population showed no evidence of committing to either a T_H1 or T_H17 canonical lineage.

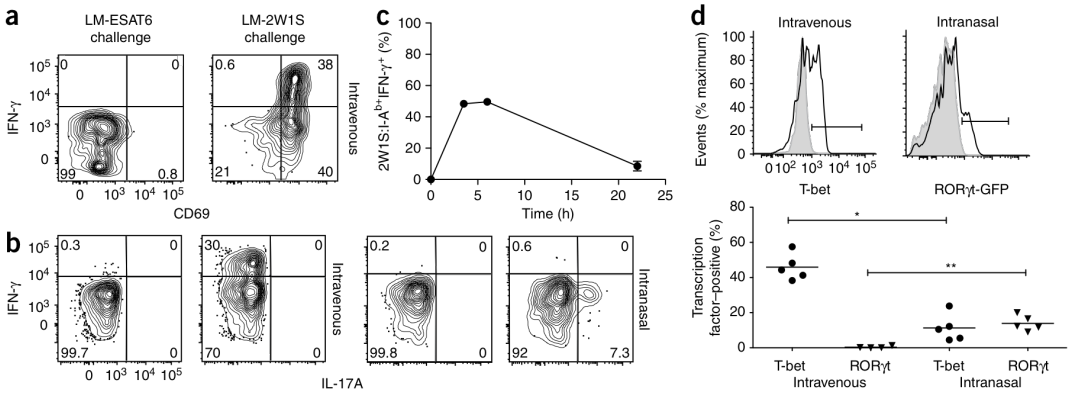

Figure 4.3. Lymphokine production by 2W–I-A^b–specific CD4$^+$ memory T cells. (**a**,**b**) Expression of CD69 (**a**) or IFN-γ (**a**,**b**) and IL-17A production (**b**) by 2W–I-A^b–specific memory T cells 2 h after challenge of mice by intravenous (**a**,**b**) or intranasal (**b**) infection with LM-ESAT6 (left) or LM-2W (right). Numbers in quadrants indicate percent of cells in each. (**c**) Frequency of 2W–I-A^b–specific IFN-γ^+ CD4$^+$ memory T cells after stimulation for 3.5 h, 6 h, or 22 h with PMA and ionomycin in the presence of brefeldin A. (**d**) T-bet expression (top left) in 2W–I-A^b–specific memory T cells (black line) induced by intravenous infection and in CD44$^+$ CD4$^+$ T-bet-deficient cells (gray filled histogram), and expression of enhanced green fluorescent protein in mice heterozygous for expression of green fluorescent protein–tagged RORgt (RORgt-GFP) (top right) in 2W–I-A^b–specific memory T cells (black line) and wild-type 2W–I-A^b–specific memory T cells (gray filled histogram) after intranasal infection. Below, frequency of T-bet$^+$ or RORgt$^+$ 2W–I-A^b–specific memory T cells in mice based on the gates above. *$P < 0.01$, T-bet samples, **$P < 0.05$, RORgt samples (a two-way analysis of variance with a Bonferroni's post-test was used to determine significance). Data are representative of three (**a**), six (**b**) or two (**c**) independent experiments, or of four or one independent experiment(s) for intracellular staining or Rorc(gt)$^{+/GFP}$ mice, respectively (**d**).

T_H17 Cells are Shorter-lived Than T_H1 Cells

We next measured the survival of IFN-γ- or IL-17A-producing T cells to determine if these subsets were equally efficient at entering the memory pool. We infected mice and then challenged them later at various times with an intravenous injection of LM-2W to identify the lymphokine-producing cells. Intravenous infection with LM-2W generated about 12,000 IFN-γ-producing 2W–I-A^b–specific effector T cells in the spleen and lymph nodes by day 7, which constituted about 10% of all 2W–I-A^b–specific T cells. At all times after the contraction phase, IFN-γ-producing cells accounted for about 25% of the 2W–I-A^b–specific memory cells (Fig. 4.4A). Therefore, IFN-γ-producing 2W–I-A^b–specific T cells were as good as or better than non-IFN-γ-producing cells at entering the memory pool.

Intranasal infection induced a pattern of 2W–I-A^b–specific $CD4^+$ T cell population expansion, contraction and memory cell formation similar to that induced by intravenous infection, albeit to a lower extent (Fig. 4.4B). The lower magnitude of this response was probably related to the fact that the nasal mucosal lymphoid tissues, which are the main sites of priming after intranasal infection (Park et al., 2004), contain many fewer naive T cells than does the spleen, where priming occurs after intravenous infection. About 2,000 IL-17A-producing 2W–I-A^b–specific effector cells were present on day 7, which, as for IFN-γ-producing cells in intravenously infected mice, constituted about 10% of all 2W–I-A^b–specific T cells at this time. However, unlike IFN-γ-producing

cells, IL-17A-producing 2W–I-A^b–specific cells were progressively lost, such that fewer than 10 cells (or 0.5% of all 2W–I-A^b–specific T cells) remained at day 110 after infection. Thus, IL-17A-producing cells did not enter the memory pool as efficiently as IFN-γ-producing cells did.

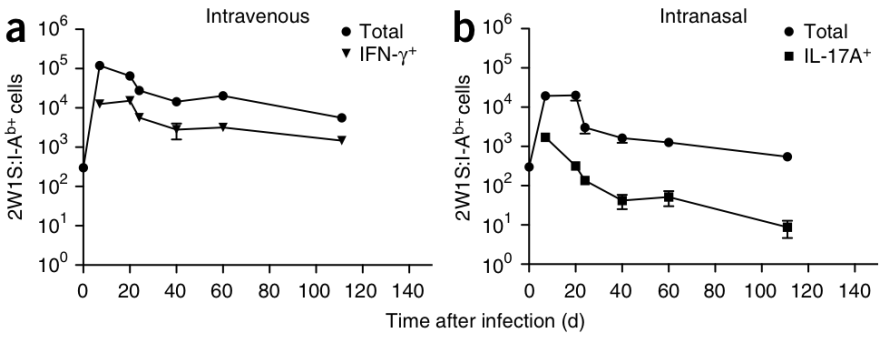

Figure 4.4 Survival of IFN-γ and IL-17A-producing 2W–I-A^b–specific CD4$^+$ memory T cells. Total 2W–I-A^b–specific CD4$^+$ T cells induced by intravenous infection (**a**) or intranasal infection (**b**), and 2W–I-A^b–specific CD4$^+$ T cells making IFN-γ but not IL-17A (**a**) or IL-17A but not IFN-γ (**b**) after challenge with LM-2W. Data are representative of three (**a**) or two (**b**) experiments (mean ± s.d. of three to five mice per time point).

CD27 Marks Functional Heterogeneity in $CD4^+$ Memory T Cells

We sought additional markers that could give clues about the differences in the longevity of IFN-γ- and IL-17A-producing $CD4^+$ T cells and determine if they fit the definition of T_{CM} cells or T_{EM} cells. Published work has demonstrated that $CD8^+$ memory T cells can be categorized on the basis of expression of the tumor necrosis factor receptor family member CD27 (Hikono et al., 2007; Snyder et al., 2008). In addition, $CD8^+$ memory cells that lack expression of CD27 have been shown to be short-lived (Dolfi et al., 2008; Hendriks et al., 2000; Hendriks et al., 2003; Snyder et al., 2008). Therefore, we assessed expression of CD27 and CCR7, a marker used to distinguish T_{CM} cells from T_{EM} cells[3]. Most of the IFN-γ^+ or T-bet^+ 2W–I-A^b–specific $CD4^+$ T cells present greater than 20 days after intravenous infection were $CCR7^{lo}CD27^+$ (Fig. 4.5A,B). Although cells with this phenotype were also present among the IFN-γ^- or T-bet^- cells in the same mice, these populations also contained many $CCR7^{hi}CD27^+$ and $CCR7^{hi}CD27^-$ cells. In contrast, most of the IL-$17A^+$ 2W–I-A^b–specific $CD4^+$ T cells present after intranasal infection were $CCR7^{hi}CD27^-$ (Fig. 4.5C), whereas the IL-$17A^-$ cells included more $CCR7^{hi}CD27^+$ and $CCR7^{hi}CD27^-$ cells like the IFN-γ^- cells in intravenously infected mice. Although the RORgt$^+$ 2W–I-A^b–specific $CD4^+$ T cells included $CCR7^{hi}CD27^-$ cells, as in the case of IL-17A-producing cells (Fig. 4.5D), the RORgt$^+$ populations also contained $CD27^+$ cells. Therefore, on the basis of CCR7 expression, the T_H1 cells resembled T_{EM} cells, whereas the T_H17 cells resembled T_{CM} cells.

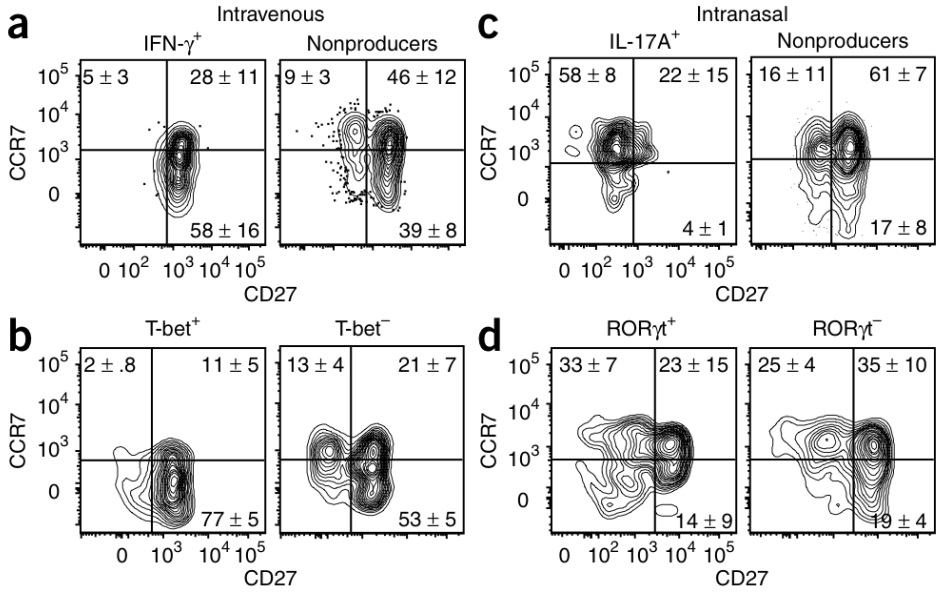

Figure 4.5. Surface phenotype of 2W–I-A^b–specific T cells. Expression of CCR7 and CD27 on 2W–I-A^b–specific T cells in mice at least 20 d after intravenous infection (**a**,**b**) or intranasal infection (**c**,**d**). (**a**) Cells producing IFN-γ but not IL-17A (left) or neither (right) after challenge with LM-2W. (**b**) T-bet$^+$ (left) or T-bet $^-$ (right) antigen-experienced cells without challenge. (**c**) Cells producing IL-17A but not IFN-γ (left) or neither (right) after challenge with LM-2W. (**d**) RORgt$^+$ (left) or RORgt $^-$ (right) antigen-experienced cells without challenge. Quadrant lines are based on 2W–I-A^{b-} CD44^{lo} naive cells in each sample; this population was uniformly CCR7^{hi} and contained CD27^{lo} and CD27^{hi} subsets. Horizontal lines are set at the lowest amount of CCR7 for the entire population; vertical lines are set at the midpoint between the CD27^{lo} and CD27^{hi} subsets. Numbers in quadrants indicate percent cells in each (mean ± s.d. of four or more mice). Data are representative of seven (**a**), four (**b**), six (**c**) or two (**d**) independent experiments.

The finding that IL-17A-producing $CD4^+$ T cells lacked CD27 and were short-lived motivated us to explore whether all $CD27^-$ $CD4^+$ memory cells had this property. We tested this possibility in an adoptive-transfer experiment involving total $CD4^+$ memory T cells, as 2W–I-A^b–specific memory cells were too infrequent to detect reliably after transfer. We sorted purified total $CD27^+$ or $CD27^-$ $CD4^+CD44^+$ T cells from *L. monocytogenes*–infected B6 mice ($CD90.2^+$) and transferred them into naive B6.PL-Thy-1^a ($CD90.1^+$) recipients (Fig. 4.6A). The $CD27^+$ $CD4^+$ memory cells survived stably over a 14-day period after adoptive transfer, whereas the number of purified $CD27^-$ $CD4^+$ memory cells decreased by about 80% (Fig. 4.6B). Thus, $CD27^-$ $CD4^+$ memory T cells were short-lived compared with $CD27^+$ $CD4^+$ memory T cells. Although this observation was based on total $CD4^+$ memory cells, it correlated with the finding that a subset of $CD27^+$ 2W–I-A^b–specific $CD4^+$ memory T cells expressed more of the Bcl-2 survival protein than did $CD27^-$ memory T cells of the same specificity (Fig. 4.6C).

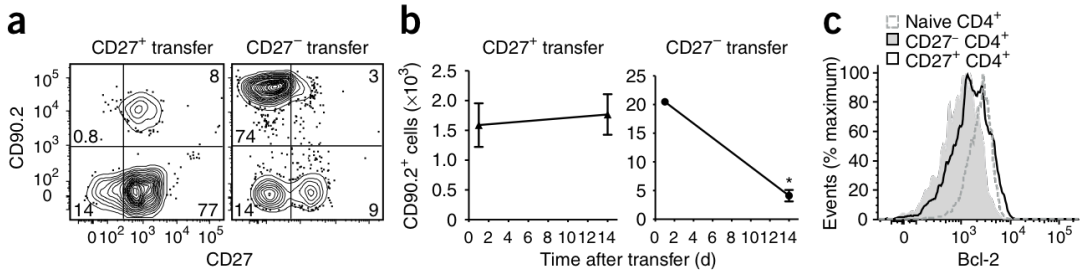

Figure 4.6. CD27$^-$ CD4$^+$ memory T cells are short-lived. (**a**) CD90.2-enriched fractions of spleen and lymph node cells from mice that received purified CD90.2$^+$ CD27$^+$ (left) or CD27$^-$ (right) total CD4$^+$ memory T cells 1 d earlier. (**b**) CD90.2$^+$ CD27$^+$ (left) or CD27$^-$ (right) cells recovered 1 or 14 d after transfer into B6.PL-Thy-1^a recipients. **P* = 0.0005, CD27$^-$ cells recovered on day 14 versus day 1 (unpaired two-tailed Student's *t*-test). (**c**) Bcl-2 expression by total naive CD4$^+$ T cells (dashed line), or CD27$^-$ (gray histogram) or CD27$^+$ (black line) 2W–I-A^{b+} memory T cells. Data are representative of three (**a**,**b**) or two (**c**) independent experiments (mean ± s.d. of three to four mice in **b**).

Minimal Homeostatic Proliferation by CD27$^-$ CD4$^+$ T Cells

It was also possible that poor homeostatic proliferation contributed to the short lifespan of CD27$^-$ CD4$^+$ memory T cells. We tested this possibility with a bromo-2-deoxyuridine (BrdU)-labeling experiment. We infected B6 mice with LM-2W and, 40 days later, gave the mice BrdU in their drinking water for 2 weeks. About 10% of the 2W–I-A^b–specific CD4$^+$ memory T cells induced by intravenous or intranasal infection labeled with BrdU (Fig. 4.7A, and data not shown). Among the 2W–I-A^b–specific CD4$^+$ memory T cells, about 15% of the CD27$^+$ cells and only 3% of the CD27$^-$ cells labeled with BrdU (Fig. 4.7A,B). The homeostatic proliferation results correlated with expression of the β-chain of the IL-15 receptor (IL-15R; also known as CD122). CD122 was expressed on some CD27$^+$ CD4$^+$ memory T cells but very few CD27$^-$ CD4$^+$ memory T

cells (Fig. 4.7C). Together these results showed that $CD27^{-}$ $CD4^{+}$ memory T cells were poor homeostatic proliferators, perhaps as a result of a lack of IL-15R expression.

To further test that hypothesis, we injected mice with IL-15–IL-15Ra complexes, which have been shown to be superagonists for IL-15R signaling *in vivo* (Rubinstein et al., 2006). Injection of IL-15–IL-15Ra complexes into B6 mice 40 d after intravenous infection with LM-2W led to an increase of ~30-fold in the fraction of 2W–I-A^{b}–specific $CD4^{+}$ memory cells that underwent homeostatic proliferation over a short 5-day BrdU-labeling period, and the populations that proliferated were enriched for $CD27^{+}$ cells (Fig. 4.7D). These results indicate that a lack of IL-15R expression limits the homeostatic proliferation of $CD27^{-}$ $CD4^{+}$ memory T cells.

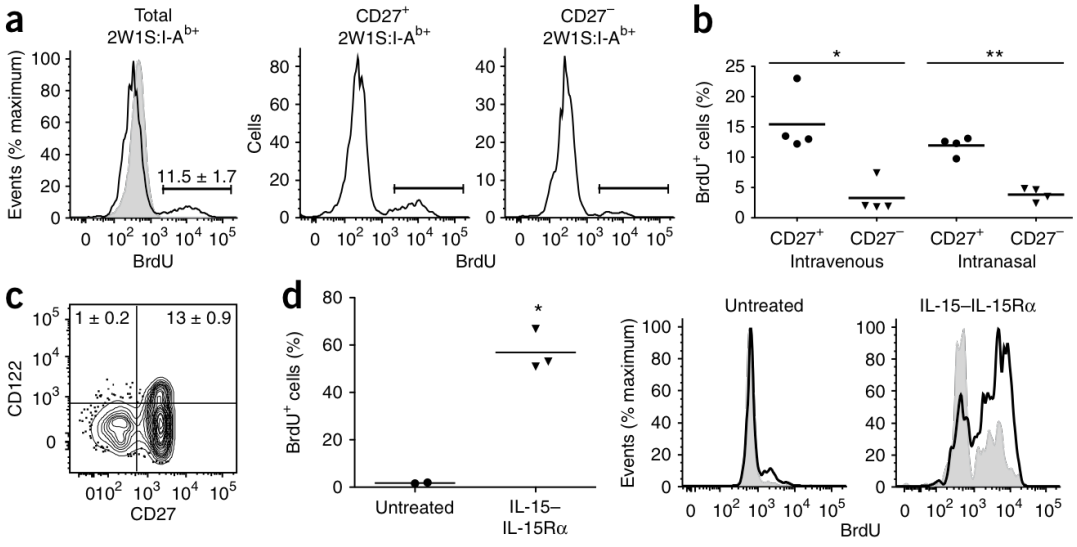

Figure 4.7. CD4$^+$ memory T cells undergo limited homeostatic proliferation. (**a**) BrdU labeling (black lines) of total (left), CD27$^+$ (middle) or CD27$^-$ (right) 2W–I-A^{b+} CD4$^+$ memory cells in mice fed BrdU for 14 d beginning 40 d after intravenous infection with LM-2W, as well as total CD4$^+$ T cells (gray) from a mouse that did not receive BrdU (left). Bracketed lines indicate gates used to identify BrdU$^+$ cells; number above bracketed (left) indicates percent BrdU$^+$ cells (mean ± s.d.). (**b**) Frequency of CD27$^+$ or CD27$^-$ BrdU$^+$ 2W–I-A^{b+} CD4$^+$ memory T cells, based on the gates shown in (**a**). Each symbol represents an individual mouse; small horizontal lines indicate the mean. **(c**) Expression of CD122 and CD27 on 2W–I-A^{b+} CD4$^+$ memory T cells induced by intravenous infection. mean ± s.d., n = 5) Frequency of CD122$^+$ cells are shown in the relevant quadrants. (**d**) Frequency of BrdU$^+$ 2W–I-A^{b+} CD4$^+$ memory cells (left) in mice left uninjected (circles) or injected with IL-15–IL-15Ra complexes (triangles) and given BrdU for 5 d beginning 20 d after intravenous infection with LM-2W, identified as described in **a**. Each symbol represents an individual mouse; small horizontal lines indicate the mean. Middle and right, BrdU incorporation by CD27$^+$ (solid line) or CD27$^-$ (gray) 2W–I-A^{b+} CD4$^+$ memory T cells in mice left uninjected (middle) or injected with IL-15–IL-15Ra complexes (right) and given BrdU for 5 d beginning 20 d after intravenous infection with LM-2W. *P = 0.003, IL-15–IL-15Ra complex versus untreated (unpaired two-tailed Student's t-test). Data are representative of three (**a**,**b**), two (**c**) or one (**d**) experiment(s).

4.4 Discussion

Here we found that intravenous or intranasal infection with LM-2W induced polyclonal 2W–I-A^b–specific $CD4^+$ memory T cells. The emergence of memory-phenotype cells was preceded by robust population expansion of naive cells, which peaked in the secondary lymphoid organs about a week after infection. In both infections, the number of 2W–I-A^b–specific $CD4^+$ T cells decreased rapidly after the peak. This contraction phase ended on day 20, after which the number of cells decreased slowly. The abrupt change in survival observed at day 20 indicated that this is when the memory phase of this response begins. Most of the 2W–I-A^b–specific $CD4^+$ T cells induced by intravenous infection were in the secondary lymphoid organs during the memory phase, with considerably fewer in the bone marrow. Thus, the secondary lymphoid organs are the main reservoir of endogenous polyclonal $CD4^+$ memory T cells induced by intravenous bacterial infection and the bone marrow is not, as described for TCR-transgenic memory cells induced by immunization with peptide plus adjuvant (Tokoyoda et al., 2009).

Our results suggest that some but not all aspects of the T_H1-or-T_H17 and T_{EM}-or-T_{CM} paradigms apply to all $CD4^+$ memory T cells. The IFN-γ-producing memory cells induced by the transient bacterial infection studied here resembled T_H1 and T_{EM} cells because of their immediate ability to produce IFN-γ but not IL-17A and lack of CCR7 expression (Sallusto et al., 1999). Similarly, the IL17A-producing cells induced by intranasal infection resembled T_H17 and T_{EM} cells because of their immediate ability to produce IL-17A but not IFN-γ. However, these cells expressed CCR7 and thus were

phenotypically similar to T_{CM} cells and were short-lived. In addition, the dominant population of memory cells induced by either infection route did not produce IFN-γ, IL-17A or IL-5 and was heterogeneous in terms of expression of CCR7 and CD27. Therefore, these cells did not fit easily into the T_H1, T_H2 and T_H17 paradigm or T_{CM} and T_{EM} paradigm. These cells may be less differentiated and thus able to become T_H1, T_H2 or T_H17 cells after secondary infection. Alternatively, these cells could be highly differentiated cells that produce lymphokines other than those that define the classical subsets.

The tendency of different routes of infection to induce different memory cells may be related to the innate cytokine environments of the relevant secondary lymphoid organs. Anatomic constraints make it likely that naive $CD4^+$ T cells first become activated in the nasal-associated mucosal lymphoid tissue after intranasal infection (Park et al., 2004). A published study has found that IL-17A-producing $CD4^+$ effector T cells are preferentially induced in mice exposed to *Francisella tularensis* organisms via the respiratory mucosa (Woolard et al., 2008). Similarly, another study has shown that infection of the upper airway with *Streptococcus pneumoniae* organisms generates a population of IL-17A-producing $CD4^+$ T cells (Zhang et al., 2009). Thus, it is possible that the environment within mucosal secondary lymphoid organs is especially conducive to the differentiation of IL-17A-producing T cells. As IL-6 is required for the differentiation of these cells (Korn et al., 2009; Weaver et al., 2006), it is noteworthy that dendritic cells from the intestinal mucosal tissue have been reported to be better IL-6 producers than are splenic dendritic cells (Sato et al., 2003). In addition, transforming

growth factor-β1, which is also essential for the differentiation of IL-17A-producing T cells, is abundant in the mucosal tissues (Kelsall, 2008). Conversely, splenic dendritic cells are potent producers of IL-12 (Reis e Sousa et al., 1997), which is required for the differentiation of IFN-γ-producing T cells (Hsieh et al., 1993).

Our results confirm the idea that the number of $CD4^+$ memory T cells decreases slowly over time, at least in some cases. Published work has reported this finding for IFN-γ-producing $CD4^+$ memory T cells induced by infection with lymphocytic choriomeningitis virus (Homann et al., 2001). We also found that the total population of 2W–I-A^b–specific $CD4^+$ memory T cells induced by intravenous bacterial infection, including those with IFN-γ-production potential, decreased slowly, with a half-life of about 40 d, between days 20 and 250 of the memory phase. It is worth noting that the aforementioned viral infection (Homann et al., 2001) and the bacterial infections studied here were cleared very quickly from the host. Thus, the decrease in the number of $CD4^+$ memory T cells described in both cases may be related to a lack of persistent antigen presentation. It will be of interest to determine if the number of $CD4^+$ memory T cells also decreases during persistent infection caused by organisms like *Salmonella enterica* serovar Typhimurium (Monack et al., 2004).

After day 250, the number of 2W–I-A^b–specific memory cells stabilized at a number only about twice that of the naive number of cells (300). This survival pattern was similar to that observed for polyclonal naive T cells (Hataye et al., 2006). Thus, it is possible that many $CD4^+$ memory T cells do not live longer than their already long-lived naive precursors.

The decrease in the number of $CD4^+$ memory T cells induced by transient infections is in contrast to the remarkable numerical stability of $CD8^+$ memory T cells (Homann et al., 2001). As IL-15 is important for the homeostatic proliferation of both types of memory cells (Surh and Sprent, 2008), it may be telling that most $CD4^+$ memory T cells induced by bacterial infection, especially those lacking CD27, did not express IL-15R. It is therefore reasonable to suspect that a low rate of IL-15-driven homeostatic proliferation contributed to the numerical decrease in $CD4^+$ memory T cell populations observed in our experiments. Our finding that increasing the availability of IL-15 in the form of IL-15–IL-15Ra complexes increased the homeostatic proliferation of $CD4^+$ memory T cells is consistent with this possibility.

IL-17A-producing effector cells did not efficiently enter the memory cell pool. One possible explanation for this finding is that these cells simply lost the ability to produce IL-17A (Korn et al., 2009). Alternatively, the IL-17A-producing cells could have died because of a lack of CD27. CD27–CD70 interactions have been shown to be important for the maintenance of $CD8^+$ memory cells (Allam et al., 2009; Hendriks et al., 2000) perhaps via CD27 signaling through the adaptor TRAF5 (Kraus et al., 2008). The lack of a CD27 signal may have also lead to lower expression of the antiapoptosis protein Bcl-2 and a greater rate of apoptosis than that of $CD27^+$ $CD4^+$ memory cells. In contrast, IFN-γ-producing memory cells may gain a survival benefit from expression of T-bet, which has been reported to control CD122 expression and thus the capacity for IL-15-dependent homeostatic proliferation (Intlekofer et al., 2005). Against this scenario is the

finding that T-bet expression is a marker of terminal differentiation and death in $CD8^+$ memory T cells (Joshi et al., 2007).

Our results have also demonstrated an association between CD27 expression and lymphokine production potential. This finding adds to other evidence indicating that signaling through CD27 is causally related to the acquisition of IFN-γ-production potential (Keller et al., 2008; Soares et al., 2007), perhaps by contributing to the induction of T-bet (van Oosterwijk et al., 2007). However, it is worth noting that about half of the $RORgt^+$ 2W–I-A^b–specific memory cells induced by intranasal infection expressed CD27 but did not produce IFN-γ or IL-17A and could have been committed to the production of IL-22 or IL-17F (Yang et al., 2008). Thus, CD27 may be necessary but not sufficient for IFN-γ production by $CD4^+$ memory cells and may be not permissive for IL-17A production. This possibility is supported by work indicating that $CD27^+$ $\gamma\delta$ T cells cannot become IL-17-producing cells (Ribot et al., 2009).

Finally, our results have implications for protective immunity. Intranasal immunization of mice with *S. pneumoniae* induces protective immunity that is dependent on IL-17A and $CD4^+$ T cells (Lu et al., 2008). Our findings suggest that this immunity may be short-lived because IL-17A-producing $CD4^+$ effector T cells do not survive to become memory cells. In support of this suggestion is the clinical observation that streptococcal infections, for example otitis media, tend to recur (Yamanaka et al., 2008).

Chapter 5:

Conclusions

5.1 Summary

Together, this work defines the role and cellular sources of IL-6 and TGF-β1, in T_H17 differentiation in response to bacterial infection *in vivo*. Additionally, it identifies that the secondary lymphoid organs of the upper respiratory tract provide a unique environment for the differentiation of these cells to become a population of T_H17 cells that are short-lived compared to T_H1 memory cells induced in a splenic environment. These studies suggest the following model. Upon intranasal infection, bacteria translocate across M cells into the NALT. A functionally specialized population of DCs residing in the NALT capture bacteria, become activated, and migrate via afferent lymph to the NALT-draining CLNs. Naïve pMHCII-specific $CD4^+$ T cells in the CLNs are activated and begin to expand upon encountering these DCs displaying cognate bacterial-pMHCII. These $CD4^+$ T cells differentiate into T_H17 effector cells in response to IL-6 and TGF-β1, produced by activated dendritic cells. T_H17 cells migrate out of CLNs, through blood and spleen, to NALT. In the NALT, bacterial pMHCII-specific T_H17 cells stimulated through their TCR secrete IL-17A, IL-17F, and IL-22, enhancing bacterial clearance at this site through epithelial cell activation and neutrophil recruitment. Upon resolution of infection, a small population of short-lived T_H17 cells remain. In the case of intravenous bacterial infection, a functionally divergent population of splenic-resident DCs capture bacteria and present bacterial-pMHCII to cognate naïve $CD4^+$ T cells located in splenic tissue. These DCs do not produce IL6, but instead more likely produce

IL-12, leading to T_H1 effector cells. The T_H1 cells that remain after resolution of intravenous infection become a long-lived population of T_H1 effector memory cells that decay more slowly than T_H17 cells induced by intranasal infection.

In our experimental system, we identified that hematopoietic cell-produced IL-6 was necessary for T_H17 differentiation and that *Il6* transcript was produced at high levels after GAS infection by $CD11c^+$ cells residing in NALT tissue. However, Nunez and colleagues report that in the intestinal lamina propria, IL-6 was not necessary for this differentiation, but rather IL-1β was required (Shaw et al., 2012). Additionally, Kuchroo and colleagues reported in the EAE model that IL-21-dependent T_H17 differentiation occurs in IL-$6^{-/-}$ mice in the absence of T_{REG}s (Korn et al., 2007).

We also showed that TGF-β1 was necessary for T_H17 differentiation after intranasal bacterial infection and the primary source was from $CD11c^+$ dendritic cells, although a modest contribution by other sources, such as paracrine production by activated T cells, could not be excluded. However, it was previously published that T_H17 cells can be isolated from the lamina propria of genetically modified mice that contain T cells lacking the TGF-β1 receptor, suggesting that T_H17 differentiation could occur *in vivo* in the absence of TGF-β signaling to $CD4^+$ T cells (Ghoreschi et al., 2010).

An explanation for these seeming disparities may simply be that there are multiple, non-overlapping, tissue-dependent cytokine signaling pathways that result in T_H17 cell differentiation rather than the universal, tissue-independent pathway observed for T_H1 and T_H2 differentiation. Alternatively, each signaling pathway could be inducing functionally independent T_H17 "subtypes", all of which produce IL-17A, but also

coordinately produce subtly different cytokine profiles. One recent study suggests that the latter idea may indeed be the reality. Sallusto and colleagues observed two different pathogen-specific T_H17 cell populations in humans that secrete a different cytokine profile after *in vitro* re-stimulation (Zielinski et al., 2012). One population secreted IL-17 and IFN-γ in response to *Candida albicans*, while the other secreted IL-17A and IL-10 in response to *Staphylococcus aureus*. These two populations were likely primed in different areas of the body and therefore differentiated within a different DC-produced cytokine milieu, becoming two different subsets of T_H17 cells. Alternatively, the pathogens may have elicited alternative cytokine production by the dendritic cells that captured them through differential pathogen recognition receptor ligation. This finding suggests that T_H17 cells may not differentiate into one homogeneous subset.

We found that LM-pMHCII-specific T_H17 effector cells induced by intranasal Lm infection decreased at a faster rate than LM-pMHCII-specific T_H1 effector memory cells generated after intravenous Lm infection. A possible explanation for this is that T_H17 cells were less likely to survive long term. This is supported by our observation that T_H1 effector memory cells expressed CD27, whereas T_H17 effector cells did not, and a lack of CD27 has been associated with short lifespan in other studies (Hendriks et al., 2003). We recently undertook experiments tracking GAS-pMHCII-specific T_H17 effector cells over time after GAS intranasal infection and observed a higher initial magnitude at the peak of expansion compared to LM-pMHCII-specific T_H17 cells after LM intranasal infection. However, we observed a similar decay rate of these cells and conclude that T_H17 cells remain short-lived, independent of the bacterial pathogen utilized. Another possibility

was that T_H17 effector cells survived, but lost the ability to produce IL-17A. Since we enumerated these cells over time by observing IL-17A production, these cells would have remained unaccounted for. A recent study supporting this possibility identified that after acute fungal infection, T_H17 cells lost the ability to produce IL-17A over time (Hirota et al., 2011). This group used a newly developed IL-17A fate-reporting mouse model to look at this and were able to track $CD4^+$ T cells that had produced-IL-17A in the past. It will be important for future studies in our lab to use this mouse under our experimental conditions to determine if this is really the case in our system.

5.2 Therapeutic Implications

Dysregulated T_H17 cell responses have been implicated in the pathogenesis of multiple autoimmune diseases such as rheumatoid arthritis and multiple sclerosis. The observation that IL-6 and TGF-β1 are necessary for T_H17 differentiation *in vivo* suggest that clinical interventions targeting these molecules may be beneficial to the treatment of these conditions. Several recent Phase III clinical trials have been undertaken to investigate the efficacy of a humanized anti-human IL-6 receptor antibody (Tocilizumab) in the treatment of rheumatoid arthritis (Alten, 2011). It was shown that Tocilizumab improved clinical symptoms of rheumatoid arthritis. Although these studies did not show a direct effect on the reduction of T_H17 cells in patients, it is plausible that treatment with this antibody acted by inhibiting further T_H17 differentiation. Additionally, neutralizing humanized anti-TGF-β1 antibodies have been developed, but are not currently being investigated in T_H17 implicated autoimmune disease treatment (Denton et al., 2007). A

future potential treatment that could be realized based on the work of this dissertation includes targeting anti-TGF-β1 antibodies to dendritic cells to inhibit secretion from this relevant source.

The finding that T_H17 effector cells are shorter-lived than their T_H1 effector memory counterparts has major implications for protective immunity as it relates to rational vaccine design. To develop an effective cell-mediated vaccine to combat pathogens in which a T_H17 response is needed for protective immunity, it may be necessary to administer multiple boosters throughout the lifetime of the patient in order to maintain enough T_H17 cells for adequate protection. This work also identifies that the intranasal route may be an important anatomical site to administer such a vaccine to ensure a strong T_H17 cell response develops.

References

Ahmed, R., and Gray, D. (1996). Immunological memory and protective immunity: understanding their relation. Science *272*, 54-60.

Allam, A., Conze, D. B., Giardino Torchia, M. L., Munitic, I., Yagita, H., Sowell, R. T., Marzo, A. L., and Ashwell, J. D. (2009). The CD8+ memory T-cell state of readiness is actively maintained and reversible. Blood *114*, 2121-2130.

Alten, R. (2011). Tocilizumab: a novel humanized anti-interleukin 6 receptor antibody for the treatment of patients with rheumatoid arthritis. Ther Adv Musculoskelet Dis *3*, 133-149.

Annunziato, F., and Romagnani, S. (2010). The transient nature of the Th17 phenotype. Eur J Immunol *40*, 3312-3316.

Aranami, T., and Yamamura, T. (2008). Th17 Cells and autoimmune encephalomyelitis (EAE/MS). Allergol Int *57*, 115-120.

Badovinac, V. P., Haring, J. S., and Harty, J. T. (2007). Initial T cell receptor transgenic cell precursor frequency dictates critical aspects of the CD8(+) T cell response to infection. Immunity *26*, 827-841.

Banchereau, J., Briere, F., Caux, C., Davoust, J., Lebecque, S., Liu, Y. J., Pulendran, B., and Palucka, K. (2000). Immunobiology of dendritic cells. Annu Rev Immunol *18*, 767-811.

Bettelli, E., Carrier, Y., Gao, W., Korn, T., Strom, T. B., Oukka, M., Weiner, H. L., and Kuchroo, V. K. (2006). Reciprocal developmental pathways for the generation of pathogenic effector TH17 and regulatory T cells. Nature *441*, 235-238.

Bettelli, E., Korn, T., Oukka, M., and Kuchroo, V. K. (2008). Induction and effector functions of T(H)17 cells. Nature *453*, 1051-1057.

Blair, D. A., and Lefrancois, L. (2007). Increased competition for antigen during priming negatively impacts the generation of memory CD4 T cells. Proc Natl Acad Sci U S A *104*, 15045-15050.

Boggs, D. R. (1984). The total marrow mass of the mouse: a simplified method of measurement. Am J Hematol *16*, 277-286.

Carapetis, J. R., Steer, A. C., Mulholland, E. K., and Weber, M. (2005). The global burden of group A streptococcal diseases. Lancet Infect Dis *5*, 685-694.

Caton, M. L., Smith-Raska, M. R., and Reizis, B. (2007). Notch-RBP-J signaling controls the homeostasis of CD8- dendritic cells in the spleen. J Exp Med *204*, 1653-1664.

Catron, D. M., Itano, A. A., Pape, K. A., Mueller, D. L., and Jenkins, M. K. (2004). Visualizing the first 50 hr of the primary immune response to a soluble antigen. Immunity *21*, 341-347.

Catron, D. M., Rusch, L. K., Hataye, J., Itano, A. A., and Jenkins, M. K. (2006). CD4+ T cells that enter the draining lymph nodes after antigen injection participate in the primary response and become central-memory cells. J Exp Med *203*, 1045-1054.

Chung, Y., Chang, S. H., Martinez, G. J., Yang, X. O., Nurieva, R., Kang, H. S., Ma, L., Watowich, S. S., Jetten, A. M., Tian, Q., and Dong, C. (2009). Critical regulation of early Th17 cell differentiation by interleukin-1 signaling. Immunity *30*, 576-587.

Chytil, A., Magnuson, M. A., Wright, C. V., and Moses, H. L. (2002). Conditional inactivation of the TGF-beta type II receptor using Cre:Lox. Genesis *32*, 73-75.

Conti, H. R., Shen, F., Nayyar, N., Stocum, E., Sun, J. N., Lindemann, M. J., Ho, A. W., Hai, J. H., Yu, J. J., Jung, J. W.*, et al.* (2009). Th17 cells and IL-17 receptor signaling are essential for mucosal host defense against oral candidiasis. J Exp Med *206*, 299-311.

Costalonga, M., Cleary, P. P., Fischer, L. A., and Zhao, Z. (2009). Intranasal bacteria induce Th1 but not Treg or Th2. Mucosal Immunol *2*, 85-95.

Cunningham, M. W. (2008). Pathogenesis of group A streptococcal infections and their sequelae. Adv Exp Med Biol *609*, 29-42.

Das, J., Ren, G., Zhang, L., Roberts, A. I., Zhao, X., Bothwell, A. L., Van Kaer, L., Shi, Y., and Das, G. (2009). Transforming growth factor beta is dispensable for the molecular orchestration of Th17 cell differentiation. J Exp Med *206*, 2407-2416.

Denton, C. P., Merkel, P. A., Furst, D. E., Khanna, D., Emery, P., Hsu, V. M., Silliman, N., Streisand, J., Powell, J., Akesson, A.*, et al.* (2007). Recombinant human anti-transforming growth factor beta1 antibody therapy in systemic sclerosis: a multicenter, randomized, placebo-controlled phase I/II trial of CAT-192. Arthritis Rheum *56*, 323-333.

Diao, H., and Kohanawa, M. (2005). Endogenous interleukin-6 plays a crucial protective role in streptococcal toxic shock syndrome via suppression of tumor necrosis factor alpha production. Infect Immun *73*, 3745-3748.

Dileepan, T., Linehan, J. L., Moon, J. J., Pepper, M., Jenkins, M. K., and Cleary, P. P. (2011). Robust antigen specific th17 T cell response to group A Streptococcus is dependent on IL-6 and intranasal route of infection. PLoS Pathog *7*, e1002252.

Dolfi, D. V., Boesteanu, A. C., Petrovas, C., Xia, D., Butz, E. A., and Katsikis, P. D. (2008). Late signals from CD27 prevent Fas-dependent apoptosis of primary CD8+ T cells. J Immunol *180*, 2912-2921.

Dombek, P. E., Cue, D., Sedgewick, J., Lam, H., Ruschkowski, S., Finlay, B. B., and Cleary, P. P. (1999). High-frequency intracellular invasion of epithelial cells by serotype M1 group A streptococci: M1 protein-mediated invasion and cytoskeletal rearrangements. Mol Microbiol *31*, 859-870.

Eberl, G., Marmon, S., Sunshine, M. J., Rennert, P. D., Choi, Y., and Littman, D. R. (2004). An essential function for the nuclear receptor RORgamma(t) in the generation of fetal lymphoid tissue inducer cells. Nat Immunol *5*, 64-73.

Engle, S. J., Hoying, J. B., Boivin, G. P., Ormsby, I., Gartside, P. S., and Doetschman, T. (1999). Transforming growth factor beta1 suppresses nonmetastatic colon cancer at an early stage of tumorigenesis. Cancer Res *59*, 3379-3386.

Ericson, S. G., Zhao, Y., Gao, H., Miller, K. L., Gibson, L. F., Lynch, J. P., and Landreth, K. S. (1998). Interleukin-6 production by human neutrophils after Fc-receptor cross-linking or exposure to granulocyte colony-stimulating factor. Blood *91*, 2099-2107.

Ertelt, J. M., Rowe, J. H., Johanns, T. M., Lai, J. C., McLachlan, J. B., and Way, S. S. (2009). Selective priming and expansion of antigen-specific Foxp3- CD4+ T cells during Listeria monocytogenes infection. J Immunol *182*, 3032-3038.

Garcia, Z., Pradelli, E., Celli, S., Beuneu, H., Simon, A., and Bousso, P. (2007). Competition for antigen determines the stability of T cell-dendritic cell interactions during clonal expansion. Proc Natl Acad Sci U S A *104*, 4553-4558.

Ghoreschi, K., Laurence, A., Yang, X. P., Tato, C. M., McGeachy, M. J., Konkel, J. E., Ramos, H. L., Wei, L., Davidson, T. S., Bouladoux, N*., et al.* (2010). Generation of pathogenic T(H)17 cells in the absence of TGF-beta signalling. Nature *467*, 967-971.

Glimcher, L. H., and Murphy, K. M. (2000). Lineage commitment in the immune system: the T helper lymphocyte grows up. Genes Dev *14*, 1693-1711.

Gonzalez, S. F., Degn, S. E., Pitcher, L. A., Woodruff, M., Heesters, B. A., and Carroll, M. C. (2011). Trafficking of B cell antigen in lymph nodes. Annu Rev Immunol *29*, 215-233.

Guilherme, L., Fae, K., Oshiro, S. E., and Kalil, J. (2005). Molecular pathogenesis of rheumatic fever and rheumatic heart disease. Expert Rev Mol Med *7*, 1-15.

Gutcher, I., Donkor, M. K., Ma, Q., Rudensky, A. Y., Flavell, R. A., and Li, M. O. (2011). Autocrine transforming growth factor-beta1 promotes in vivo Th17 cell differentiation. Immunity *34*, 396-408.

Harker, J. A., Lewis, G. M., Mack, L., and Zuniga, E. I. (2011). Late interleukin-6 escalates T follicular helper cell responses and controls a chronic viral infection. Science *334*, 825-829.

Harrington, L. E., Hatton, R. D., Mangan, P. R., Turner, H., Murphy, T. L., Murphy, K. M., and Weaver, C. T. (2005). Interleukin 17-producing CD4+ effector T cells develop via a lineage distinct from the T helper type 1 and 2 lineages. Nat Immunol *6*, 1123-1132.

Harrington, L. E., Janowski, K. M., Oliver, J. R., Zajac, A. J., and Weaver, C. T. (2008). Memory CD4 T cells emerge from effector T-cell progenitors. Nature *452*, 356-360.

Hataye, J., Moon, J. J., Khoruts, A., Reilly, C., and Jenkins, M. K. (2006). Naive and memory CD4+ T cell survival controlled by clonal abundance. Science *312*, 114-116.

Heinrich, P. C., Behrmann, I., Haan, S., Hermanns, H. M., Muller-Newen, G., and Schaper, F. (2003). Principles of interleukin (IL)-6-type cytokine signalling and its regulation. Biochem J *374*, 1-20.

Hendriks, J., Gravestein, L. A., Tesselaar, K., van Lier, R. A., Schumacher, T. N., and Borst, J. (2000). CD27 is required for generation and long-term maintenance of T cell immunity. Nat Immunol *1*, 433-440.

Hendriks, J., Xiao, Y., and Borst, J. (2003). CD27 promotes survival of activated T cells and complements CD28 in generation and establishment of the effector T cell pool. J Exp Med *198*, 1369-1380.

Hikono, H., Kohlmeier, J. E., Takamura, S., Wittmer, S. T., Roberts, A. D., and Woodland, D. L. (2007). Activation phenotype, rather than central- or effector-memory phenotype, predicts the recall efficacy of memory CD8+ T cells. J Exp Med *204*, 1625-1636.

Hirota, K., Duarte, J. H., Veldhoen, M., Hornsby, E., Li, Y., Cua, D. J., Ahlfors, H., Wilhelm, C., Tolaini, M., Menzel, U.*, et al.* (2011). Fate mapping of IL-17-producing T cells in inflammatory responses. Nat Immunol *12*, 255-263.

Hogquist, K. A., Baldwin, T. A., and Jameson, S. C. (2005). Central tolerance: learning self-control in the thymus. Nat Rev Immunol *5*, 772-782.

Homann, D., Teyton, L., and Oldstone, M. B. (2001). Differential regulation of antiviral T-cell immunity results in stable CD8+ but declining CD4+ T-cell memory. Nat Med *7*, 913-919.

Hsieh, C. S., Macatonia, S. E., Tripp, C. S., Wolf, S. F., O'Garra, A., and Murphy, K. M. (1993). Development of TH1 CD4+ T cells through IL-12 produced by Listeria-induced macrophages. Science *260*, 547-549.

Hyland, K. A., Brennan, R., Olmsted, S. B., Rojas, E., Murphy, E., Wang, B., and Cleary, P. P. (2009). The early interferon response of nasal-associated lymphoid tissue to Streptococcus pyogenes infection. FEMS Immunol Med Microbiol *55*, 422-431.

Hyland, K. A., Wang, B., and Cleary, P. P. (2007). Protein F1 and Streptococcus pyogenes resistance to phagocytosis. Infect Immun *75*, 3188-3191.

Intlekofer, A. M., Takemoto, N., Wherry, E. J., Longworth, S. A., Northrup, J. T., Palanivel, V. R., Mullen, A. C., Gasink, C. R., Kaech, S. M., Miller, J. D.*, et al.* (2005). Effector and memory CD8+ T cell fate coupled by T-bet and eomesodermin. Nat Immunol *6*, 1236-1244.

Ishigame, H., Kakuta, S., Nagai, T., Kadoki, M., Nambu, A., Komiyama, Y., Fujikado, N., Tanahashi, Y., Akitsu, A., Kotaki, H.*, et al.* (2009). Differential roles of interleukin-17A and -17F in host defense against mucoepithelial bacterial infection and allergic responses. Immunity *30*, 108-119.

Ivanov, II, McKenzie, B. S., Zhou, L., Tadokoro, C. E., Lepelley, A., Lafaille, J. J., Cua, D. J., and Littman, D. R. (2006). The orphan nuclear receptor RORgammat directs the differentiation program of proinflammatory IL-17+ T helper cells. Cell *126*, 1121-1133.

Iwasaki, A. (2007). Mucosal dendritic cells. Annu Rev Immunol *25*, 381-418.

Iwasaki, A., and Kelsall, B. L. (2001). Unique functions of CD11b+, CD8 alpha+, and double-negative Peyer's patch dendritic cells. J Immunol *166*, 4884-4890.

Jameson, S. C., Hogquist, K. A., and Bevan, M. J. (1995). Positive selection of thymocytes. Annu Rev Immunol *13*, 93-126.

Janeway, C. A., Jr., and Medzhitov, R. (2002). Innate immune recognition. Annu Rev Immunol *20*, 197-216.

Jenkins, M. K., Chu, H. H., McLachlan, J. B., and Moon, J. J. (2010). On the composition of the preimmune repertoire of T cells specific for Peptide-major histocompatibility complex ligands. Annu Rev Immunol *28*, 275-294.

Jenkins, M. K., Khoruts, A., Ingulli, E., Mueller, D. L., McSorley, S. J., Reinhardt, R. L., Itano, A., and Pape, K. A. (2001). In vivo activation of antigen-specific CD4 T cells. Annu Rev Immunol *19*, 23-45.

Jenkins, M. K., and Moon, J. J. (2012). The role of naive T cell precursor frequency and recruitment in dictating immune response magnitude. J Immunol *188*, 4135-4140.

Jiang, D., Liang, J., Fan, J., Yu, S., Chen, S., Luo, Y., Prestwich, G. D., Mascarenhas, M. M., Garg, H. G., Quinn, D. A.*, et al.* (2005). Regulation of lung injury and repair by Toll-like receptors and hyaluronan. Nat Med *11*, 1173-1179.

Joshi, N. S., Cui, W., Chandele, A., Lee, H. K., Urso, D. R., Hagman, J., Gapin, L., and Kaech, S. M. (2007). Inflammation directs memory precursor and short-lived effector CD8(+) T cell fates via the graded expression of T-bet transcription factor. Immunity *27*, 281-295.

Jung, H. C., Eckmann, L., Yang, S. K., Panja, A., Fierer, J., Morzycka-Wroblewska, E., and Kagnoff, M. F. (1995). A distinct array of proinflammatory cytokines is expressed in human colon epithelial cells in response to bacterial invasion. J Clin Invest *95*, 55-65.

Kaech, S. M., Hemby, S., Kersh, E., and Ahmed, R. (2002). Molecular and functional profiling of memory CD8 T cell differentiation. Cell *111*, 837-851.

Keller, A. M., Schildknecht, A., Xiao, Y., van den Broek, M., and Borst, J. (2008). Expression of costimulatory ligand CD70 on steady-state dendritic cells breaks CD8+ T cell tolerance and permits effective immunity. Immunity *29*, 934-946.

Kelsall, B. (2008). Recent progress in understanding the phenotype and function of intestinal dendritic cells and macrophages. Mucosal Immunol *1*, 460-469.

Khoruts, A., Mondino, A., Pape, K. A., Reiner, S. L., and Jenkins, M. K. (1998). A natural immunological adjuvant enhances T cell clonal expansion through a CD28-dependent, interleukin (IL)-2-independent mechanism. J Exp Med *187*, 225-236.

Kopf, M., Baumann, H., Freer, G., Freudenberg, M., Lamers, M., Kishimoto, T., Zinkernagel, R., Bluethmann, H., and Kohler, G. (1994). Impaired immune and acute-phase responses in interleukin-6-deficient mice. Nature *368*, 339-342.

Korn, T., Bettelli, E., Gao, W., Awasthi, A., Jager, A., Strom, T. B., Oukka, M., and Kuchroo, V. K. (2007). IL-21 initiates an alternative pathway to induce proinflammatory T(H)17 cells. Nature *448*, 484-487.

Korn, T., Bettelli, E., Oukka, M., and Kuchroo, V. K. (2009). IL-17 and Th17 Cells. Annu Rev Immunol *27*, 485-517.

Kraus, Z. J., Haring, J. S., and Bishop, G. A. (2008). TNF receptor-associated factor 5 is required for optimal T cell expansion and survival in response to infection. J Immunol *181*, 7800-7809.

Lee, P. P., Fitzpatrick, D. R., Beard, C., Jessup, H. K., Lehar, S., Makar, K. W., Perez-Melgosa, M., Sweetser, M. T., Schlissel, M. S., Nguyen, S.*, et al.* (2001). A critical role for Dnmt1 and DNA methylation in T cell development, function, and survival. Immunity *15*, 763-774.

Lee, Y. K., Turner, H., Maynard, C. L., Oliver, J. R., Chen, D., Elson, C. O., and Weaver, C. T. (2009). Late developmental plasticity in the T helper 17 lineage. Immunity *30*, 92-107.

Letterio, J. J., and Roberts, A. B. (1998). Regulation of immune responses by TGF-beta. Annu Rev Immunol *16*, 137-161.

Li, H., Nooh, M. M., Kotb, M., and Re, F. (2008). Commercial peptidoglycan preparations are contaminated with superantigen-like activity that stimulates IL-17 production. J Leukoc Biol *83*, 409-418.

Li, J., Huston, G., and Swain, S. L. (2003). IL-7 promotes the transition of CD4 effectors to persistent memory cells. J Exp Med *198*, 1807-1815.

Li, M. O., and Flavell, R. A. (2008). TGF-beta: a master of all T cell trades. Cell *134*, 392-404.

Li, M. O., Wan, Y. Y., and Flavell, R. A. (2007). T cell-produced transforming growth factor-beta1 controls T cell tolerance and regulates Th1- and Th17-cell differentiation. Immunity *26*, 579-591.

Lin, Y., Ritchea, S., Logar, A., Slight, S., Messmer, M., Rangel-Moreno, J., Guglani, L., Alcorn, J. F., Strawbridge, H., Park, S. M.*, et al.* (2009). Interleukin-17 is required for T helper 1 cell immunity and host resistance to the intracellular pathogen Francisella tularensis. Immunity *31*, 799-810.

Lohning, M., Hegazy, A. N., Pinschewer, D. D., Busse, D., Lang, K. S., Hofer, T., Radbruch, A., Zinkernagel, R. M., and Hengartner, H. (2008). Long-lived virus-reactive memory T cells generated from purified cytokine-secreting T helper type 1 and type 2 effectors. J Exp Med *205*, 53-61.

Love, P. E., and Bhandoola, A. (2011). Signal integration and crosstalk during thymocyte migration and emigration. Nat Rev Immunol *11*, 469-477.

Lu, Y. J., Gross, J., Bogaert, D., Finn, A., Bagrade, L., Zhang, Q., Kolls, J. K., Srivastava, A., Lundgren, A., Forte, S.*, et al.* (2008). Interleukin-17A mediates acquired immunity to pneumococcal colonization. PLoS Pathog *4*, e1000159.

Lyakh, L. A., Sanford, M., Chekol, S., Young, H. A., and Roberts, A. B. (2005). TGF-beta and vitamin D3 utilize distinct pathways to suppress IL-12 production and modulate rapid differentiation of human monocytes into CD83+ dendritic cells. J Immunol *174*, 2061-2070.

Mangan, P. R., Harrington, L. E., O'Quinn, D. B., Helms, W. S., Bullard, D. C., Elson, C. O., Hatton, R. D., Wahl, S. M., Schoeb, T. R., and Weaver, C. T. (2006). Transforming growth factor-beta induces development of the T(H)17 lineage. Nature *441*, 231-234.

Martin, J. M., Green, M., Barbadora, K. A., and Wald, E. R. (2004). Group A streptococci among school-aged children: clinical characteristics and the carrier state. Pediatrics *114*, 1212-1219.

Marzo, A. L., Klonowski, K. D., Le Bon, A., Borrow, P., Tough, D. F., and Lefrancois, L. (2005). Initial T cell frequency dictates memory CD8+ T cell lineage commitment. Nat Immunol *6*, 793-799.

Masopust, D., Vezys, V., Marzo, A. L., and Lefrancois, L. (2001). Preferential localization of effector memory cells in nonlymphoid tissue. Science *291*, 2413-2417.

McGeachy, M. J., Chen, Y., Tato, C. M., Laurence, A., Joyce-Shaikh, B., Blumenschein, W. M., McClanahan, T. K., O'Shea, J. J., and Cua, D. J. (2009). The interleukin 23 receptor is essential for the terminal differentiation of interleukin 17-producing effector T helper cells in vivo. Nat Immunol *10*, 314-324.

Mohrs, M., Shinkai, K., Mohrs, K., and Locksley, R. M. (2001). Analysis of type 2 immunity in vivo with a bicistronic IL-4 reporter. Immunity *15*, 303-311.

Monack, D. M., Mueller, A., and Falkow, S. (2004). Persistent bacterial infections: the interface of the pathogen and the host immune system. Nat Rev Microbiol *2*, 747-765.

Moon, J. J., Chu, H. H., Hataye, J., Pagan, A. J., Pepper, M., McLachlan, J. B., Zell, T., and Jenkins, M. K. (2009). Tracking epitope-specific T cells. Nat Protoc *4*, 565-581.

Moon, J. J., Chu, H. H., Pepper, M., McSorley, S. J., Jameson, S. C., Kedl, R. M., and Jenkins, M. K. (2007). Naive CD4(+) T cell frequency varies for different epitopes and predicts repertoire diversity and response magnitude. Immunity *27*, 203-213.

Muller, W. J., Orgun, N. N., Dong, L., Koelle, D. M., Huang, M. L., and Way, S. S. (2008). Recombinant Listeria monocytogenes expressing an immunodominant peptide

fails to protect after intravaginal challenge with herpes simplex virus-2. Arch Virol *153*, 1165-1169.

Murphy, K. M., and Reiner, S. L. (2002). The lineage decisions of helper T cells. Nat Rev Immunol *2*, 933-944.

Nishikawa, Y., Shibata, R., Ozono, Y., Ichinose, H., Miyazaki, M., Harada, T., and Kohno, S. (2000). Streptococcal M protein enhances TGF-beta production and increases surface IgA-positive B cells in vitro in IgA nephropathy. Nephrol Dial Transplant *15*, 772-777.

Osterlund, A., Popa, R., Nikkila, T., Scheynius, A., and Engstrand, L. (1997). Intracellular reservoir of Streptococcus pyogenes in vivo: a possible explanation for recurrent pharyngotonsillitis. Laryngoscope *107*, 640-647.

Oukka, M. (2008). Th17 cells in immunity and autoimmunity. Ann Rheum Dis *67 Suppl 3*, iii26-29.

Pahlman, L. I., Morgelin, M., Eckert, J., Johansson, L., Russell, W., Riesbeck, K., Soehnlein, O., Lindbom, L., Norrby-Teglund, A., Schumann, R. R.*, et al.* (2006). Streptococcal M protein: a multipotent and powerful inducer of inflammation. J Immunol *177*, 1221-1228.

Pape, K. A., Merica, R., Mondino, A., Khoruts, A., and Jenkins, M. K. (1998). Direct evidence that functionally impaired CD4+ T cells persist in vivo following induction of peripheral tolerance. J Immunol *160*, 4719-4729.

Park, H., Li, Z., Yang, X. O., Chang, S. H., Nurieva, R., Wang, Y. H., Wang, Y., Hood, L., Zhu, Z., Tian, Q., and Dong, C. (2005). A distinct lineage of CD4 T cells regulates tissue inflammation by producing interleukin 17. Nat Immunol *6*, 1133-1141.

Park, H. S., Costalonga, M., Reinhardt, R. L., Dombek, P. E., Jenkins, M. K., and Cleary, P. P. (2004). Primary induction of CD4 T cell responses in nasal associated lymphoid tissue during group A streptococcal infection. Eur J Immunol *34*, 2843-2853.

Park, H. S., Francis, K. P., Yu, J., and Cleary, P. P. (2003). Membranous cells in nasal-associated lymphoid tissue: a portal of entry for the respiratory mucosal pathogen group A streptococcus. J Immunol *171*, 2532-2537.

Peck, A., and Mellins, E. D. (2010). Plasticity of T-cell phenotype and function: the T helper type 17 example. Immunology *129*, 147-153.

Pepper, M., and Jenkins, M. K. (2011). Origins of CD4(+) effector and central memory T cells. Nat Immunol *12*, 467-471.

Pepper, M., Linehan, J. L., Pagan, A. J., Zell, T., Dileepan, T., Cleary, P. P., and Jenkins, M. K. (2010). Different routes of bacterial infection induce long-lived TH1 memory cells and short-lived TH17 cells. Nat Immunol *11*, 83-89.

Portnoy, D. A., Auerbuch, V., and Glomski, I. J. (2002). The cell biology of Listeria monocytogenes infection: the intersection of bacterial pathogenesis and cell-mediated immunity. J Cell Biol *158*, 409-414.

Quinn, R. W., and Federspiel, C. F. (1973). The occurrence of hemolytic streptococci in school children in Nashville, Tennessee, 1961-1967. Am J Epidemiol *97*, 22-33.

Rees, W., Bender, J., Teague, T. K., Kedl, R. M., Crawford, F., Marrack, P., and Kappler, J. (1999). An inverse relationship between T cell receptor affinity and antigen dose during CD4(+) T cell responses in vivo and in vitro. Proc Natl Acad Sci U S A *96*, 9781-9786.

Reiner, S. L., and Locksley, R. M. (1995). The regulation of immunity to Leishmania major. Annu Rev Immunol *13*, 151-177.

Reinhardt, R. L., Khoruts, A., Merica, R., Zell, T., and Jenkins, M. K. (2001). Visualizing the generation of memory CD4 T cells in the whole body. Nature *410*, 101-105.

Reis e Sousa, C., Hieny, S., Scharton-Kersten, T., Jankovic, D., Charest, H., Germain, R. N., and Sher, A. (1997). In vivo microbial stimulation induces rapid CD40 ligand-independent production of interleukin 12 by dendritic cells and their redistribution to T cell areas. J Exp Med *186*, 1819-1829.

Reynolds, J. M., Pappu, B. P., Peng, J., Martinez, G. J., Zhang, Y., Chung, Y., Ma, L., Yang, X. O., Nurieva, R. I., Tian, Q., and Dong, C. (2010). Toll-like receptor 2 signaling in CD4(+) T lymphocytes promotes T helper 17 responses and regulates the pathogenesis of autoimmune disease. Immunity *32*, 692-702.

Ribot, J. C., deBarros, A., Pang, D. J., Neves, J. F., Peperzak, V., Roberts, S. J., Girardi, M., Borst, J., Hayday, A. C., Pennington, D. J., and Silva-Santos, B. (2009). CD27 is a thymic determinant of the balance between interferon-gamma- and interleukin 17-producing gammadelta T cell subsets. Nat Immunol *10*, 427-436.

Rubinstein, M. P., Kovar, M., Purton, J. F., Cho, J. H., Boyman, O., Surh, C. D., and Sprent, J. (2006). Converting IL-15 to a superagonist by binding to soluble IL-15R{alpha}. Proc Natl Acad Sci U S A *103*, 9166-9171.

Rutz, S., Noubade, R., Eidenschenk, C., Ota, N., Zeng, W., Zheng, Y., Hackney, J., Ding, J., Singh, H., and Ouyang, W. (2011). Transcription factor c-Maf mediates the TGF-beta-dependent suppression of IL-22 production in T(H)17 cells. Nat Immunol *12*, 1238-1245.

Sallusto, F., Geginat, J., and Lanzavecchia, A. (2004). Central memory and effector memory T cell subsets: function, generation, and maintenance. Annu Rev Immunol *22*, 745-763.

Sallusto, F., Lenig, D., Forster, R., Lipp, M., and Lanzavecchia, A. (1999). Two subsets of memory T lymphocytes with distinct homing potentials and effector functions. Nature *401*, 708-712.

Sato, A., Hashiguchi, M., Toda, E., Iwasaki, A., Hachimura, S., and Kaminogawa, S. (2003). CD11b+ Peyer's patch dendritic cells secrete IL-6 and induce IgA secretion from naive B cells. J Immunol *171*, 3684-3690.

Scheibner, K. A., Lutz, M. A., Boodoo, S., Fenton, M. J., Powell, J. D., and Horton, M. R. (2006). Hyaluronan fragments act as an endogenous danger signal by engaging TLR2. J Immunol *177*, 1272-1281.

Seder, R. A., and Ahmed, R. (2003). Similarities and differences in CD4+ and CD8+ effector and memory T cell generation. Nat Immunol *4*, 835-842.

Shaw, M. H., Kamada, N., Kim, Y. G., and Nunez, G. (2012). Microbiota-induced IL-1beta, but not IL-6, is critical for the development of steady-state TH17 cells in the intestine. J Exp Med *209*, 251-258.

Shull, M. M., Ormsby, I., Kier, A. B., Pawlowski, S., Diebold, R. J., Yin, M., Allen, R., Sidman, C., Proetzel, G., Calvin, D., and et al. (1992). Targeted disruption of the mouse transforming growth factor-beta 1 gene results in multifocal inflammatory disease. Nature *359*, 693-699.

Sigurdardottir, T., Bjorck, V., Herwald, H., Morgelin, M., Rutardottir, S., Tornebrant, J., and Bodelsson, M. (2010). M1 protein from streptococcus pyogenes induces nitric oxide-mediated vascular hyporesponsiveness to phenylephrine: involvement of toll-like receptor activation. Shock *34*, 98-104.

Singer, A., Adoro, S., and Park, J. H. (2008). Lineage fate and intense debate: myths, models and mechanisms of CD4- versus CD8-lineage choice. Nat Rev Immunol *8*, 788-801.

Snyder, C. M., Cho, K. S., Bonnett, E. L., van Dommelen, S., Shellam, G. R., and Hill, A. B. (2008). Memory inflation during chronic viral infection is maintained by continuous production of short-lived, functional T cells. Immunity *29*, 650-659.

Soares, H., Waechter, H., Glaichenhaus, N., Mougneau, E., Yagita, H., Mizenina, O., Dudziak, D., Nussenzweig, M. C., and Steinman, R. M. (2007). A subset of dendritic

cells induces CD4+ T cells to produce IFN-γamma by an IL-12-independent but CD70-dependent mechanism in vivo. J Exp Med *204*, 1095-1106.

Sriskandan, S., Faulkner, L., and Hopkins, P. (2007). Streptococcus pyogenes: Insight into the function of the streptococcal superantigens. Int J Biochem Cell Biol *39*, 12-19.

Starr, T. K., Jameson, S. C., and Hogquist, K. A. (2003). Positive and negative selection of T cells. Annu Rev Immunol *21*, 139-176.

Stephen, J., Kuruvilla, A., Johnson, J., Chandi, S., Krishnaswami, S., and Brahmadathan, K. N. (1998). Pharyngeal colonisation, ADNB response and development of cardiac lesions in mice following intranasal inoculation with group A beta haemolytic streptococcus M type 18. Indian J Exp Biol *36*, 292-297.

Stoklasek, T. A., Schluns, K. S., and Lefrancois, L. (2006). Combined IL-15/IL-15Ralpha immunotherapy maximizes IL-15 activity in vivo. J Immunol *177*, 6072-6080.

Stranges, P. B., Watson, J., Cooper, C. J., Choisy-Rossi, C. M., Stonebraker, A. C., Beighton, R. A., Hartig, H., Sundberg, J. P., Servick, S., Kaufmann, G.*, et al.* (2007). Elimination of antigen-presenting cells and autoreactive T cells by Fas contributes to prevention of autoimmunity. Immunity *26*, 629-641.

Surh, C. D., and Sprent, J. (2008). Homeostasis of naive and memory T cells. Immunity *29*, 848-862.

Swain, S. L., Hu, H., and Huston, G. (1999). Class II-independent generation of CD4 memory T cells from effectors. Science *286*, 1381-1383.

Szabo, S. J., Kim, S. T., Costa, G. L., Zhang, X., Fathman, C. G., and Glimcher, L. H. (2000). A novel transcription factor, T-bet, directs Th1 lineage commitment. Cell *100*, 655-669.

Taghon, T., and Rothenberg, E. V. (2008). Molecular mechanisms that control mouse and human TCR-alphabeta and TCR-gammadelta T cell development. Semin Immunopathol *30*, 383-398.

Tart, A. H., Walker, M. J., and Musser, J. M. (2007). New understanding of the group A Streptococcus pathogenesis cycle. Trends Microbiol *15*, 318-325.

Tokoyoda, K., Zehentmeier, S., Hegazy, A. N., Albrecht, I., Grun, J. R., Lohning, M., and Radbruch, A. (2009). Professional memory CD4+ T lymphocytes preferentially reside and rest in the bone marrow. Immunity *30*, 721-730.

van Oosterwijk, M. F., Juwana, H., Arens, R., Tesselaar, K., van Oers, M. H., Eldering, E., and van Lier, R. A. (2007). CD27-CD70 interactions sensitise naive CD4+ T cells for IL-12-induced Th1 cell development. Int Immunol *19*, 713-718.

Vanden Berghe, W., Vermeulen, L., De Wilde, G., De Bosscher, K., Boone, E., and Haegeman, G. (2000). Signal transduction by tumor necrosis factor and gene regulation of the inflammatory cytokine interleukin-6. Biochem Pharmacol *60*, 1185-1195.

Veldhoen, M., Hocking, R. J., Atkins, C. J., Locksley, R. M., and Stockinger, B. (2006). TGFbeta in the context of an inflammatory cytokine milieu supports de novo differentiation of IL-17-producing T cells. Immunity *24*, 179-189.

Wang, B., Dileepan, T., Briscoe, S., Hyland, K. A., Kang, J., Khoruts, A., and Cleary, P. P. (2010). Induction of TGF-beta1 and TGF-beta1-dependent predominant Th17 differentiation by group A streptococcal infection. Proc Natl Acad Sci U S A *107*, 5937-5942.

Wang, B., Li, S., Southern, P. J., and Cleary, P. P. (2006). Streptococcal modulation of cellular invasion via TGF-beta1 signaling. Proc Natl Acad Sci U S A *103*, 2380-2385.
Weaver, C. T., Harrington, L. E., Mangan, P. R., Gavrieli, M., and Murphy, K. M. (2006). Th17: an effector CD4 T cell lineage with regulatory T cell ties. Immunity *24*, 677-688.

Wilson, N. J., Boniface, K., Chan, J. R., McKenzie, B. S., Blumenschein, W. M., Mattson, J. D., Basham, B., Smith, K., Chen, T., Morel, F.*, et al.* (2007). Development, cytokine profile and function of human interleukin 17-producing helper T cells. Nat Immunol *8*, 950-957.

Woolard, M. D., Hensley, L. L., Kawula, T. H., and Frelinger, J. A. (2008). Respiratory Francisella tularensis live vaccine strain infection induces Th17 cells and prostaglandin E2, which inhibits generation of gamma interferon-positive T cells. Infect Immun *76*, 2651-2659.

Yamanaka, N., Hotomi, M., and Billal, D. S. (2008). Clinical bacteriology and immunology in acute otitis media in children. J Infect Chemother *14*, 180-187.

Yang, X., Letterio, J. J., Lechleider, R. J., Chen, L., Hayman, R., Gu, H., Roberts, A. B., and Deng, C. (1999). Targeted disruption of SMAD3 results in impaired mucosal immunity and diminished T cell responsiveness to TGF-beta. EMBO J *18*, 1280-1291.

Yang, X. O., Pappu, B. P., Nurieva, R., Akimzhanov, A., Kang, H. S., Chung, Y., Ma, L., Shah, B., Panopoulos, A. D., Schluns, K. S.*, et al.* (2008). T helper 17 lineage differentiation is programmed by orphan nuclear receptors ROR alpha and ROR gamma. Immunity *28*, 29-39.

Zaph, C., Rook, K. A., Goldschmidt, M., Mohrs, M., Scott, P., and Artis, D. (2006). Persistence and function of central and effector memory CD4+ T cells following infection with a gastrointestinal helminth. J Immunol *177*, 511-518.

Zhang, Z., Clarke, T. B., and Weiser, J. N. (2009). Cellular effectors mediating Th17-dependent clearance of pneumococcal colonization in mice. J Clin Invest *119*, 1899-1909.

Zhou, L., Chong, M. M., and Littman, D. R. (2009). Plasticity of CD4+ T cell lineage differentiation. Immunity *30*, 646-655.

Zielinski, C. E., Mele, F., Aschenbrenner, D., Jarrossay, D., Ronchi, F., Gattorno, M., Monticelli, S., Lanzavecchia, A., and Sallusto, F. (2012). Pathogen-induced human TH17 cells produce IFN-γamma or IL-10 and are regulated by IL-1beta. Nature *484*, 514-518.

Zygmunt, B. M., Rharbaoui, F., Groebe, L., and Guzman, C. A. (2009). Intranasal immunization promotes th17 immune responses. J Immunol *183*, 6933-6938.